EXPERIMENTAL AND NUMERICAL ANALYSIS OF EFFECT OF CURING TIME ON MECHANICAL PROPERTIES OF THIN SPRAY-ON LINERS

A THESIS SUBMITTED TO
THE GRADUATE SCHOOL OF APPLIED AND NATURAL SCIENCES
OF
MIDDLE EAST TECHNICAL UNIVERSITY

BY

DOĞUKAN GÜNER

IN PARTIAL FULFILLMENT OF THE REQUIREMENTS
FOR
THE DEGREE OF MASTER OF SCIENCE
IN
MINING ENGINEERING

MAY 2014

Approval of the thesis:

EXPERIMENTAL AND NUMERICAL ANALYSIS OF EFFECT OF CURING TIME ON MECHANICAL PROPERTIES OF THIN SPRAY-ON LINERS

submitted by **DOĞUKAN GÜNER** in partial fulfilment of the requirements for the degree of **Master of Science in Mining Engineering Department, Middle East Technical University** by,

Prof. Dr. Canan Özgen _____

Dean, Graduate School of **Natural and Applied Sciences**

Prof. Dr. Ali İhsan Arol _____

Head of Department, **Mining Engineering**

Assoc. Prof.Dr. Hasan Öztürk _____

Supervisor, **Mining Engineering Dept., METU**

Examining Committee Members:

Prof. Dr. Celal Karpuz _____

Mining Engineering Dept., METU

Assoc. Prof. Dr. Hasan Öztürk _____

Mining Engineering Dept., METU

Assoc. Prof. Dr. Levend Tutluoğlu _____

Mining Engineering Dept., METU

Assoc. Dr. Hakan Başarır _____

Mining Engineering Dept., METU

Dr. İ. Ferid Öge _____

Freelance Mining Engineer

Date: 29.05.2014

I hereby declare that all information in this document has been obtained and presented in accordance with academic rules and ethical conduct. I also declare that, as required by these rules and conduct, I have fully cited and referenced all material and results that are not original to this work.

Name, Last Name: Doğukan GÜNER

Signature :

ABSTRACT

EXPERIMENTAL AND NUMERICAL ANALYSIS OF EFFECT OF CURING TIME ON MECHANICAL PROPERTIES OF THIN SPRAY-ON LINERS

GÜNER, Doğukan
M.Sc., Department of Mining Engineering
Supervisor: Assoc. Prof. Dr. Hasan Öztürk

May 2014, 154 pages

This research study investigates the effect of curing time on elastic material properties (Young's modulus, Poisson's ratio) and tensile, compressive strength of thin spray on liners (TSL). TSLs are fast curing, comparatively thin (3-5mm) and widely used rock support system in mining and civil engineering excavations. They have advantages of low volume, rapid application and low operating cost. The major ingredients of current TSLs are divided as polyurethane/ polyurea or Portland cement based latex products. One of the important parameters that control the support mechanisms of TSLs' is the tensile and compression strength behaviour of them. There are many different testing set-ups and tests have been conducted considering the physical properties of them. In this study, two different TSL products supplied by two TSL manufacturers are tested comparatively. During laboratory studies, samples that are prepared in the laboratory conditions with different curing times (1, 7, 14, 21 and 28 days) are tested based on ASTM standards. In addition, distinct element numerical modelling of the test results are carried out using PFC2D in an attempt to simulate the tests numerically, since the constitutive behaviour of the TSLs are yet to be determined. It is concluded that the increase in the curing time improves the tensile and compressive strength of the TSLs (2 to 9 times). Moreover, as an extra conclusion from the testing procedure, the difference between the common malpractices of measuring the sample displacement

from the grips of the loading machine versus from the sample's gauge length is observed to be significant (1 to 13 times). In addition, PFC numerical models with the tests enabled the derivation of two important parameters of TSLs; such as, bond strength and bond elastic modulus values of TSLs which can be used for numerical modelling of TSLs` support mechanisms in PFC by the researchers.

Keywords: Thin Spray-on liner (TSL), curing time, Discrete Element Method (DEM), Mechanical properties, Particle Flow Code (PFC)

ÖZ

KÜR SÜRESİNİN PÜSKÜRTÜLEN İNCE KAPLAMALARIN MEKANİK ÖZELLİKLERİNE ETKİSİNİN DENEYSEL VE SAYISAL OLARAK İNCELENMESİ

GÜNER, Doğukan
Yüksek Lisans, Maden Mühendisliği Bölümü
Tez Yöneticisi: Doçent Doktor Hasan Öztürk

Mayıs 2014, 154 sayfa

Bu çalışma püskürtülen ince kaplamaların (PİK) elastik malzeme özelliklerini (Elastik modulü, Poisson oranı), çekme ve basma dayanımlarını belirlemeye dayanır. PİK'ler hızlı prizlenen, nispeten ince (3-5mm), madencilik ve inşaat kazılarında yaygın olarak kullanılan bir tahkimat sistemidir. PİK'lerin uygulama kolaylığı, düşük işletme maliyetine sahip olması ve ince kalınlıklarda kullanılması sebebiyle düşük hacim gereksinimi gibi pek çok avantajı bulunmaktadır. Mevcut PİK'ler çoğunlukla poliüretan / poliüre veya Portland çimentosu bazlı lateks ürünlerdir. Çekme ve basma dayanımı değerleri, bu ürünlerin tahkimat mekanizmasını kontrol eden önemli parametrelerdendir. Bu parametrelerin tespiti için geliştirilen pek çok deney düzeneği mevcuttur. Bu çalışmada, literatürde ilk kez, iki farklı üretici tarafından sağlanan farklı içeriklere sahip PİK örnekleri test edilmiştir. Deney örnekleri farklı kür sürelerinde hazırlanmış (çekme deneyleri için 1, 7, 14, 21 ve 28 gün, basma deneyleri için 2, 7, 14, 21 ve 28 gün) ve deneyler yapılmıştır. Bu testlerde ASTM' ye (American Society for Testing and Materials) ait mevcut standartlar esas alınmıştır (D-638 ve D-695-10). Ayrıca henüz PİKlerin temel davranışı bilinmediğinden deneylerin sayısal simulasyonu çabasıyla, deneylerin Ayrık Elemanlar sayısal yöntemiyle modellenmesi PFC2D adlı programla yapılmıştır. Sonuç olarak kür süresindeki artış PİKlerin çekme ve basma dayanımında da artışa neden olmaktadır (2 -9 katı). Ek olarak örnek

deplasmanının ölçümünde yaygın olarak kullanılan yükleme cihazının örneği tutan uçları arasında yapılan ölçüm tekniği ile örneğin gague uzunluğuna bağlanan ekstansometreden ölçülen deplasman değerleri arasında büyük farklılıklar bulunduğu gözlemlenmiştir(1-13 katı). Ayrıca, yapılan testlerin PFC2D programında kalibrasyonu programda PİKlerin iki önemli parametresi olan ve ilerde PİKlerin tahkimat sistemini PFC'de sayısal modellemek isteyecek araştırmacılarca kullanılabilecek, bağ mukavemeti ve bağ elastik modülü değerlerinin bulunmasına olanak vermiştir.

Anahtar Kelimeler: Püskürtülen İnce Kaplama (PİK), Kür süresi, Ayrık Elemanlar Yöntemi (AEY), mekanik malzeme özellikleri, PFC

To My Parents

for their infinite love and trust

ACKNOWLEDGEMENTS

I express my sincere gratitude and heartfelt thanks to my advisor Assoc. Prof. Dr. Hasan Öztürk for his constructive guidance, insightful wisdom, valuable suggestions and continuing patience throughout this study. Being able to work with him was indeed a privilege for me. I also present my special thanks to the examining committee members, Prof. Dr. Celal Karpuz, Assoc. Prof. Dr. Levend Tutluoğlu, Assoc. Prof. Dr. Hakan Başarır and Dr. Ferid Öge for serving on the M.Sc. thesis committee.

This research was supported by METU Scientific Research Projects Coordination Center (BAP-08-11-2012-104). Also thanks are extend to TSL suppliers BASF and South African Mining & Engineering Supplies Cc.

I must offer acknowledgement to Hakan Uysal, Tahsin Işıksal and Sami Kılıç for their help and invaluable guidance during laboratory work.

I would also like to thank to my friends and colleagues for their support and help, Onur Gölbaşı, Ahmet Güneş Yardımcı, Deniz Tuncay, Uğur Alkan, Selahattin Akdağ and Gamze Aysu Kara.

Finally, I feel grateful to my family and I want to dedicate this dissertation to my family Most of all, I would like to express my sincere gratitude to my mother Zehra Güner, my father Bülent Güner for their unconditional support and encouragement, which have been the real inspiration during my studies.

TABLE OF CONTENTS

LIST OF TABLES

TABLES

LIST OF FIGURES

FIGURES

CHAPTER 1

INTRODUCTION

Adventure of humanity with mining started from the first ages. Human-being firstly has utilized the minerals located near surface and with the proceeding times he has recognized the potential of minerals deeper under the surface which has caused the commence of underground mining. Later on, the need for safety requirements in underground openings forced the development of the support systems. Timber support is the first type of these reinforcement systems. With the technological improvements, industrial need for various mineral types has raised. This induced the increases in production amounts and the need for wider underground openings eventually. Especially in recent decades, there have been many academical and industrial studies for the development of different underground supports to ensure health and safety of the miners. These studies have assisted in the increase of various support systems with different functions.

Underground supports systems are classified into 2 groups as passive and active. Active support transfers a reinforcing load to the rock by the mechanical tightening of a nut against an anchor point (tensioned). Mechanical rockbolts, tensioned rebar, tensioned cables are the foremost used active supports in ground control.

On the other hand, passive support systems are activated under load only when the rock moves. These systems are held in place by cement grout or friction (non-tensioned). Untensioned rebar, cable bolts, Swellex, split-sets, cable slings, shotcrete, timber & steel sets, mesh, screen & straps, backfill are the common passive support systems utilized in underground openings. Wire mesh and shotcrete arrangement, discovered in 1940s, is the most commonly used passive support system in ground control.

1.1 General Remarks and Definitions

At the beginning of 1990s, in order to decrease the underground mine injuries during support installation, to help decrease the delay in mining cycle and to apply support to the limited accessible excavations a new support alternative to wire mesh and shotcrete was discovered in simultaneous studies performed in Canada and South Africa. Performance of this liner was considered to be satisfactory by the mining society after the initial trials in some underground openings. After the workshop of "1st International Seminar on Mine Surface Support Liners: Membrane, Shotcrete and Mesh" arranged in Perth, Australia in 2001, all products falling into the description of "thin layer of surface support made from plastic, polymer or cement based compositions" were called as "Thin Spray-on Liner (TSL)".

General definition of TSL accepted by the whole mining society is "generally cement, latex, polymer-based and also reactive or non-reactive, multi-component materials applied to the rock surface sprayed by nozzle, in a layer of generally 6 mm or less (3-5 mm) thickness material".

As mentioned above, TSLs are known as the new form of shotcrete. However, in order to verify the comparative advantages of TSLs against shotcrete, most of the mechanical properties and benefits of TSLs should be tested and proved in details. This study aims to contribute to determination of elastic material properties, tensile and compressive strength determination of different TSLs as a function of curing time.

1.2 Problem Statement

TSL products are predicted to be effective support systems; however, mechanical behavior of this relatively new support material is still questionable, due to lack of understanding the supporting mechanism. Researchers have studied to understand the support mechanism of TSLs using numerical, analytical methods and laboratory studies (Lau *et al.*, 2008). In order to model TSLs numerically or analytically, researchers perform various laboratory tests such as tensile strength, uniaxial

compressive strength, Punch, bonding strength, double sided shear strength, plate pull, linear block support, gap shear load and coated core compression tests (Yilmaz, 2011)

There is not any testing standard in laboratory studies yet, since TSLs are relatively new product. However, some of the tests such as tensile and tensile bond strength tests gained the acceptance, because the field studies shows that tensile failure mechanism is one of the commonly observed yield type in TSLs (Kuijpers *et al.* 2004)

TSLs are accepted as elastic materials; and researchers made assumption on the elastic properties (E, ν) of TSLs (Mason and Stacey, 2008; Mason and Abelman, 2009; Fowkes et al., 2008; Wang and Tannant, 2002; Dirige and Archibald, 2009). However, mechanical properties of TSLs are strongly related to the curing time (Tannant, 1999) Definition of the properties regarding the time-dependent variation is critically important for a complete definition of TSLs' mechanical property. One of the purposes of this study is to determine the change of mechanical properties of two different TSL products with different curing times.

Another aim of this study is the distinct element numerical modelling of the tests using a two dimensional numerical code; Particle Flow Code software (PFC2D) (Itasca, 2008). In an attempt to simulate the test results numerically. Since the constitutive behavior of TSLs' are yet to be determined calibration of the PFC models with the tests will help researchers with the PFC modelling of TSLs support system.

1.3 Research Objectives of the Study

In the scope of this study; mechanical properties of two different TSLs will be determined for different curing times (1, 7, 14, 21, 28 days for tensile testing, 2, 7, 14, 21, 28 days for compression testing).

These mechanical properties are;

- Tensile strength
- Young's modulus (tensile modulus)

- Uniaxial compressive strength
- Modulus of elasticity
- Poisson's ratio

In order to compare two different TSLs having different mechanical properties, a great care was paid attention to the chemical compositions of the TSLs during selection process. Two TSLs, one being more brittle compared to the other are chosen.

After the laboratory tests, numerical modelling part of this study will be initiated. The tensile and uniaxial testing of the laboratory specimens will be simulated by discrete element models, using PFC2D (Itasca consulting trademark). PFC numerical models by the tests will enable the derivation of two important parameters of PFC; such as, bond strength and bond elastic modulus values of TSLs which can be used for the future studies of numerical modelling of TSLs' support mechanisms.

1.4 Research Methodology

The methodology of this research includes the following steps;

- Determination and request of the TSLs from different manufacturers (MasterRoc TSL 865 by BASF from Istanbul, Tunnel Guard by South African Mining & Engineering Supplies from South Africa),
- Purchasing the data acquisition system, the tensile load cell and the tensile extensometer,
- Seting-up of the testing apparatus and checking the whole setup with some trial tests,
- Preparation of tensile and compression TSL samples in accordance with standards. (ASTM D-638, D695),
- Tensile and compression testing of samples with different curing times,
- Evaluation of test results,
- Modelling of test specimens using PFC2D.
- Comparison of tests with numerical studies.

- Derivation of bond strength and bond elastic modulus values of the two TSL products which can be used for the future studies of numerical modelling of TSLs` support mechanisms.

1.5 Thesis Outline

This study is composed of six chapters and 3 appendices, which are organized as described. Chapter 1 presents general remarks, problem statement, and research objective of the study and thesis outline in brief. Chapter 2 mentions literature review, background and the future of TSLs. In chapter 3, details of the laboratory test take a part. After general information about the products and the test procedure presented, test results and calculations are discussed. Chapter 4 covers the discrete element model and the theory behind it. Tensile and compression test model results are also included in this chapter. Lastly, conclusions and recommendations are presented in chapter 5.

In Appendix A, stress-strain curves of tensile tests and specimen photos before and after tests are illustrated for each curing time. In Appendix B, stress-strain curves of compression tests and specimen photos before and after tests are presented for each curing time, In Appendix C, the numerical study results and the obtained stress-strain curves are presented.

CHAPTER 2

LITERATURE SURVEY

This chapter presents some relevant literature studies of TSLs that is an overview and development of TSLs covering the field of applications, merits and demerits, previous laboratory studies of TSLs. Finally, 2D discrete element numerical modelling review and TSL test simulations are presented.

2.1.Literature Review of TSLs

2.1.1. History & Overview

Shotcrete is one of the primary means of support in underground excavations since invention of New Austrian Tunneling Method (NATM), beginning of 1970's (Mirzamani *et al.*, 2011). During the rapid technological advancements in mining industry, the improvement in mechanical properties of shotcrete became necessary. Although many researchers studied on this subject, the advances are very limited to improve these properties.

In the early 90's shotcrete was used as the liner support system of choice in mine support. By using remotely operated spraying equipment, the worker was now removed from unsupported ground conditions at the face and roof. However, implementing the necessarily large quantities of shotcrete in mines where material handling systems were restrictive due to depth and widely spread underground workings was still a problem. Therefore, for deep mines using shotcrete in mine cycle became a problem.

The objective of using TSL was to replace the loose supporting or retaining function of screen, between the primary ground support system of bolts, with a thin deformable liner (Swan and Henderson, 1999)

In the late 1980's, MIROC (Canadian Mining Industry Research Organization) initiated a detailed research with the support of the private companies, in order to develop an alternative material to shotcrete. As a result of this research, they improved the first TSL, a polyurethane-based product, Mineguard™. General definition of TSL accepted by the whole mining society is "generally cement, latex, polymer-based and also reactive or non-reactive, multi-component materials applied to the rock surface sprayed by nozzle, in a layer of generally 6 mm or less (3-5mm) thickness material".

Detailed laboratory tests about the chemical composition of Mineguard™ continued until the end of 90's (Archibald *et al.*, 1997; Archibald *et al.*, 1999). During the same years in South Africa, latex-based spray liner material, known as Everbond, was developed (Wojno and Kuijpers, 1997). These studies immediately attracted the attention of the world mining industry to TSLs. Due to the advantages such as the ease of use and the reduction in mining costs, mining companies began to prefer TSLs instead of shotcrete. In 2001, 55 different mining companies started to use TSLs for ground support purpose and this number gradually increased (Tannant, 2001).

Cost of covering an excavation with a 1mm of MasterRoc TSL 865 is 15Euro /m^2 in Turkey excluding labour and transportation etc.(BASF, 2013) A shotcrete and TSL cost comparison also can be seen in Table 2.1 Cost Comparison of Shocrete and TSL (Esterhuizen and Bosman, 2009).

Table 2.1 Cost Comparison of Shocrete and TSL (Esterhuizen and Bosman, 2009).

	4 mm TSL	8 mm TSL	25mm Shotcrete*	50 mm Shotcrete*
Total Cost (€/m^2)	10.9	16.0	14.8	17.9

The above cost does not include transportation cost

* Not fibre reinforced

Mining sector showed a great interest for surface rock support in 2000's. Three different international surface support symposiums carried out in Australia (2001), South Africa (2002) and Canada (2003), respectively. More than 70 different studies were presented ranging from laboratory to in-situ support liner performance testing, health & safety issues to case studies that reflect the current state of surface rock support technology. These publications were released during the 5th International Symposium on Ground Support in Mining and Underground Construction (Lacerda, 2004).

Currently more than 30 different TSL products are available in trading or out of trading on global marketplace. During 2nd Int. TSL Seminar in 2002, 21 different TSL products were presented in workshops. Also, Yilmaz (2009) prepared a list of TSL products either available in commercially or under developing by research and development department of companies. List of all TSL products and manufacturers are presented in Table 2.2 Available and Developing TSL Products in Marketplace. (2nd Int. TSL Seminar, 2002, Rispin and Garshol, 2003, Yılmaz, 2009).

Table 2.2 Available and Developing TSL Products in Marketplace. (2nd Int. TSL Seminar, 2002, Rispin and Garshol, 2003, Yılmaz, 2009)

Liner Name	**Manufacturer Name**
3M Liner	Minnesota Mining and Manufacturing Company (3M)
Ardumin TM 020	Ardex
Meyco TSL-865	**BASF**
Carbontech	A-Seal, V-Seal
Superseal	Cementation Lining Products (CLP)
CHC TSL	CHC
Chryso TSL	Chryso
D21H; Concor Standard TSL	CONCOR
Rockguard	Engineered Coatings Ltd.
Fosroc	Polyshield SS-100
Geo-Mining	Geo-Mining TSL
Guyric Pipe Company	GPC TSL
Hydroflex Pty. Ltd.	Diamondguard
Kohlbergerer Enterprises Pty Ltd	Polyurethane TSL
Master Builders Inc. (MBT)(Degussa)	MasterSeal 840R01A; 850C

Table 2.2 (continued)

Master Builders Inc. (MBT)(Degussa)	Masterseal CS1251; 845A; CE1286; CT1266
Minova	Capcem, Tekflex, Rapseal
Mondi Mining Supplies	Rock Hold
Nico Du Rand Consultants (NDRC)	Super lining
NS Consultancy	Ultraskin
Precrete	Rockliner A; F2; T1; 916; D50
Conseal	Pumachem CC
Tunnel Guard	**Southern African institute of Mining (SAIMM)**
Polyurea TSL	Speciality Products Int. Pty. Ltd.
Rockweb	Spray-On Plastics
Everbond; Evermine	Stratabond SA Pty Ltd (Mead Mining
TAL	TAL
Mıneguard	Urylon Plastics Canada

Note that some of the products listed above table are not currently available in marketplace due to its limited mechanical properties. Research and development departments are still working to improve mechanical properties. For example, in 2009, BASF Company had to put on hold a product, Meyco TSL- 845, and in 2011 a new product took the place of TSL-845, called TSL 865. Moreover, according to BASF authorities, next year (2014) they will introduce a new liner into the market which has outstanding features than previous products.

Recently, 3M designed a new 2-part composite polymeric TSL comprising a foam primer and a tough polymer top coat. It can be modified to meet the demands in the mining industry in terms of its strength, elasticity, toughness, and adhesion. The primer has the advantage of adhering to damp rock and the primer tends to smooth out the rock surface and seal gaps, allowing the top coat to mobilize its key physical properties such as tensile strength, elongation and toughness as the load is generated due to eventual loose rock failure. The top coat is preferably 3-4mm thick and comprised of hybrid polyurea chemistry, known for its high tensile strength and toughness. In order to form an adequate ground support, the liner requires support by a standard bolting pattern as with shotcrete and screen. (Swan *et al.* 2012)

2.1.2. Application Areas of TSLs in Underground Openings

Thin Spray on liners are traditionally used in hard rock mines, generally in Canada, South Africa and Australia. Moreover during 2000's underground coal mines have also noticed the potential benefits.

According to Saydam (2011), there are wide application areas for TSLs, which can assist to various forms of wall support. Some different researchers also pointed out these application areas (Archibald, 2004, EFNARC, 2008). TSL applications can be also implemented as a different part of underground opening as mentioned below. Those mentioned application areas are still in improvement.

- Support between rock anchors
- Supporting areas with limited access and/or logistics constraints
- Mesh replacement
- After blasting immediately supporting as a primary support
- Temporary support (before shotcrete)
- Temporary support in TBM tunnels (poor ground)
- Reduction in rock burst damage
- Pillar reinforcement
- Face support
- Large machine borehole lining and stabilization
- Stabilization of return air tunnel
- Rehabilitation
- Prevention of rock falls
- Rigid ventilation seals
- Ground degradation (weathering fretting, swelling, slaking)
- Ground alteration (moisture, heat, humidity, chemical contamination)
- Gas barrier in coal mines.

2.1.3. Advantages and Disadvantages of TSLs

According to the literature review, TSLs have many substantial advantages. In literature these advantages are divided into two different subgroups as geotechnical and non-geotechnical. The merits regards the issues such as ground stability, support performance, rock reinforcement, mechanical properties as geotechnical advantages. Operational, logistics-handling, unit cost, health and safety merits are reviewed in non-geotechnical advantages category (Yılmaz, 2011).

Geotechnical advantages can be listed as follows;

- Reducing the required bolt number, enabling bolt optimization (Tannant, 2001; Lacerda *et al.*, 2002),
- During small rock deformation (millimeters), providing active support and prevent rockfalls (Spearing *et al.*, 2000; Archibald, 2001; Stacey, 2001; Stacey &Yu, 2004),
- Improbable to blast damage (Spearing *et al.*, 2000; Lacerda *et al.*, 2002),
- Fast curing rate and reach adequate mechanical properties in few hours after application (Hannon A., 2009; Lacerda, 2004; Yılmaz, 2007),
- Relatively higher adhesion capability, bond strength, (Tannant, 2001; Pappas *et al.*, 2003; Kuijpers *et al.*, 2004; Archibald & Dridge, 2006; Lukey *et al.*, 2008, Ozturk, 2012a),
- Discardable rebound amount and wastage during spraying process (Smith, 2012; Spearing *et al.*, 2009; Lacerda, 2004),
- Providing a barrier against gas, moisture degradation and radiation leaks, (EFNARC, 2008; Archibald & Drige, 2006; Potvin, 2002),
- Wide displacement range (elongation ratio), (Tannant, 2001; Archibald & Dridge, 2006; Pappas *et al.*, 2003; Lukey *et al.*, 2008; Kuijpers *et al.*, 2004),

Non-geotechnical advantages can be listed as follows;

- Ease of application and fast application rate (Pappas, 2003; Tannant, 2001; Lacerda, 2004; Yılmaz, 2011; Saydam, 2011; Ozturk, 2011),

- Spraying with small equipment (Pritchard *et al.*, 1998; Tannant, 2001; Laurance, 2001),
- Not any damaging effects to processing equipment (crusher, mill etc.) (Yılmaz, 2009),
- Improvement in the illumination of working area (reflection of light due to its color) (Potvin, 2002; Tannant, 2001),
- Less material handling with respect to other ground support products (logistic benefits) (Tannant, 2001; Archbald, 2001; Steyn *et al.*, 2008; Pappas, 2003),
- Reducing the cycle times in underground operations (Steyn *et al.*, 2008; Archibald, 2001; Smith, 2012),
- Reduction in the risk of accidents, increases the safety of working environment (Hannon, 2009; Archibald, 2001; Smith, 2012; Archibald & Dridge, 2006; Pappas, 2003),
- Decrease in the operating costs (Tannant, 2001; Yılmaz, 2009; Smith, 2012; Spearing *et al.*, 2009),
- Applicability of the material in thinner thicknesses with respect to other surface support systems (Archibald, 2001; Tannant, 2001; Spearing *et al.*, 2009; EFNARC, 2008; Pappas, 2003; Pritchard *et al.*, 1998; Ozturk, 2011).

Despite the mentioned merits, there are also few disadvantages of using TSL that are claimed by some researchers. Major demerits are as follows;

- Mechanical properties of TSLs are directly related to mixing ratio; and in U/G openings it is hard to achieve proper ratio between mixing components of TSL,
- Small deficiencies such as tear on the surface of the TSL because of blasting operations or tear from underground equipment operations can cause the crack propagation on the whole liner.
- Dust, diesel fumes and oil, decrease bonding capability of TSL to substrate. TSL bonding needs clean surface before application (Yılmaz, 2011; Archibald, 2001; Tannant, 2001; Spearing *et al.*, 2001; Ozturk, 2005; Ozturk, 2012)
- Direct exposure of TSL may leads to allergic sensitization (Archibald, 2001), health and safety might be a concern for some TSLs (Boeg- Jensen, P. 2013)

- The support mechanism of TSL is not fully understood (Archibald, 2001; Kuijpers *et al.*, 2004)
- Shelf-life of TSLs are relatively low (3-12 months) due to chemical ingredients,
- Constitutive behaviour of TSLs are not well understood (Wang and Tannant, 2001)
- TSLs might show creep and viscoelastic properties which has not been studied extensively, there is only limited data on this issue (Ozturk, 2012b; Ozturk and Tannant, 2007)

2.2. Previous Laboratory Testing of TSLs

Over the last decades, various types of laboratory and in-situ tests have been conducted in order to better understand the properties and interaction behavior of TSLs with rock. Detailed reviews of previous laboratory tests are conducted by Potvin *et al.*.(2004). They classified laboratory tests into 2 groups as chemical and mechanical. Flammability and durability tests are listed as chemical tests. On the other hand, mechanical tests are divided into 2 subgroups namely, small and large scale. Tensile, adhesion, coated core, tear, UCS, core to core adhesive bond strength test can be listed as small scale tests. Figure 2.1 represents the schematic view of classified test types of TSLs (Modified after Potvin, 2002)

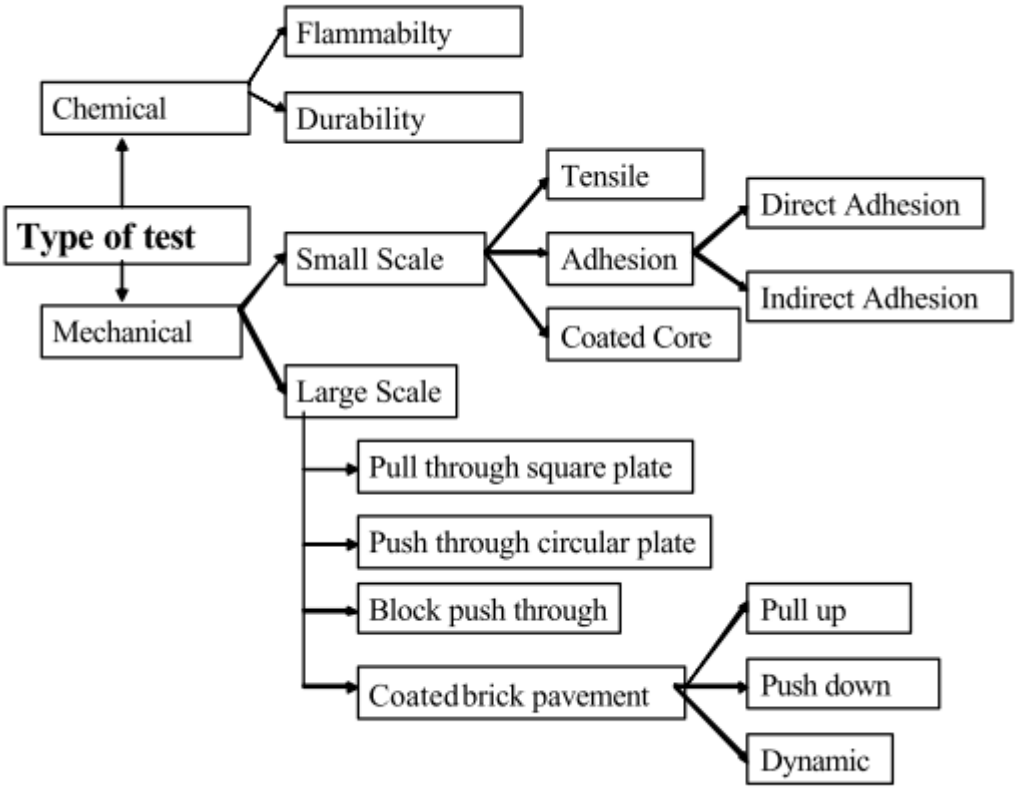

Figure 2.1 Classification of Test Types for TSLs (Potvin, 2002)

TSL society is mainly focused on the following laboratory tests;

- Tensile strength & elongation (Tannant *et al.*, 1999; Archibald, 2001; Spearing and Gelson, 2002; Yilmaz, 2011; Ozturk, 2011)
- Uniaxial compressive strength (Ozturk, 2011),
- Punch (Spearing *et al.*, 2001; Kuijpers, 2001; Stacey and Kasangula, 2003),
- Bonding strength (Lewis, 2001; Spearing, 2001; Tannant and Ozturk,2003; Yilmaz, 2011),
- Double sided shear strength (Saydam and Stacey, 2004),
- Plate pull (Tannant *et al.*, 1999; Archibald, 2001; Finn, 2001),
- Linear block support (EFNARC; 2008),
- Gap shear load test (EFNARC; 2008),
- Coated core compression tests (Espley *et al.*, 1999; Archibald and DeGagne, 2000; Kuijpers, 2001).
- Large scale laboratory loading (Zhenjun *et al.*, 2014)

Among them, only two of the small scale test methods gained the acceptance in TSL society so far. These tests are tensile (elongation) and tensile-bond (adhesion) strength tests (Kuijpers *et al.*, 2004).

As it is mentioned in the previous chapter, the laboratory studies of this thesis consist of two different tests, tensile and compression. Therefore, the literature review is only focused on these tests and the theory behind them.

2.2.1. Relevant Literature on Tensile (Elongation) Test

Tensile strength test is the most frequently used test among all. In underground openings the cracks may form due to highly stressed ground, stress relieved ground, blasting, seismicity, etc. Crack dilations and outward movements along cracks play an important role in tensioning TSL, as seen in Figure 2.2. When a crack contacts with an adjacent or pre-existing weakness planes, wedges or blocks would be formed. Depending on the orientation of cracks and the shear strength characteristics of the weakness planes, the rock blocks may become loose and fall down especially from the roof and sidewalls of the excavation due to gravitational force (Yılmaz, 2011)

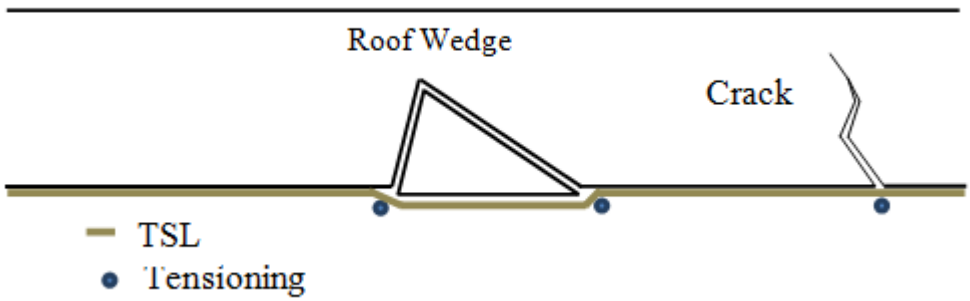

Figure 2.2 Tensile Load Mechanism in Underground Opening (Yilmaz, 2011)

Most of the researchers have selected this test methodology as a primary liner characterization test (Kuijpers *et al*., 2004). In addition to tensile strength of TSL, other material properties related with tensile failure such as the tensile modulus, elongation capacity or tensile extension at failure can also be found in the scope of this test.

TSL tensile test was firstly conducted by Tannant *et al.* (1999). They used the Standard Test Method for Tensile Properties of Plastics (ASTM D638, 1998) for test set up and testing progress. (Detailed information for this standard will be explained in Chapter 3). They recommended the usage of Type I specimen dimensions based on their experience.

In 2001, Archibald carried out tensile tests for 4 different TSL products. He suggests that at least 10 specimens should be tested for each material and tests should be conducted at the end of the 7th curing day. Moreover, he also followed ASTM D-638 standards in his study. He measured the displacement change during tests and investigated tensile strength, elongation capacity, modulus of deformation for 4 different products having different thickness range.

Spearing and Gelson (2002), Ozturk (2011), Yilmaz (2010) also conducted similar tests. Ozturk, (2011) conducted tensile test for 2 different products with 7 days cured samples. As a result of this study, he concluded that extensive studies were necessary to determine the elastic properties of TSLs.

The most detailed TSL tensile test study in literature is conducted by Yilmaz (2010). He carried out tests for 20 different TSLs and 1 shotcrete sample. Moreover in this study, effect of curing time was examined by testing each liner in curing interval of 28 days. As a result of this study, it was concluded that the tensile strength grows up with increasing curing period. Moreover, one of the significant contributions of this study was the strength development categorization part. According the results obtained from the laboratory tests, Yilmaz (2010) categorized TSLs' strength development into 4 different groups namely, weak, medium, strong and very strong based on tensile strengths.

One of the biggest issues with the previous testings are the way of measuring the displacement of the specimen under tension. Although, the standards (ASTM D-638) states that the displacement of the gauge length of the specimen has to be measured,

researchers has not taken this into account either because of practical difficulties in measuring displacement of this portion of the sample or because of not having proper extensometers or because of the lack of knowledge of these standards. For the first time in this study, proper measurements of the gauge length displacement is carried out during tensile tests.

In addition, although some researchers did some analytical and numerical solutions on the TSLs' support mechanism assuming TSL behaves linear elastically (Mason and Stacey, 2008; Mason and Abelman, 2009; Fowkes et al., 2008; Wang and Tannant, 2002; Dirige and Archibald, 2009), there is not enough information in the literature regarding the other important mechanical properties of TSLs; such as, Young's modulus, elongation ratio, Poisson's ratio, cohesion and internal friction angle etc. This thesis study will also present these properties of TSLs.

Previous studies offer very similar test set-ups and specimen dimensions as suggested standard (ASTM D-638, 1998). Figure 2.3 shows the test set-ups of some previous studies.

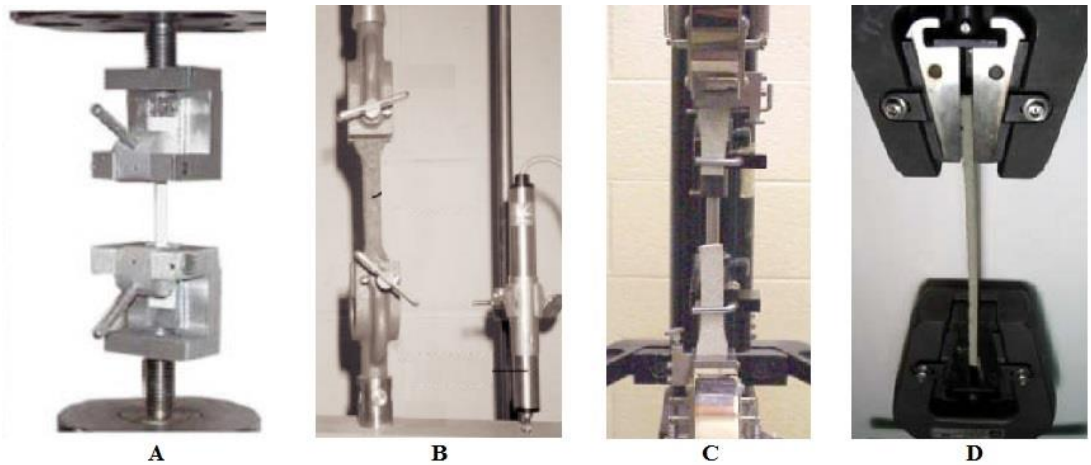

Figure 2.3 Previous Test Setups and Specimens (A: Archibald, 2001, B: Tannant, 1999, C: Spearing and Gelson, 2002, D: Ozturk, 2010)

2.2.2. Relevant Literature on Compression Test

Unfortunately, very few studies were conducted on compression tests of TSLs. The reason why compression studies are not interested in the literature is that it is believed that TSL does not experience compressive forces during its support function. Researchers mainly focus on in-situ loading mechanism of TSLs as being tensile loading. However, in recent studies, TSLs are modelled numerically in order to understand the support mechanisms; and these studies requires some elastic input parameters such as unconfined compressive strength, modulus of elasticity, Poisson's ratio. Compression test is the only way to find out these parameters.

In the literature only two studies are conducted in this field. Ozturk (2011) performed UCS tests for two different TSL products with 7 days cured samples. In this study, cylindrical test specimens were prepared with 38 mm diameter and 87 mm length. At the end of the 7th curing day, samples were tested under 2mm/min cyclic loading. Figure 2.4 shows the test setup of the experiment. During the tests, load, axial and lateral displacement were recorded and elastic material properties were found. Consequently, Ozturk (2011) suggested that more experimental studies are necessary to determine the actual elastic parameters of TSLs.

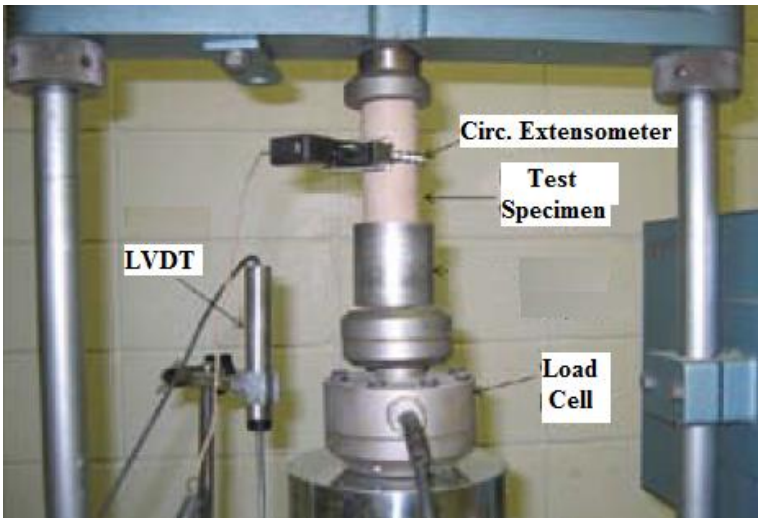

Figure 2.4 Compression Test Setup (Ozturk, 2011)

Mpunzi (2012) conducted different laboratory tests for three different types of TSL, namely, Brazilian, compression, three point bending strength. The major purpose of this study was the investigation of the failure mechanism behavior of liners for rock support through laboratory tests. The weakest point of the study is that this testing method is not used in literature before. Therefore, it does not point out any standard testing technique. As a result of compression tests, he focused on the dependency of maximum strength value over curing time and as expected, increasing curing time also improved the maximum strength value of specimen.

Although this testing method was not mentioned in the previous literature section, the results showed analogousness to previous tensile tests. The study set-up had not adopted from any standard testing methods.

2.3.Literature Review of Numerical Modelling of TSLs

Although there are many numerical modelling for many different types of materials; such as, rocks, soils, and plastics in the literature, only few of them are about TSLs. The constitutive behaviour of TSLs are not well understood. Some researchers (Mason and Stacey, 2008; Mason and Abelman, 2009; Fowkes et al., 2008; Dirige and Archibald, 2009) assumed linear elastic behaviour for these materials. However laboratory and field experience shows that most of TSLs behave linear elastic up to some load then it becomes ductile and visco-elastic (Ozturk, 2012; Tannant 2011). Therefore, continuum modelling of TSLs might not be true for all of liners. For this reason, PFC modelling which uses discrete element method were assumed to be appropriate for TSL modelling (Tannant & Wang, 2003).

Tannant and Wang (2003) modelled thin tunnel liners with particle flow code, PFC2D (Itasca, 1999). PFC2D models materials assumed that they are composed of small discs connected with bonds. During their study, model calibration was initially conducted. They simulated laboratory tensile tests and coated block punch models in order to reproduce the peak strength, the elongation at peak strength and stress strain curve path obtained from a tensile test on a TSL material.

As a result of the model calibration, they found material input parameters to be used for tunnel modeling of TSL with PFC. Table 2.3 Shows result of calibration study.

Table 2.3 TSL Tensile Test Calibration Results (Tannant and Wang, 2003)

TSL Tensile Test Calibration PFC2D Input Parameter	
Min. particle radius (mm)	0.75
Max. particle radius (mm)	1.25
Liner model thickness (mm)	25
Friction coefficient	0.25
Particle density (kg/m^3)	1,500
Material porosity	0.2
Particle-particle contact modulus (MPa)	0.5
Particle normal/Shear stiffness ratio	1
Mean contact bond and shear strength (MPa)	0.5

As a result of the test simulations, Tannant and Wang (2003) mentioned that more sophisticated PFC2D models were required in order to obtain the full shape of the stress-strain or load-displacement curve for a TSL material. Moreover, as a result of tunnel modelling at PFC, they observed that TSL had very little effect on the generation and growth of fractures in the rock around the tunnel; and TSL was able to control and decrease rock displacements around the tunnel. In other words, a liner could be considered helpful to maintaining the overall structure of rocks.

Harding (2008) performed a study to simulate the modified double sided shear and the coated core compression tests of TSLs in FLAC software. He reached similar failure patterns for simulations in modified double sided shear test as observed during laboratory tests. On the other hand, coated core simulation results did not demonstrate a good correlation.

Another publication with this subject was by Richardson and Saydam (2009). This study was about the bending and double sided shear test simulations by FLAC software. The major purpose of the paper was to find a quantitative parameter which would enable to compare TSL products and to investigate support mechanisms of the liners. As a result of this study, bending test model was not compatible with the

laboratory studies. However, the double sided shear test required finer calibration and more detailed studies in numerical modelling; and finally they focused on the great research potential of numerical test simulations of TSLs.

Dirige and Archibald (2006) studied on the support potential of TSLs in highly stressed and rockburst prone rock conditions by numerical modelling (FLAC3D). During this study, they constructed a tunnel model supported with TSL and shotcrete respectively. Typical input parameter of liner is presented in Table 2.4.

Table 2.4 Model Input Parameters of a TSL (Dirige and Archibald, 2009)

Properties	**TSL**
Modulus of Deformation or Young's modulus, (MPa)	111.69
Tensile Strength (MPa)	8.92
Cohesion (MPa)	8
Internal Friction Angle (Deg.)	35
Density (kg/m^3)	1,050
Shear Modulus (MPa)	39.89
Bulk Modulus (MPa)	186.15
Poisson's Ratio (ν)	0.4

In addition, Ahn (2011) modelled TSL using ABAQUS assuming the properties given in Table 2.5

Table 2.5 TSL ABAQUS Model Parameters (Ahn, 2011)

Parameter	**Value**
Initial tangent elastic modulus (E)	100 MPa
Poisson's ratio (ν)	0.3
Density	1100 kg/cm3
Initial yield stress	5.5 MPa
Tensile failure stress	8 MPa
Model behaviour	Elastoplastic strain-hardening

Moreover PFC2D is also commonly used in simulation for rock mechanics tests. Following literatures are related with rock mechanics test modelling.

Tannant and Wang (2007) used PFC2D to model uniaxial and biaxial tests on oil sands.

Xia *et al.* (2009) studied uniaxial compressive strength test simulation of brittle rock on PFC2D software. They succeeded simulation on 2 different UCS tests of brittle rocks. Obtaining a 99% correlation with the laboratory results.

In the literature assumed mechanical properties of TSLs are shown in Table 2.6

Table 2.6 Assumed Elastic modulus and Poisson's ratio parameters in the literature

E (MPa)	**ν**	**Source**
100, 1000	0.40, 0.30	Mason and Stacey, 2008
111	0.40	Dirige and Archibald, 2009
1000	0.30	Mason and Abelman, 2009
100	0.30	Ahn, 2011
13	0.25	Ozturk, 2011

CHAPTER 3

TSL TESTING

This chapter presents two different testing methodologies for compression and tensile tests of TSLs. First of all, detailed information will be given about the tested TSLs. Then, significant test parameters will be detailed according to the methodology of the testing. Finally, test standards, procedures, calculations and results of the TSL tests for tensile and compression test will be presented.

3.1 General Information about the TSLs Tested

The laboratory tests are conducted on two different, widely used TSL products. Moreover, when selecting the products it was also focused to obtain different chemical compositions in order to observe the importance of ingredients of products. According to the literature review, MasterRoc® TSL 865 (Formerly MEYCO® TSL 865) produced by BASF Company and Tunnel Guard produced by South African Mining & Engineering Supplies Company are selected. This part presents important features of the selected products.

3.1.1 Liner 1: MasterRoc® TSL 865 (Formerly MEYCO® TSL 865)

BASF's currently available TSL product was known as a name of MEYCO® TSL 865. However, the company modified the name of the liner in October 2013 as MasterRoc® TSL 865.

Liner 1 is a one-component polymer based powder for spray application on rock or coal faces for surface support and protection against many conditions, especially weathering problem. Company claims that the liner has high elasticity, tensile strength

and improves ground stability due to polymer component. Moreover, sprayed concrete or shotcrete can be applied on the membrane. One of the most beneficial sides of the liner is about its setting time. Laboratory tests proved that the setting of the mixture takes few minutes. Besides the curing time benefit, this liner has a great ability to bond rock, concrete and coal it also has no safety issues regarding toxicity. However, the thesis study is mostly focused on tensile and compressive properties of the material.

Amount of TSL application is determined as 1 kg of dry powder per square meter and per mm thickness as advised by the manufacturer. Product consumption generally depends on surface roughness of the applied face. Suggested mixing ratio amount of the polymer powder is twice of the water by weight, mixing and application can be done by a single operator (Figure 3.1). Detailed technical data and safety information are given in Table 3.1. Polymer powder composition is as follows;

- 10.0 - 30.0 % Limestone
- 10.0 - 30.0 % Calcium oxide
- 7.0 - 13.0 % Cement, alumina, chemicals*
- 1.0- 5.0 % Kaolin
- 0.1- 1.0 % crystalline silica (percent of weight)

*Due to confidential items, ingredient chemicals are out of public sharing.

Shelf life can be considered as a drawback for this product. Suggested shelf life is about 12 months for 20-25 kg packages for under 40° C storage conditions. Moreover, it is also stated that opened packages should be consumed within a week.

Figure 3.1 Application & Applied Face of Liner 1 (retrieved from BASF, Turkey)

Table 3.1Technical and Safety Information of Liner 1 (BASF, 2013)

Form	Powder
Color	White
Bulk Density (g/L)	690 ±90
Consumption	0.9 kg/m^2 per mm
Application Thickness	2 to 10 mm
Application Temperature	5-45 °C
Tensile Strength (MPa)	
After 4 Hours	> 0.20
After 1 Day	> 0.40
After 7 Days	> 2.00
After 56 Days	> 5.00
Elongation at Break (%)	
After 4 Hours	> 100
After 1 Day	> 50
After 7 Days	> 60
After 56 Days	> 30
Bond Strength to Concrete After 14 Days (MPa)	1.7
Flammability	Self-Extinguishing
pH Value	About 11

3.1.2 Liner 2: Tunnel Guard

The major application area of the liner is generally on deeper tabular gold deposits in addition to various ranges of minerals such as platinum, diamond and copper for both structural support and weathering protection in South Africa (Spearing *et al.*, 2009).

This liner was shipped from Johannesburg, South Africa to METU by the manufacturer.

Liner 2 is a Portland cement-based mixture in combination with a polypropylene fiber additive that exhibits excellent binding, sealing and structural support characteristics. It is packaged in a 25 kg of 2 units powder and 1 unit liquid form (Figure 3.2). Three components are mixed all together with the help of a portable pump, which also has ability of spraying the mixture on to the surface. Due to the cement ingredient of the product, setting time can take a longer time (few hours) than the previously discussed TSL product. Compositions of mentioned three components are not shared by the manufacturer.

Figure 3.2 Mixing Components of Liner 2.

Mixing ratio of components is as follows;

- 49-51 % Cementitious Product (with polypropylene fiber)
- 29-31 % Aggregate (silica sand)
- 18-20 % Binder Liquid (synthetic latex, water)

Application rate is also significant merit for this product. If preparation of host rock is suitable for the application, 200 square meters wall can be covered in one shift. This enables the very high speed development. (South African Mining & Engineering Supplies cc., 2006)

The preparation of the opening wall is explained by the company as: “It is imperative to wash down the rock surface of all dust and it is also necessary to bar down any

larger loose rocks to improve application safety. When the surface cannot be washed down the dust needs to be blown off using compressed air to ensure maximum bonding." (South African Mining & Engineering Supplies cc., 2006). All given mechanical properties are only valid for correctly prepared surfaces. Figure 3.3 shows the photos of before and after the Liner 2 application.

Shelf life is almost the same with the previous liner that is about 12 months within standard storage conditions. Moreover, this liner is twice as denser than Liner 1. Almost 2.1 kg of dry powder per square meter and per mm thickness can be utilized as a guideline. Product consumption generally depends on the roughness of applied surface. Detailed technical data and safety information are given in Table 3.2.

Figure 3.3 Liner 2 Application (Left: Just Before, Right: After) (South African Mining & Engineering Supplies cc., 2006)

One of the weakest properties of this liner can be considered as the limited elongation capability due to cement component. On the other hand, this cement component provides enhancement for the strength value of the product.

Table 3.2 Technical and Safety Information of Liner 2 (South African Mining & Engineering Supplies cc., 2006)

Form	Powder, Powder and Liquid
Color	Grey, sand colored, dark brown
Bulk Density (g/l)	2010 (mixed components)
Consumption	2.08 kg/m^2 per mm
Application Thickness	3 to 5 mm
Application Temperature	5-40 °C
Tensile Strength (MPa)	
After 1 Day	> 3.17
After 2 Days	> 3.98
After 7 Days	> 3.81
After 31 Days	> 4.70
Compressive Strength (MPa)	32.50
Flexural Strength (MPa)	4.30
Bond Strength (MPa)	3.75
Shear Strength (MPa)	17.90
Odour	Odourless, slight ammoniaca
Flammability	Non-flammable
pH Value	About 7 (mixed components)
Water Solubility	Partially soluble

3.2 Test Parameters

Laboratory testing is a labor intensive process since innumerable parameters should be considered during all the stages of testing and specimen preparation. Suggested testing methodologies for polymers and shotcrete and their standard parameters are utilized in the scope of TSL testing. In addition, some other factors that can be underestimated in the evaluation of shotcrete or polymers are also included for laboratory assessment of TSL. Some significant parameters are explained in the sub-topics.

3.2.1 Chemical Composition

As mentioned before, TSLs are composed of mixture of powder-water or powder-liquid. Chemical composition of dry powder can directly affect the mechanical properties. Cement-based TSLs are expected to fail in higher loads since cement is

known with limited elongation capacity. This property causes brittle load-displacement behavior for cement based TSL.

3.2.2. Shelf Life

TSLs have different material specifications compared to shotcrete. Shotcrete has long shelf life under dry and warm conditions. However TSLs have only few months or at most 1 year shelf life. Moreover, available TSLs are in 20-25 kg packages in market and expire date is about 2 weeks after the package opened. This will cause time restriction in utilization of TSLs for researchers. A researcher should be very careful for material expire date in laboratory studies to obtain admissible results.

3.2.3. Mixing Ratio

Generally, each liner should be mixed in constant ratios to ensure the manufacturer's suggestions. In field applications, TSLs are mixed by special equipment. In laboratory studies, this mixing equipment cannot be used since small scale of TSL quantities are utilized in laboratory conditions compared to field applications. Therefore, different mixing options were adopted for this purpose in the literature. In the previous studies, researchers mixed TSL materials by 3 different ways: (i) Initial trials are done by hand mixing. However since settling time is very short in some TSLs, this method is not applicable for mixing. (ii) The second mixing device is a kitchen mixer. Researchers widely used kitchen mixer due to multi-functional mixing velocity option. Even in low rotational speeds, kitchen mixers can cause bubbling and therefore air entrapped in the TSL mixture. However, kitchen mixers can have inability of mixing dense compositions due to insufficient motor power. (iii) Bit attachment for a power drill mixer can be used in the cases where the mixture is too dense. Strong motor mixing dense materials efficiently. In addition, this tool have ability to prevent vortex occurrence in less dense mixtures by using slow rotational speed option.

Mixing time varies for every product, i.e. 60-90 seconds with medium rpm speed for Liner 2, 4 minutes mixing with slow rpm speed for Liner 1. Since Liner 1 has low

density, mixture of it tends to cause a vortex and air bubble in the process. Slowest rpm speed is selected to have homogenous mixture of the material.

3.2.4. Laboratory Conditions

One of the major purposes of this thesis is to try to mimic mining environment in the laboratory. However, according to the laboratory studies it is observed that TSLs are very sensitive to laboratory environment such as temperature, humidity. Since numerous testing are carried for different curing time, these parameters should be kept constant, as much as possible, during required curing time and testing. Yılmaz (2011) mentioned about the optimum TSL laboratory conditions for temperature and humidity. Researchers used 22ºC-28ºC for temperature and 50%-60% range for humidity. Also, specimens should not be exposed to airflow and direct sunlight. Although there is also need for researches in assessment of temperature and humidity effects in TSL testing, this thesis study mainly focuses on curing time change within room temperature and humidity condition.

3.2.5. Shrinkage

It is observed that generally water based testing samples are prone to shrinkage during the curing time because of its water content. Due to evaporation, dimensions of the specimens decrease and it can result in bending. Shrinkage is an inevitable problem for such samples. Bend samples cannot be tested, because test specimen should be symmetrical for both tensile and compression tests.

Since Liner 1 is a water based product, shrinkage problem arises during sample preparation steps. Figure 3.4 shows standard (top) and shrunk test specimen (bottom).

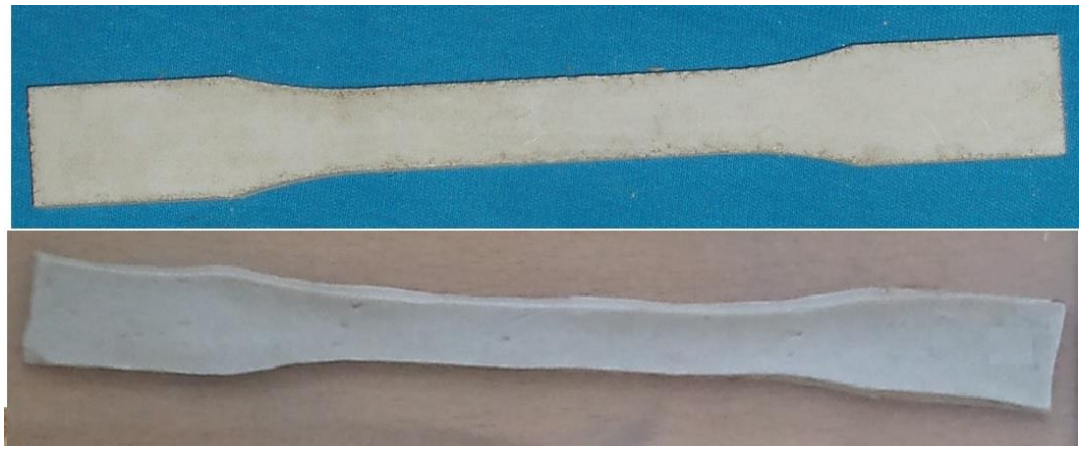

Figure 3.4 Standard and Shrunk Test Specimens

Each sample dimension should be re-measured at the end of the curing time when test samples are molded or stamped according to standards. Some small variations in the dimensions up to 10 % shortening may be acceptable.

3.2.6. Test Specimen Dimensions

There are many factors affecting the selection of optimum test specimen. Test specimen should be representative, cost effective, easy to prepare, compatible with testing machine. Some standardization organizations, ASTM, ISO etc. have published various test standards for different types of materials and suggested standard sample dimensions.

Since TSLs are relatively new product there is not any standard testing methodology yet. Previous researches on TSL testing used mostly modified standard test methodologies for plastics in order to conduct tensile tests.

Previous researchers modified ASTM-D638 test standard for tensile testing purpose. Two different specimen dimensions were used in previous studies namely, type I and type IV. These specimen shapes and dimensions are presented in Figure 3.5.

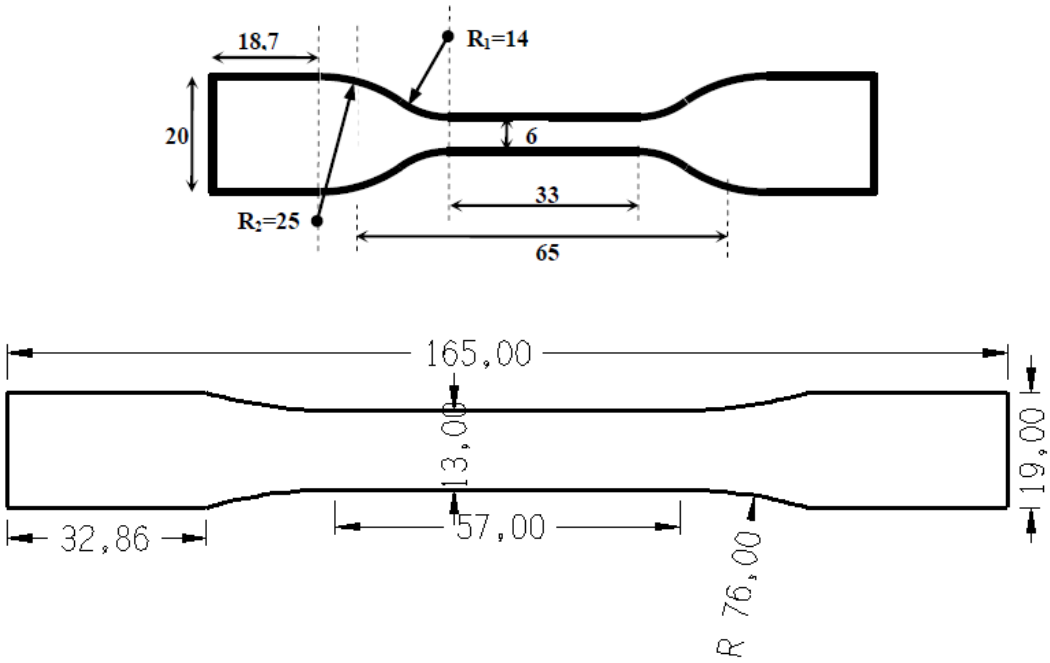

Figure 3.5 Type I (Bottom) & Type IV (Top) Specimen Dimensions in mm.

Specimen thickness of tensile test is directly related with application thickness of TSL. Since general application thickness is about 3-5 mm in field, researchers prepared 3-5 mm thick samples similarly. In this study, 4 mm sample thickness is selected.

Moreover, thickness uniformity is another important measure. Sample should be prepared with uniformly.

3.2.7. Curing Time

Curing time is defined as the period of time for proper setting of the material. This statement is commonly mentioned in studies for thermoplastics and cement materials. In TSL society, researchers are defining curing time as “time elapsing from the completion of specimen preparation to testing” (Yilmaz, 2006).

As mentioned in the previous chapters, one of the objectives of this study is understanding the effect of curing time to mechanical properties. In this sense, curing time varied 1, 7, 14, 21 and 28 days for tensile test and 2, 7, 14, 21 and 28 days for

compression test. Previous studies show that mechanical properties of TSLs are strongly depend on curing time.

3.2.8. Load Rate

During the laboratory studies, relevant load rate standards are applied. Each standard has its own loading rate. Load rate has significant effect on testing time. When performing a laboratory test, for validity and the acceptance of study, researchers should apply each specification of standard testing methods. Suggested and applied load rates will be stated in the following part of this chapter.

3.2.9. Specimen Number

Test procedure should be repeated more than one time to validate the results statistically. Number of the trials is specified in between 3 and 5 according to the literature studies. Conducted test per each curing time is 5 valid trials.

3.2.10. Outlier Test

Test results acquired in the experiments can be out of expected ranges, in very high or very low values. This resultant data can be due to improper test conditions and they should be detected and eliminated using outlier tests. Since only 5 trials were done for each curing time, most of the outlier test are unavailable due to limited number of tests.

Q test by Dean and Dixon (1951) is practically used for chemical experiments with small trials as the trials in this study. Q value is a ratio defined as the difference of the suspect value from its nearest one divided by the range of the values as giving in the following equation:

$$Q = \frac{X_{2nd\ min} - X_{min}}{X_{max} - X_{min}} \qquad [3.1]$$

If the calculated ratios for each test value are above the limits stated in Q test table according to confidence intervals and sample sizes, these values are called as outlier.

For confidence intervals with 90 %, 95 % and 99 %, Q values are obtained as 0.642, 0.710 and 0.821, respectively. Detection and elimination of outlier data from the sample space gave opportunity to obtain higher R-squared values which provides higher correlation and more sensitive plots between the variables.

3.3 Tensile Testing

As mentioned in the previous chapters, tensile test is most widely used mechanical testing method for surface support liners among TSL society. Unfortunately, the number of publications on this issue is limited (Yilmaz, 2011). During previous studies (Tannant *et al.* (1999), Archibald (2001), Spearing and Gelson (2002), Ozturk (2011), Yilmaz, (2011)), researchers made reference to ASTM D638 in their tensile testing studies since there is not any accepted standard for TSLs. This standard is originally having been published for determination of the tensile properties of unreinforced and reinforced plastics with defined test conditions. As TSLs are generally polymer based products, this testing methodology can easily be adopted. Moreover, International Organization for Standardization (ISO) has also very similar test standards called as ISO 527. However, this study again follows the methodology considering ASTM standards similar with the previous literature researches.

The following parts present important factors, test set up, calculations and results of tensile tests.

3.3.1 Test Standard & Procedure

In order to prove the validity of the conducted tests, standard testing methods should be followed step by step. Since TSL tests are not usually performed in mining engineering applications, a detailed summary of test standards will be discussed under this chapter. As stated in Chapter 1, this study is based on 2 different laboratory tests of 2 different TSL materials as tensile and compressive tests.

In tensile tests, 2 different test standards, ASTM and ISO, are accepted laboratory standards. Since ASTM standards are widely used in the previous studies, in this study ASTM standards are preferred as the base of the experiment procedure, to be able to compare the results of this study with the previous researchers results.

10 important test parameters were already explained in Chapter 3.2. Standard testing methodology also covers some additional parameters that will be necessary for the correct explanation of TSL characteristics. These parameters are discussed as follows;

- Testing machine should have a constant loading rate between grips; one grip should be fixed and other should movable member.
- 4 different test specimens are described, generally type I specimens are preferred among TSL society. However, type IV specimens can also be selected especially for testing of higher elongation capacity specimens. Specimen dimensions can be seen in Figure 3.5.
- Even testing material is isotropic material; at least 5 different valid tests (for each curing time) should be performed in order to ensure the validity of tests. Moreover, test specimens should break in narrow cross-section, otherwise the test should be discarded.
- Test specimens can be prepared by machining operations like die cutting or molding process. However, test specimen should be symmetrical and thickness should also be uniform. Otherwise, unexpected failure zones can be observed, that makes the test invalid.
- Load rate should be in 5 to 50mm/min range (ASTM D-638-10)
- Best testing condition is suggested as 23°C and 50 % relative humidity for tensile testing where specimen thickness is less than 7 mm. Moreover, during tests of different specimens, temperature and humidity should be kept constant.
- Dimensions of test specimens should be re-measured just before test.
- At the beginning of the test, specimen should be placed between grips in vertical alignment; misalignment may cause progressive failure. Figure 3.6 shows the importance of specimen alignment. Specimen axis and machine

pulling direction should be as shown with Figure 3.6-A. On the other hand, the alignment as in Figure 3.6-B causes progressive failure.

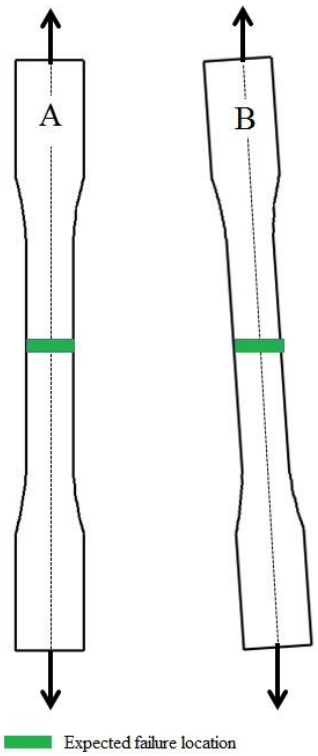

Figure 3.6 Importance of Specimen Alignment.

- During test, load and displacement values should be recorded continuously. Displacement should be measured from the gauge length of the test specimen when the specimen is stretched. During the calculation part, stress versus strain curve should be plotted. Tensile strength, modulus of elasticity, elongation ratio and some other important material properties can be obtained with the help of this curve.
- Finally, failure should be in the gauge section of the sample. If the specimen fails out of this section, test should be discarded.

3.3.2 Sample Preparation

Specimen preparation is also one of the most important steps. Though it seems easy to prepare a test specimen, there are some difficulties encountered in this step. Test specimens should be representative of the field application, identical and conforming described test standards.

In order to obtain homogenous test specimens, all test specimens were prepared in one mixing progress. TSL products are available in the market with different packaging; and it is prepared by mixing with water or different solutions, using mixing and spraying machine in application area under the manufacturer's suggestion. Such a mixing and spraying procedure is not practical for small-scale sample preparation in a laboratory. Therefore, power drill mixer with different rpm speeds and bit attachment is utilized for sample preparation as discussed in section 3.2.3. According to the manufacturer suggestion, each TSL material is prepared with a different mixing ratio.

Figure 3.7 Power Drill Mixer and Bit Attachment

Liner 2 can be mixed in any rpm level due to its chemical composition. However, during sample preparation of Liner 1, standard rpm speed causes vortex occurrence in water-powder mixture; and this vortex leads to air bubbles in the mixture. Air bubbles decrease the actual cross-section area of the specimen and cause failure of the

specimen in underestimated levels during tensile testing. This problem is eliminated by adjusting the drill machine speed to the lowest level.

After few minutes of mixing procedure, mixture gets ready for molding. As mentioned before, there are two approaches to prepare specimen as molding and die cutting. Die cutting is easier way to prepare specimen. However, in some rigid materials (Liner 2), this process might damage the specimen. Molding and die cutting methods can be viewed in Figure 3.8. Moreover, it is sometimes hard to remove specimen from the casting mold since TSLs have higher adhesion capability, during molding process. An additional releasing agent; such as, thin machine oil or special product for this purpose, should be used to prevent bonding of specimens to steel or perspex molds.

Figure 3.8 Die Cutting (Left) & Molding (Right) Process

Setting time of mixture should be considered as another significant issue. Liner 1 has a very short setting time, about 5 minutes, therefore molding process should be done as fast as possible.

Plastic flat working sheet should be placed under the perspex or steel casting mold, in order to satisfy thickness uniformity of test specimen. Glass working surface should not be preferred, due to higher bond capability between TSL and glass. Initial trials were performed by using glass working surface without any releasing agent. As seen in Figure 3.9, removing of specimen for glass surfaces is almost impossible.

Figure 3.9 Difficulties of Removal of the Specimen

Also, casting is carried out by pouring homogenous mixture on perspex mold. Dog-bone shape mold set-up and poured-levelled mixture of Liner 2 can be seen in Figure 3.10.

Figure 3.10 Just Before and After Molding Process

Unlike the previous studies, in order to satisfy exact field conditions, top of the mold was not covered with another plastic sheet. This enables the top surface of specimen being in contact with air during curing period. Therefore, top of the Perspex mold should be levelled with the help of a plastic spatula.

At the end of the curing time, test specimens are removed from the plastic or steel molds. Since releasing agent is used before the process, unmolding operation of the specimens does not face with any difficulties. Finally, small undesired parts at the edges of the specimens should be cleaned with a knife to ensure that the specimen has exactly the same dimensions as suggested standard as shown in Figure 3.11.

Figure 3.11 Cleaning of Unwanted Extensions

During sample preparation, 40 test specimens are molded for each product. 74 different tensile strength tests are conducted during this study. As emphasized, at least 5 valid tests are required for the investigation of 5 different curing time. 10 extra dummy specimens are prepared in case of having discarded specimens to obtain 25 valid test results per product. Table 3.3 shows the amount of conducted tests for each curing time.

Table 3.3 Conducted Test Amounts in Tensile Testing

	Liner 1						**Liner 2**					
Curing Time (Days)	**1**	**7**	**14**	**21**	**28**	**Total Number of Tests**	**1**	**7**	**14**	**21**	**28**	**Total Number of Tests**
Number of Tensile Tests	6	6	7	6	8	33	6	8	8	9	11	40

Testing Apparatus and Test Set-up

Although direct tensile test is not commonly used in Rock Mechanic tests, Middle East Technical University, Rock Mechanics laboratory has a direct tensile testing machine. Machine has 2 different loading rate options as slow and fast. Tests are conducted under slow strain option which is about 6-7 mm/ min and maximum measurable load capacity is about 500 kgf. Moreover, machine also has an analogue load indicator.

During the tests, this testing machine is modified in order to record data continuously by a data acquisition system which has a data reading rate of 8 data per second. Load

amount is measured by S-type tensile load cell with 500 kgf maximum capacity. Axial displacement is measured by two different ways; (i) axial extensometer with 50 mm gauge length and 100% strain reading capacity, mounted to gauge length of test specimen and (ii) LVDT transducer mounted on the grips of the testing machine.

First of all, extensometer is attached to the gauge length of the specimen as shown in Figure 3.12. The specimen should be aligned vertically to the loading (pulling) direction. In order to satisfy this alignment, a very small load can be applied before the test. In the literature, previous researchers measured the displacement between two grips of the machine, not between the gauge length of the specimen as suggested by ASTM D-638 In this study, displacement both from axial extensometer and lvdt are used to see the difference. The test apparatus is shown in Figure 3.13. During the test; load, gauge length axial displacement, time and displacement between grips readings are recorded by a data acquisition system. Data acquisition system can record 8 different readings per second. This enables getting more sensitive test results. This system also enables to visualize load versus displacement curves during tests.

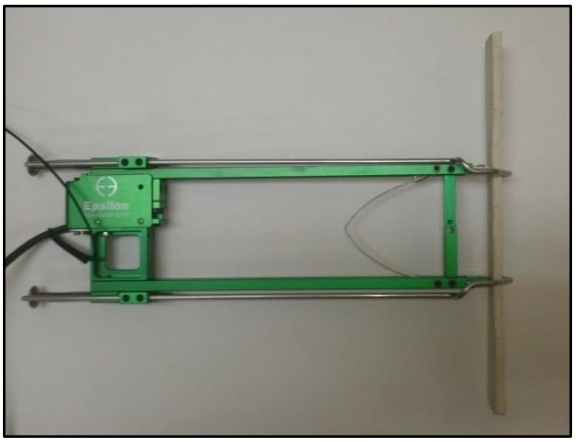

Figure 3.12 Clamping of Extensometer to Gauge Length of Specimen

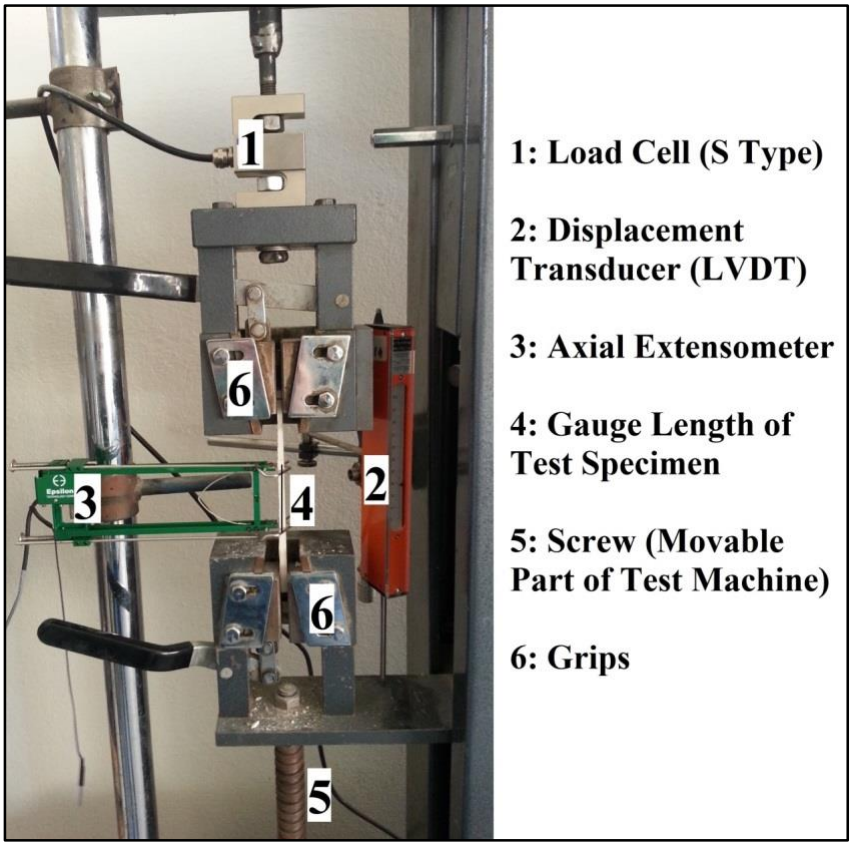

Figure 3.13 Tensile test Set-up

At the end of the test, 3 important considerations should be satisfied, in order to be sure about the validity of tests. These considerations are;

1) As mentioned in the previous chapter, specimen failure is expected in the gauge length. If the specimen fails out of this region, the test is not taken as a valid test. Figure 3.14 shows the validity of tensile testing in terms of the failure location.

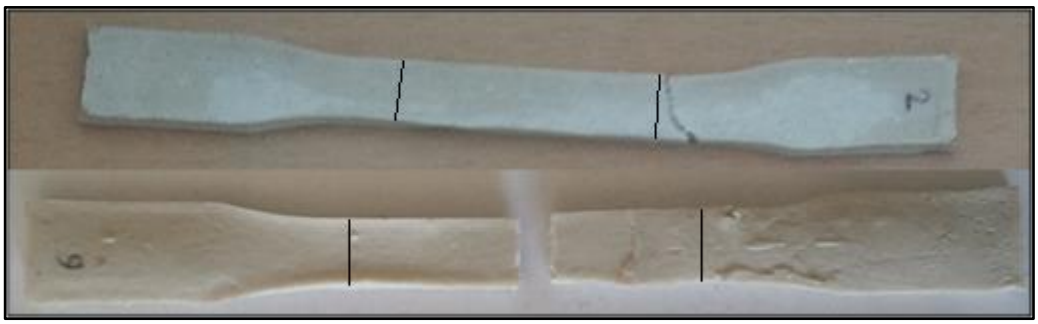

Figure 3.14 Invalid & Valid Failure Locations

2) Power drill mixer and the bit attachment sometimes cause improper blending and agglomeration of powder mixture. Tests with these lumps can neglected with outlier results. Failed section should be checked regarding this situation. In case of seeing these undesired conditions, the test should be discarded. Also air bubbles can cause similar problems. Figure 3.15 shows invalid testing due to air bubbles lumps and valid testing sections.

Figure 3.15 Invalid and Valid Test Due to Air Bubbles and Lumps in Failure Section

3) Expected failure should be a straight section across the width of liner in the gauge length portion as shown in Figure 3.14, is in linear section of gauge length. However, the failure is sometimes not straight section as in Figure 3.16. In this situation, failure area should be recalculated and the calculations should be computed considering the new failure area.

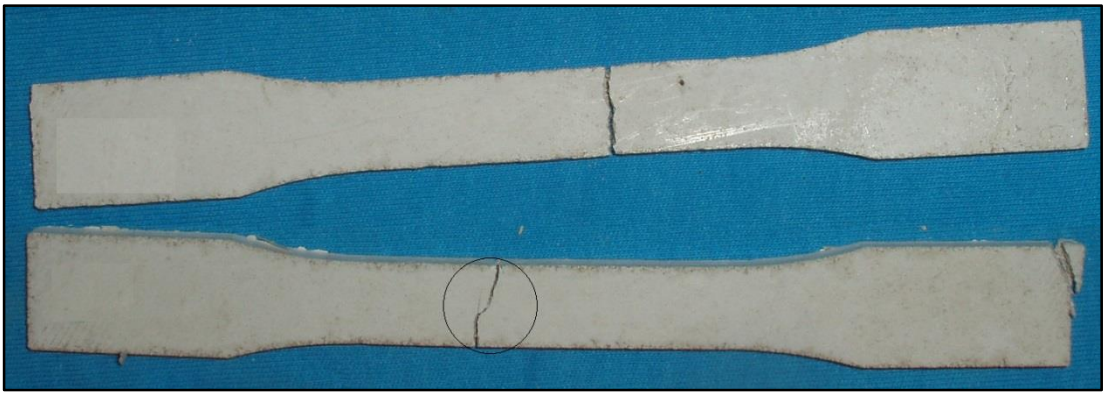

Figure 3.16 Straight & not Straight Failure Surface

3.3.3 Calculations & Results

As a result of the tensile tests, 3 important parameters will be investigated namely as:

1) Tensile Strength (σ_t)
2) Tensile modulus (E_t)
3) Elongation at break in %

Tensile strength (σ_t) is defined as maximum tensile load per unit area of minimum original cross-section and calculated by division of maximum load by the original cross section area of gauge section (area after the curing time). The following formula is used for calculating tensile strength in MPa:

$$\sigma_t = \frac{F}{A} \qquad [3.2]$$

Where;

F : Maximum load during test in N

A: Cross-sectional area of narrow section of specimen in mm^2.

Tensile modulus (modulus of elasticity, tangent modulus) (E_t) is defined as the ratio of stress to corresponding strain below the elastic limit of test specimen; and it is the ratio between stress and strain induced by the applied load. Unit of modulus of elasticity is GPa for rocks, and MPa for plastic materials. Formula of modulus of elasticity is as follows:

$$E_t = \frac{\sigma_t}{\varepsilon} \qquad [3.3]$$

Where;

σ_t : Stress in MPa

ε: Strain in % (Axial Displacement / gauge length)

Moreover, E_t should be calculated on the linear elastic region of the slope in stress-strain curve constituted by continuous data acquisition. Sample stress versus strain curve for a ductile TSL sample and linear elastic portion are given in Figure 3.17.

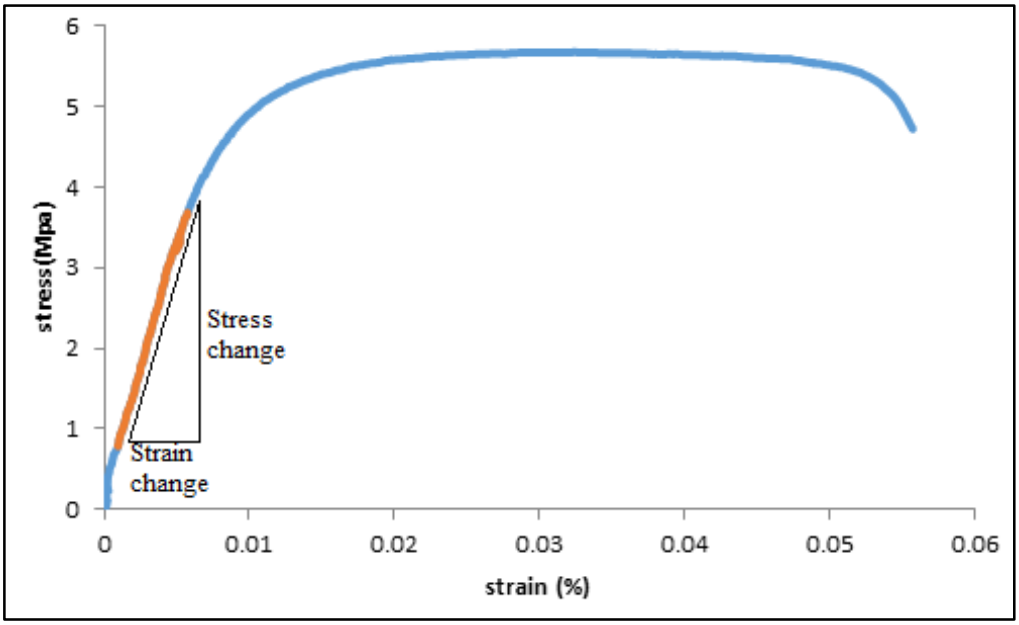

Figure 3.17 Sample stress- strain curve to find E_t

Percent elongation is defined as the change in gauge length at the point of specimen rupture. The given formula is using to find percent elongation;

$$Percent\ elongation\ = \frac{\Delta_L}{L} \qquad [3.4]$$

Where;

Δ_L : Total gauge length change of specimen

L: Initial gauge length of specimen

After the initial trials, it is observed that Liner 2 is more rigid than Liner 1. Figure 3.18 shows 2 different specimens at the end of the tensile test. Necking difference during failure of the specimens is significant in Figure 3.18.

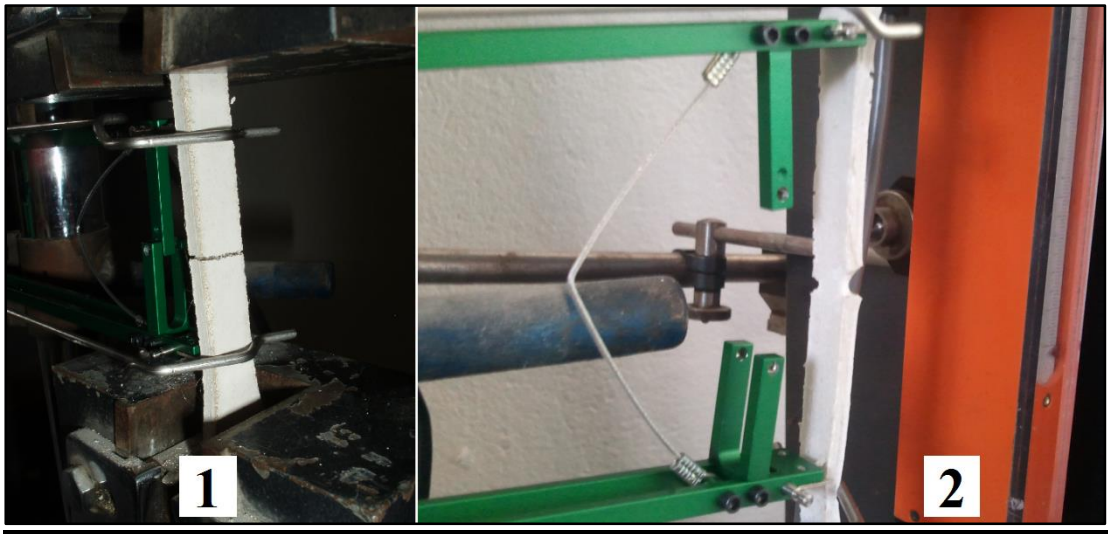

Figure 3.18 Failure of Liner 2 (1), and Liner 1 (2) Specimens

Test results will be presented for Liner 1 and Liner 2 separately. Following section will discuss the test results of Liner 1.

Tensile Test Results of Liner 1

40 tensile test specimens, 10 of them as spare specimens, are prepared for Liner 1. According to the data acquired from 25 different valid tests, stress strain curves are plotted for each one. The overall test time is recorded as 4 minutes per sample; constant load rate is applied, (6.5 mm/min). Since the liner has relatively ductile and soft behavior, it enables to measure the displacement change in 2 ways during tests:

1) Displacement change between the grips, measured with LVDT
2) Displacement chance in gauge length of specimen, measured with axial extensometer.

In order to find out elastic modulus and elongation capability of the product, displacement change is required. The previous studies specified this parameter by recording length change between the grips of the loading machine. In this study, for the first time in the literature, displacement change is investigated by measuring the change of gauge length of specimen as suggested ASTM D638.

Figure 3.19 shows the raw load displacement curves of one sample for 5 different curing time.

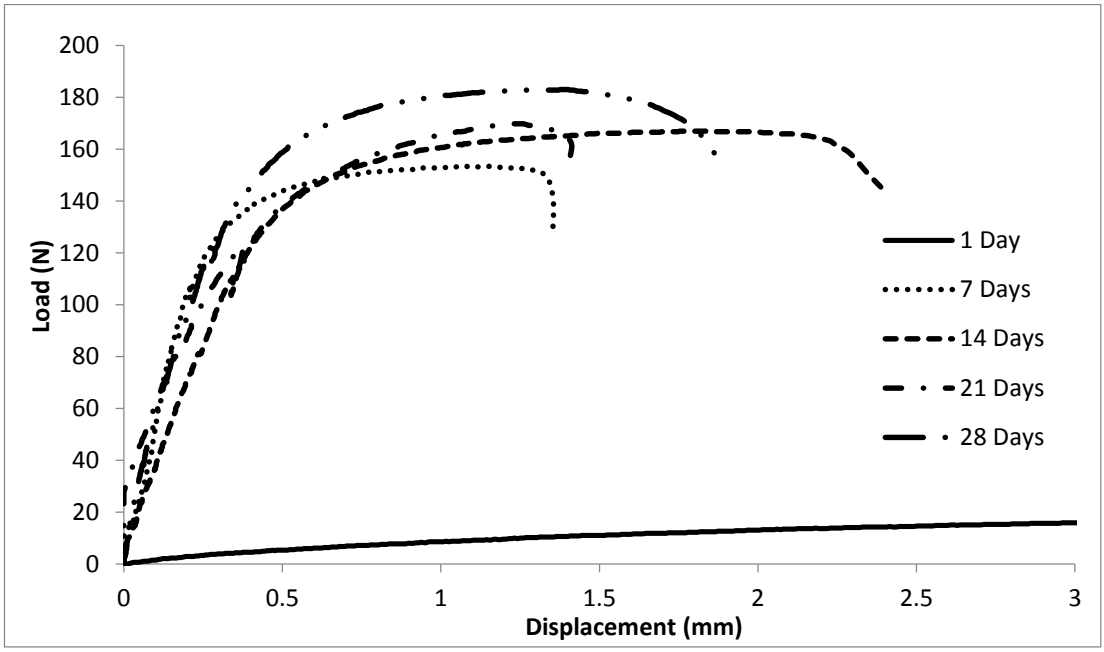

Figure 3.19 Representative Load-Displacement Curves for 5 Different Curing Time.

As a result of the laboratory studies, tensile strength versus curing period, elastic module versus curing period and tensile strength versus elastic module graphs are plotted. Since the displacement change is measured by 2 ways, a total of 5 different summary curves are investigated.

Moreover, outlier test (Q test) is conducted for some suspicious results. The test computation proves that there is no over- or under-estimated value in tensile test results of Liner 1.

All valid test results, stress strain curves and sample photographs (before and after test) are presented in Appendix A. Here, some most important findings are illustrated. Figure 3.20 shows the relationship between tensile strength and curing time. As seen in Figure 3.20 tensile strength strongly depends on curing time, the relationship can be express with a logarithmic equation.

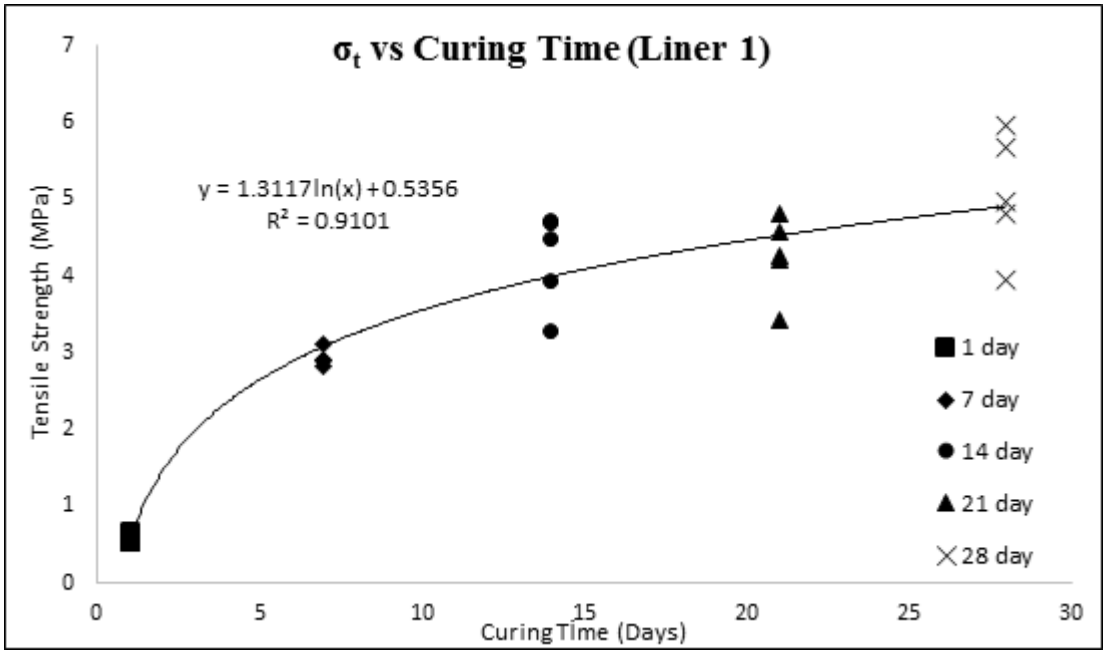

Figure 3.20 Tensile Strength Results of Liner 1

Strong correlation coefficient is observed for the graph in Figure 3.20 (0.91). This means that 91 % of tensile strength growth can be identified by the increase in curing time. However, as curing time increases, sample standard deviation is increasing unexpectedly due to scattered test results. This might be considered as a small scale problem of the laboratory study, because the previous researchers also faced with the same problem.

Average tensile strength results for the specified curing time are presented in Table 3.4. As can be seen from Table 3.4, increase in curing time causes 5 to 9 times increase of Liner 1's tensile strength

Table 3.4 Tensile Strength Growth versus Curing Time of Liner 1

Curing Time	**Average Tensile Strength (MPa)**
1 Day	0.58 ± 0.05
7 Days	2.93 ± 0.10
14 Days	4.21 ± 0.61
21 Days	4.26 ± 0.52
28 Days	5.08 ± 0.79

Figure 3.21 and Figure 3.22 show the effect of curing time on elastic modulus variation. Since the displacement measurements are recorded in 2 separate ways, 2 different curves are obtained.

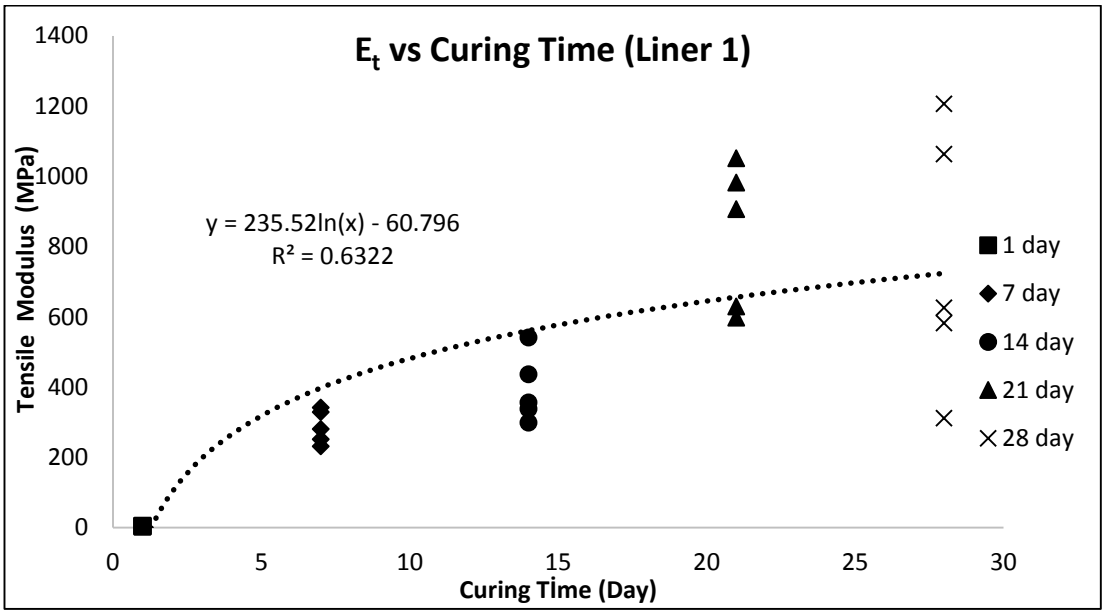

Figure 3.21 Elastic Modulus Growth and Curing Time (Based on Extensometer Readings)

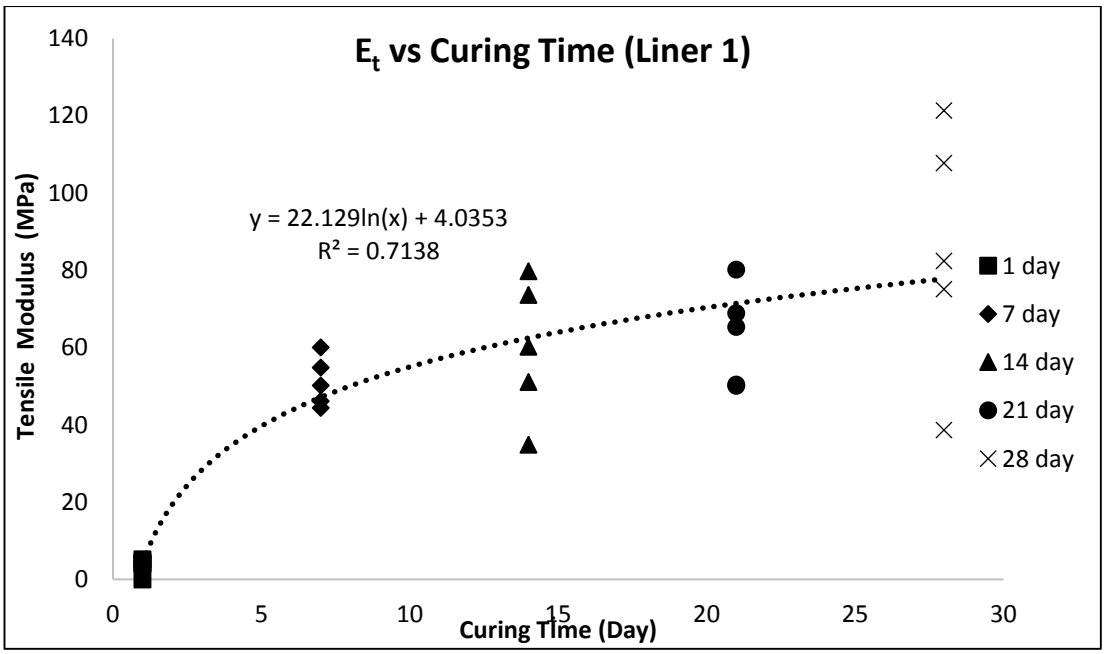

Figure 3.22 Elastic Modulus Growth versus Curing Time (Based on LVDT Readings)

In Figure 3.21, axial extensometer readings (displacement measured in gauge length) are used to find elastic modulus. On the other hand, in Figure 3.22, LVDT readings (displacement change between machine grips) are utilized to find elastic modulus. First method, given in Figure 3.21, shows 63% correlation between the tensile modulus and curing time where this value increases %71 for the second method. Average elastic modulus results are presented in Table 3.5

Table 3.5 Elastic Modulus Growth versus Curing Period

Curing Time	**Avg. Et (MPa) Extensometer**	**Avg. Et (MPa) LVDT**	**Ratio**
1 Day	4.51 ± 1.03	4.51 ± 0.51	1.0
7 Days	286.91 ± 47.98	51.13 ± 6.41	5.6
14 Days	394.27 ± 96.27	59.92 ± 17.96	6.6
21 Days	833.77 ± 207.32	63.01 ± 12.85	13.2
28 Days	758.2 ± 367.91	93.08 ± 45.50	8.2

Graphs and table demonstrate that there is a significant difference between 2 readings. 1 day curing time test results are almost similar. However, as the curing time increases, the readings become highly incompatible. In other words, findings of the previous researchers studies failed to exhibit realistic results. Because as can be seen from Table 3.5, there is almost an order of magnitude difference between two different displacement measurement techniques. Therefore, it can be said that the previous researchers might have underestimated elastic modulus by an order of magnitude. Since ASTM test standards suggest that displacement change should be measured from gauge length of specimen, the first graph should be considered as the realistic one. The relationship between elastic modulus versus curing time can be expressed in logarithmic curve function as shown in Table 3.7.

The 3rd result parameter is about elongation ratio change versus curing time. 2 different elongation ratio curves are obtained as in elastic modulus part. (It should be noted that elongation for lvdt case is found by displacement divided by total sample length, while

for extensometer case it is found by displacement divided by sample gauge length. Figure 3.23, Figure 3.24)

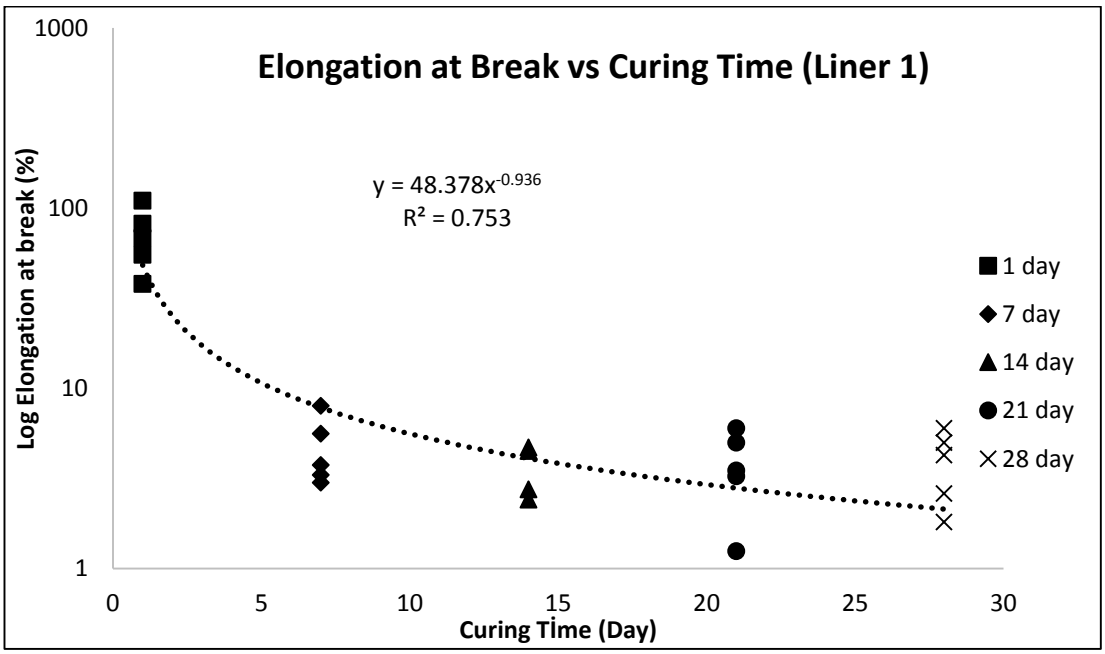

Figure 3.23 Log Elongation at break versus curing time (Based on extensometer readings)

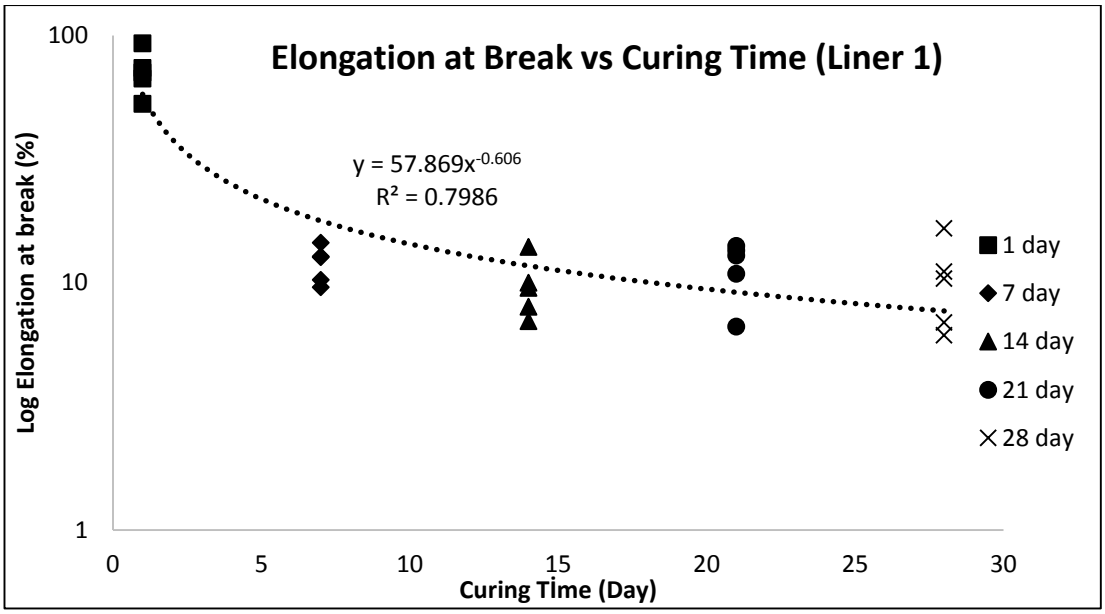

Figure 3.24 Log Elongation at break versus curing time (Based on LVDT readings)

The effect of curing time is expressed by both logarithmic and power trend line equation on Figure 3.23 and Figure 3.24. Also, the most suitable relationships way of elongation at break change versus curing time is by a power curve according to R-squared correlation coefficient. Since elongation capability has a sharp decrease between first to seventh curing time, the power trendline is selected to show better visualization.

As seen in Table 3.6 if displacement is measured from the grip distances, almost three times higher values of elongation are obtained.

Table 3.6 Elongation at break change versus curing period

Curing Time	**Avg. Elongation at Break (%) Extensometer**	**Avg. Elongation at Break (%) LVDT**	**Ratio**
1 Day	70.60± 27.36	71.60± 14.41	0.99
7 Days	4.73± 2.08	11.99± 2.01	0.39
14 Days	3.05± 1.57	9.71± 2.68	0.31
21 Days	3.80± 1.81	11.62± 3.03	0.33
28 Days	3.93± 1.71	10.23± 4.15	0.38

To sum up, tensile strength and elastic modulus parameters of Liner 1 are directly related with the curing time. As the curing time rises, tensile strength and elastic modulus also increases. These relationships can be defined by an either logarithmic or a power equation. Table 3.7 presents all the related equations and the correlation coefficients of the resultant graphs. Moreover, as elastic moduli increase with the curing time, material behaves stiffer. In other words, the elongation capability decreases with curing time. This relationship can be expressed by a power curve; relevant equation and correlation coefficient are also presented in Table 3.7.

Table 3.7 . Equations and Correlation Coefficients of Given Curves

Equation Name (y)	**Equation**	**R^2**
Tensile strength	y = 1.3117ln(x) + 0.5356	0.91
Elastic modulus (extensometer)	y = 235.52ln(x) - 60.796	0.63
Elastic modulus (LVDT)	y = 22.129ln(x) + 4.0353	0.71
Elongation at break % (extensometer)	$y = 48.378x^{-0.936}$	0.75
Elongation at break % (LVDT)	$y = 57.869x^{-0.606}$	0.80

x is the curing time in days.

Finally, tensile strength and elastic modulus correlation equation is also plotted based on extensometer readings. This equation enables practical elastic modulus estimation for ductile type TSLs. As a result, this graph gives the following equation;

$$Tensile\ strength\ (MPa) = 0.7698x \ln\big(Tensile\ Modulus\ (MPa)\big) - 0.8379 \qquad [3.5]$$

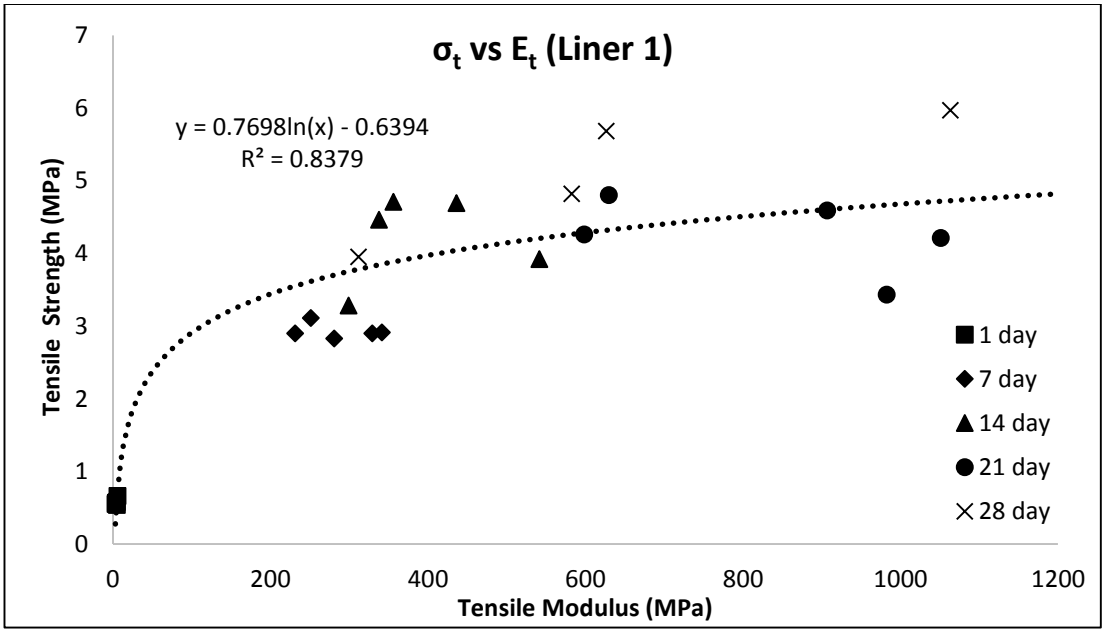

Figure 3.25. Tensile Strength versus Tensile Modulus

Tensile Test Results of Liner 2

Initial test trials show that Liner 2 is a more brittle material. It means that even some little misalignment of test specimen, the failure can easily occur out of gauge length. Therefore, 45 test specimens are prepared in order to get 25 valid test results.

Axial extensometer is the most commonly used instrument for displacement measurement in tensile testing of plastics. However, specimen clamping to external axial extensometer is troublesome for rigid specimens. When the machine is started to move, extensometer clamps tend to slide on specimen surface. The similar situation is observed in this material. Therefore, only displacement change of grip could be measured during the tests. In order to find out the elastic modulus and elongation capacity of the product, displacement should be identified. Figure 3.26 shows the raw load displacement curves of one sample specimen for 5 curing time for Liner 2.

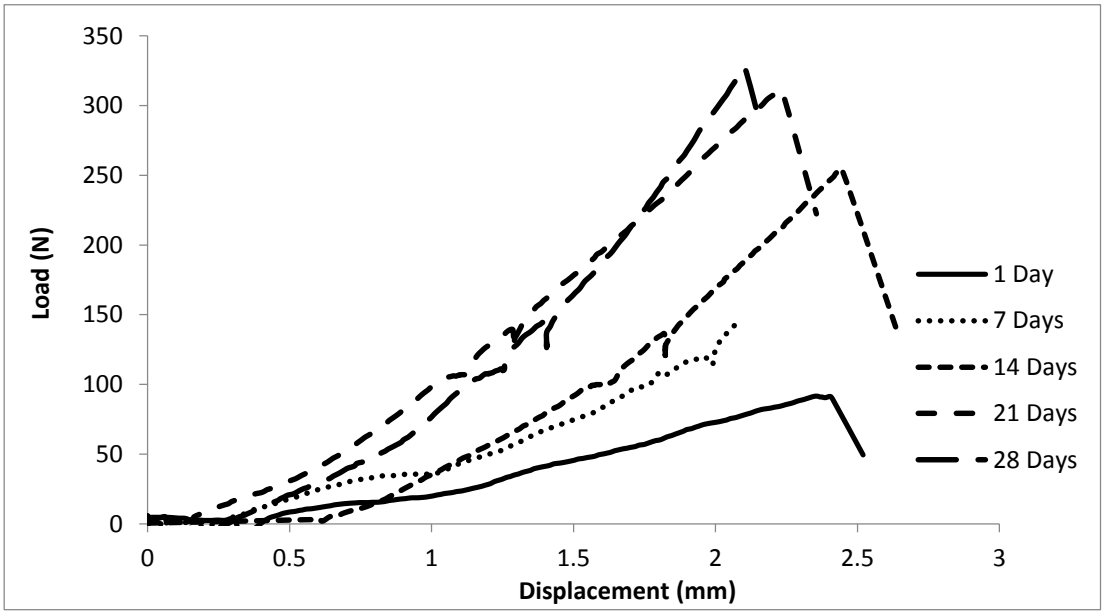

Figure 3.26. Representative Load-Displacement Curves for 5 Different Curing Time

All valid test results, stress strain curves and sample photographs (before and after test) are presented in Appendix 1. As mentioned in the previous chapters, 3 important tensile properties and their relationships with curing time will be investigated in this

part. For this purpose, 3 different result graphs are generated. Figure 3.27 shows the tensile strength growth versus the curing time.

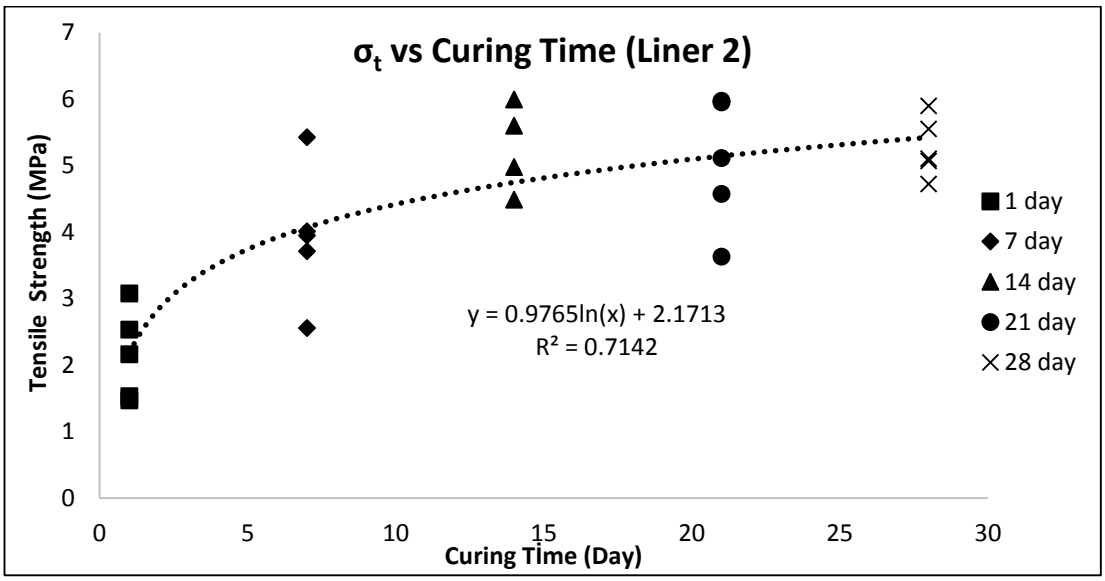

Figure 3.27 Tensile strength results of Liner 2

Tensile strength growth can be expressed by a logarithmic equation. Relatively high correlation coefficient (0.71) is observed in Figure 3.27. In other words, 71% of tensile strength growth can be expressed by given logarithmic function. In data checking for statistical compatibility, Q test results show the detection of an outlier value for 14th day. Therefore14th day results are represented by 4 valid test values discarding the outlier. Table 3.8 shows the average tensile strength results for specified curing time. As can be seen from Table 3.8, increase in curing time causes 1.5 to 2.5 times increase of Liner 2's tensile strength

Table 3.8 Tensile Strength Growth versus Curing Period

Curing Time	**Average Tensile Strength (MPa)**
1 Day	2.15 ± 0.68
7 Days	3.93 ± 1.02
14 Days	4.97 ± 0.67
21 Days	5.05 ± 0.98
28 Days	5.27 ± 0.45

Elastic module growth can also be presented in Figure 3.28. Since Liner 2 is relatively brittle material and overall test time is about 30 seconds per sample, gauge length displacement cannot be measured by axial extensometer. Displacement change is measured only by distance change between grips with an LVDT.

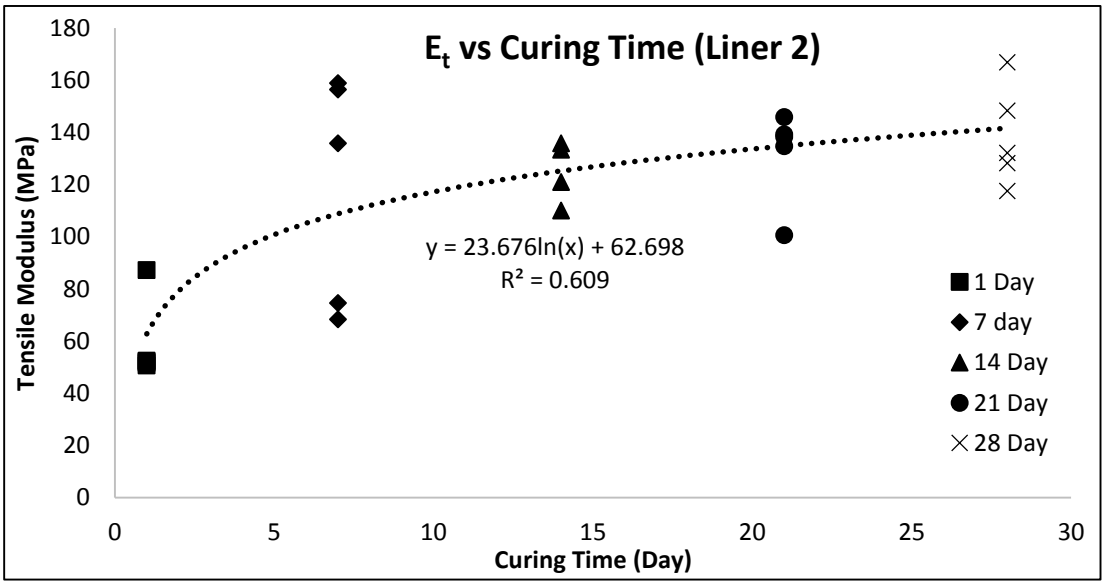

Figure 3.28 Elastic Modulus Growth of Liner 2 (Based on LVDT Readings)

As a result of this graph, as expected, elastic modulus increases with curing time. Logarithmic trend line is most representative trend line for this data. Analyses show that there is an outlier possibility in the data of 14th curing day. Therefore, this data is eliminated; and 14th day is presented by only 4 data. Average elastic modulus test results are given in Table 3.9.

Table 3.9 Average Elastic Modulus versus Curing Time

Curing Time	Average Elastic Modulus (MPa)
1 Day	58.82 ± 15.91
7 Days	118.78 ± 44.18
14 Days	125.04 ± 11.96
21 Days	131.75 ± 17.88
28 Days	138.61 ± 19.29

Since the values on Table 3.9 are based on LVDT readings, one might expect elastic modulus to be more, like in Liner 1 results. Therefore, it might be said that Liner 2's elastic modulus is 2 to 9 times of the numbers in Table 3.9 depending on curing time.

The third parameter aimed to be determined is the elongation capability of the TSL; and its variation with respect to increasing curing time. As opposed to the previous graphs, the correlation between elongation at break (%) versus curing time cannot be determined since there is no correlation between the parameters. Figure 3.29shows the elongation capability change versus curing time.

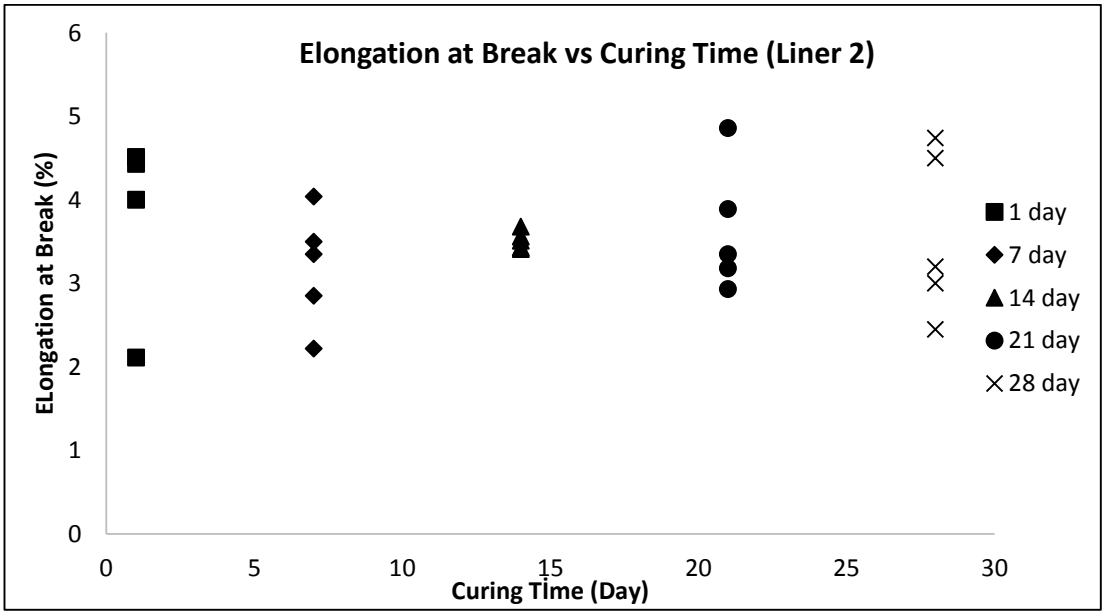

Figure 3.29. Elongation at Break versus Curing Time (Based on LVDT Recordings)

As seen in Figure 3.29, elongation capability of Liner 2 does not depend on the curing time. Average elongation capability of Portland cement-based brittle Liner (2) is found to be 3.5 %. Average results for the elongation at break are presented in Table 3.10.

Table 3.10 Average Elongation at Break versus Curing Time (Liner 2)

Curing Time	**Elongation at Break (%)**
1 Day	3.91± 1.03
7 Days	3.19± 0.69
14 Days	3.52± 0.11
21 Days	3.64± 0.76
28 Days	3.58± 0.99
Average:	3.57± 0.76

As a result of Liner 2 tensile tests, the effect of curing time to tensile strength, elastic modulus and elongation capability are investigated. As the curing time increases, tensile strength and elastic modulus also increases. Best curve fitting between these parameters can be expressed by logarithmic equations. Table 3.11 presents all the related equations and the correlation coefficients of given graphs. Contrary to the general opinion, Portland cement-based and/ or fiber added TSL materials has almost constant elongation capacity.

Table 3.11. Equations and correlation coefficients of given curves

Equation Name (y)	**Equation**	**R^2**
Tensile strength	y = 0.9765ln(x) + 2.171	0.71
Elastic modulus (LVDT)	y = 23.676ln(x) + 62.698	0.61

x: curing time in days.

Finally, tensile strength versus elastic modulus correlation equation is also plotted for Liner 2. This equation enables the practical elastic modulus estimation for brittle type TSLs. Equation of the curve is as follows:

$$Tensile\ strength\ (MPa) = 2.8146\, x \ln\left(Tensile\ Modulus\ (MPa)\right) - 8.8672 \qquad [3.6]$$

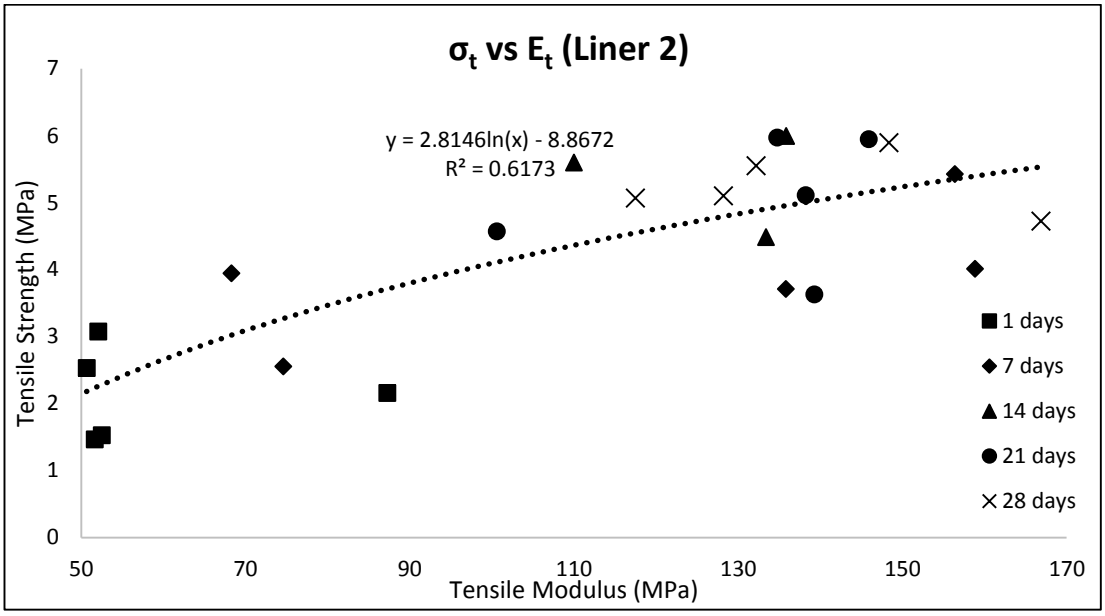

Figure 3.30. Tensile Strength versus Tensile Modulus

Comparison of Tensile Strength Properties of two products

This part presents the tensile strength, elastic modulus and percent elongation comparison of Liner 1 and Liner 2. Representative stress strain curves of two products are given in Figure 3.31.

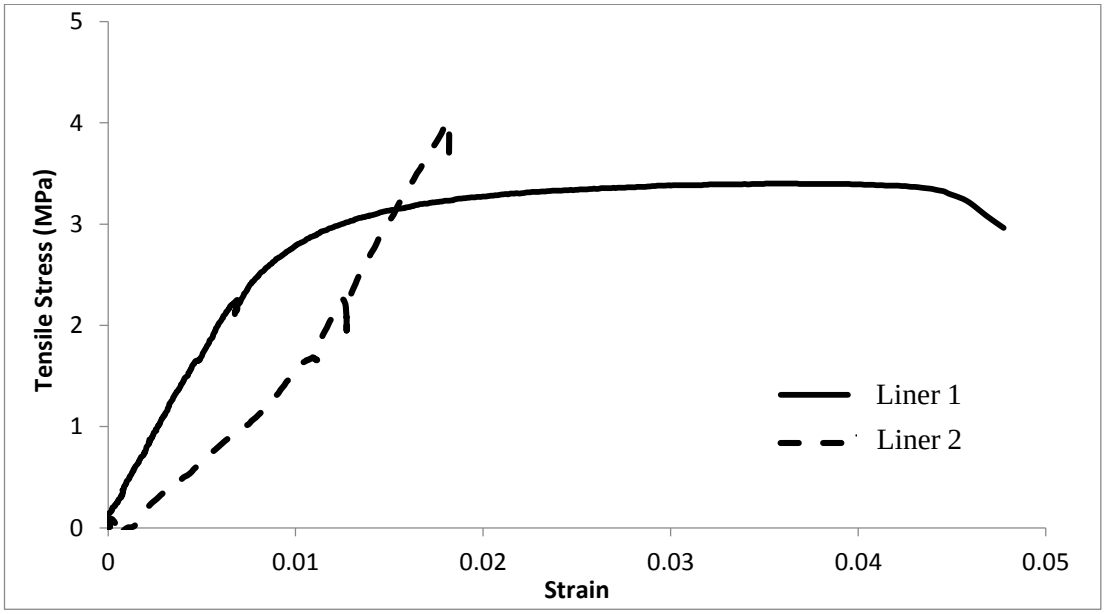

Figure 3.31 Representative Stress strain curves of two products (7 days)

During the laboratory studies, in order to compare testing products, all variables are kept constant (load rate, curing time, specimen properties etc.). Liner 1 has higher elongation capability than Liner 2. One of the major reason is that the chemical ingredient varies for both products. Liner 1 is a copolymer based TSL; and major component enables to hold higher strain capability. On the other hand, Liner 2 has ingredients of Portland cement and polypropylene fibers. These components make the liner stiffer and stronger; however, restrict its elongation capability.

Figure 3.32 shows logarithmic curve expressions of tensile strength growth versus curing time of two products. Both products are best expressed by logarithmic curve plots. Due to its chemical compositions and fibers in it, Liner 2 is a little bit stronger then 2nd one. At the end of a month curing time, tensile strength values can reach up to about 5 MPa.

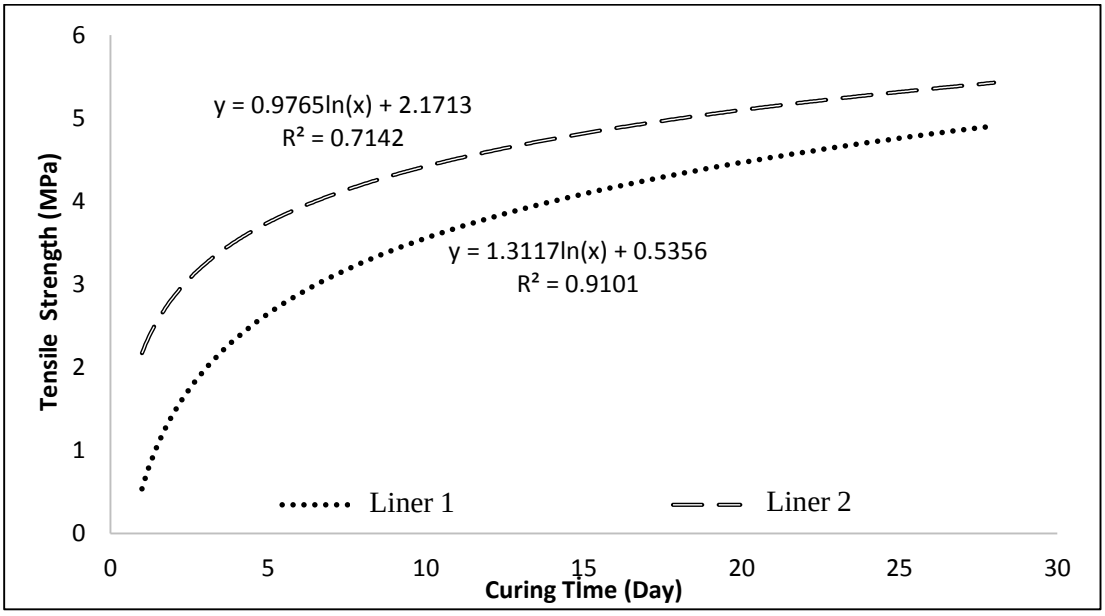

Figure 3.32. Tensile Strength Curing Time Relationships

Elastic modulus also increases as curing time increases. It is expected that Liner 2, the brittle one, has higher elastic modulus value. Graphs are presented in Figure 3.33. Since stiffer material can gain load easily, elastic module of Liner 2 is relatively higher than the other one.

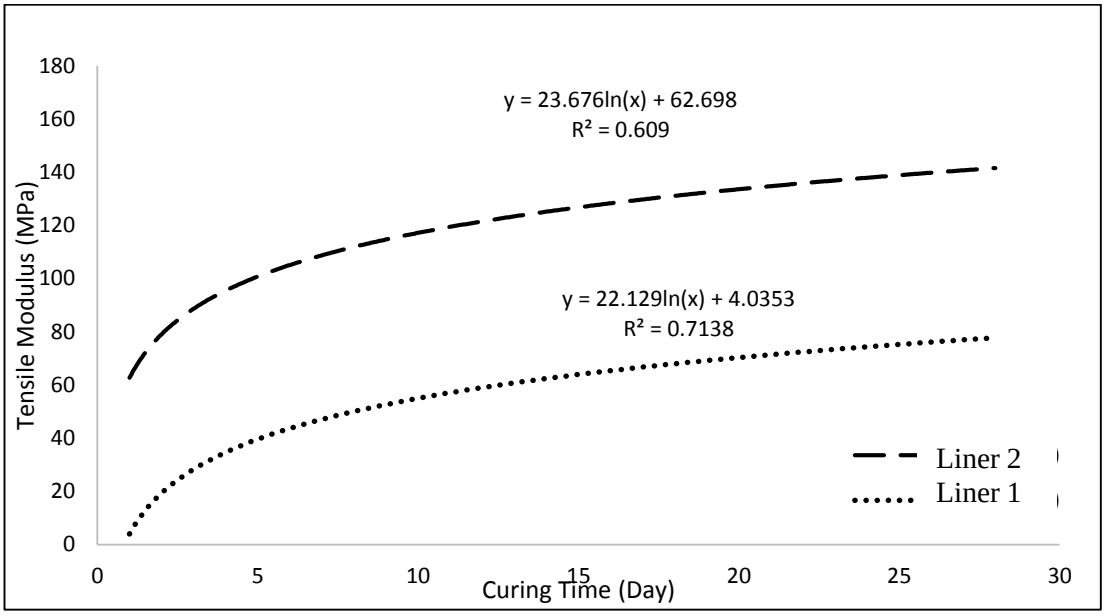

Figure 3.33 Elastic Modulus Growths versus Curing Time (Both LVDT Reading)

Note that elastic modulus growth of both Liners are calculated by measuring grip displacement change in Figure 3.33. Since Liner 1 behaves as a ductile material, elastic modulus of Liner 1, is significantly less than Liner 2.

Elongation ratio is also important property for TSLs. As a result of the laboratory studies, it is found that elongation ratio of Liner 1 strongly depends on curing time. However, Liner 2 has no any dependency on curing time. At the end of a month, average elongation rate is found to be very similar for both products, which is between 3 - 4 %.

3.4 Compression Testing

Compression testing is not a commonly used TSL testing method among TSL researchers. In the literature, only two studies on compression testing of TSL exist. Ozturk (2011) conducted a compression test for 2 different TSL products; and Mpunzi (2012) performed a similar study for 3 different products. Detailed information of these studies is given in the literature survey section.

In numerical modelling of underground openings, some material property inputs such as unconfined uniaxial compressive strength, elastic modulus and Poisson's ratio are required to be found. Researchers generally assume some values for those parameters while performing numerical models. (Drige and Archibald, 2009) The only way to find these properties is to carry out compression tests.

Previous studies were not based on any standard testing methodology during compression test studies. Moreover, they did not attempt to analyse the effect of curing time over these parameters; and they mainly focused on compression strength of TSL material.

One of the main contributions of this study is not only finding these mechanical properties, but also revealing the relationships between these parameters versus a specified curing time (2, 7, 14, 21, 28 days). As in the tensile tests, this study is also based on ASTM test standards. "Standard Test Method for Compressive Properties of Rigid Plastics, ASTM- D695-10" is the most suitable testing standards for TSL materials.

There are various factors taken into account during the laboratory test. Each factor is standardized in ASTM D695-10. Following parts present the stated factors, test set up, calculations and the results of compression tests.

3.4.1 Test Standards & Procedure

To generate a background for the further studies, test parameters are clearly identified under this title. 10 different testing parameters were explained in chapter 3.2. Some additional important considerations should also be mentioned before, during and after compression test studies.

Substantial compression test considerations are listed as follows;

- Any suitable testing machine can be used, as long as having ability to control the rate of crosshead movement in constant level. However, it is better to perform these tests by using a test machine with a displacement controlled one.
- Two different specimen dimensions are mentioned in the standards. Specimen should be in a form of cylinder or prism whose length is twice its diameter or width. Most suitable specimen size is 0.5 in. (12.7mm) diameter or width by 1 in. (25.4 mm) length.
- Preparation of such cylindrical specimens is almost impossible by molding process. Therefore, it is better to prepare a cylindrical sample by coring a cured mixture with a diameter of 25.4 mm drill bit. For water soluble products, it is preferred to use dry coring technique.
- As in the tensile tests, at least 5 different test specimens should be tested and validated.
- According to the test standards, load rate should be between 1 and 1.6 mm/min. In this study, the load rate of 1.45 mm/min is used
- Laboratory conditions are the same as in the tensile tests. The best laboratory condition is about 23°C and 50 % relative humidity to provide a consistent compression test outputs. Moreover, test specimens should be evaluated in constant temperature and humidity during curing a test period of 28 days to obtain comparable test results. Displacement measurement tools are also very sensitive to instant temperature changes. These considerations should not be ignored during tests.
- Test specimen dimensions should be re-measured just before testing due to the shrinkage problem.
- When placing the specimen between the compression test platens, it is required to take the top and bottom surface of the specimens into the parallel level with compression tools.
- Since there might be some bubbles in specimen, axial displacement change should be measured by using at least 2 different measuring tools. Moreover, instead of strain gauge to measure lateral displacement, it is better to use circumferential extensometer due to its capability to measure circumferential displacement variation.

- During test, parameters such as load, axial displacement, lateral displacement, time reading should be recorded continuously. Visualization of load-displacement curves under loading condition has a benefit of comparing results for different tests.
- It is possible to observe that some TSLs may not be fail during test. The chemical composition converts them in to a rubber-like material.
- During calculations part, stress-strain and axial-lateral strain curves should be plotted, and related mechanical properties can be obtained by using these curves.

3.4.2 Sample Preparation

Initial procedure for the specimen preparations is the same as tensile testing part. The major difference is the molding part. Since compression test specimens have relatively small cylindrical shape, molding is very time consuming and ineffective way to prepare a test specimen.

After mixing of liner components by power drill mixer and the bit attachment, the mixture is poured into a wide-mouth container. After the mixture gains some strength (2 day in this study), specimens are prepared by using diamond core drilling machine. Machine should be operated as much low speed as possible not to disturb the core specimen. Moreover, the dry coring process should be done. Figure 3.34 shows the coring process of TSL samples.

Figure 3.34 Specimen Preparations by Coring Technique

Note that mixture preparation of products for each curing time should be done separately in order to get homogenous specimens. After the coring process, top and bottom surface of the core specimen should be smoothed out by a chainsaw for the standardized length to diameter ratio.

During sample preparation, 40 test specimens are prepared for each product. 73 compression tests are carried out in this study. 10 out of 40 specimens are utilized for the calibration of the testing equipment. Finally, tests are continued until acquiring 5 valid test results for each curing time. Table 3.12 presents the number of tests for each curing time and product.

Table 3.12 Conducted Test Numbers in Compression Tests

	Liner 1						**Liner 2**					
Curing Time (Days)	**2**	**7**	**14**	**21**	**28**	**Total Number of Tests**	**2**	**7**	**14**	**21**	**28**	**Total Number of Tests**
Number of Tests	6	8	10	7	9	40	10	5	6	5	6	32

Testing Apparatus and Test Set-up

Compression tests are conducted with a displacement controlled MTS machine which has a 500 kN load capacity.

Since MTS machine does not enable to visualize load displacement curve during tests, a data acquisition system is attached to the test set up. Moreover, this system can record 8 data reading per second; it helps to obtain more sensitive test results. A load cell of 5 tonnes capacity is used.

Circumferential and axial displacement measurement tools have 10 mm capacity with ± 0.001mm sensitivity. In some soft products, this capacity may not be enough to measure upper limits. However, elastic moduli and Poisson’s ratio are calculated in

elastic loading part of the tests. Therefore, 10 mm measurement range is enough for the conducted tests. Compression test set-up can be seen in Figure 3.35.

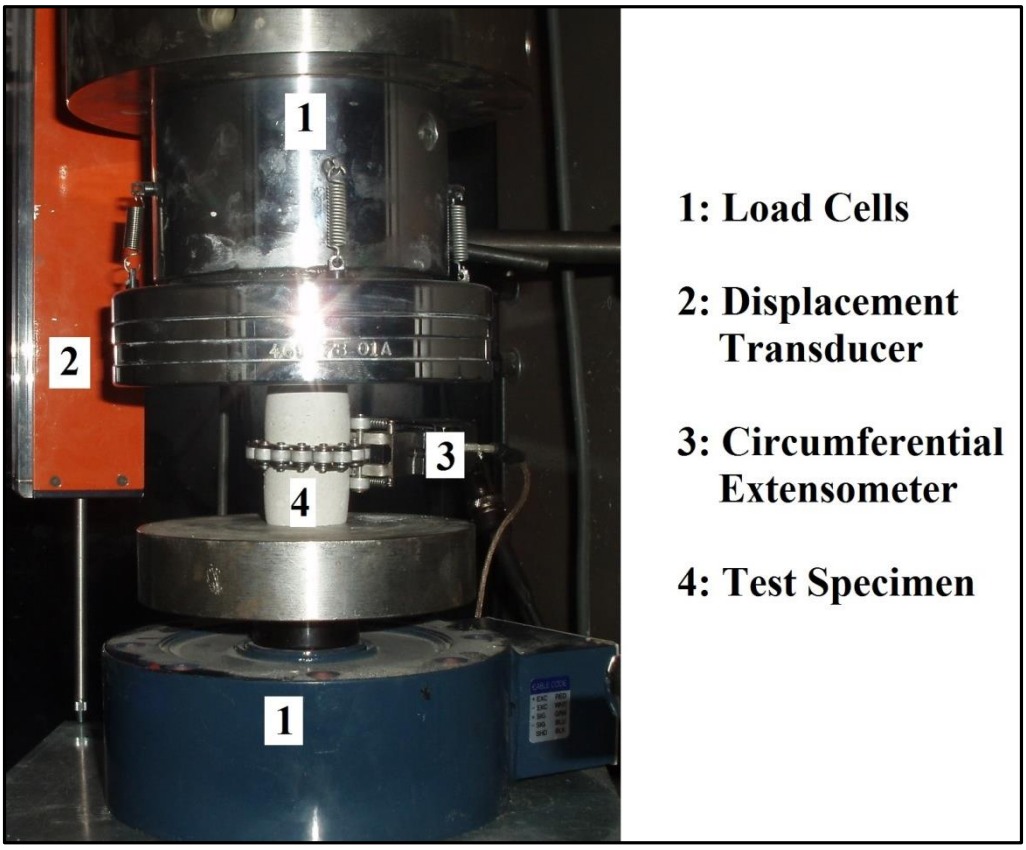

Figure 3.35 . Compression Test Apparatus

3.4.3 Calculations & Results

As a result of compression tests, following 3 important parameters will be investigated;

1) Unconfined compressive strength (σ)
2) Elastic modulus (E)
3) Poisson's ratio (ν)

Unconfined Compressive Strength (UCS) is defined as the maximum compressive load per unit area of minimum original cross-section and calculated by dividing the maximum load by the original area (area after curing). The following formula is used for calculating UCS in MPa:

$$\sigma_t = \frac{F}{A} \qquad [3.7]$$

Where;

F: Maximum load during test in N

A: Cross-sectional area of applied load in mm^2.

Elastic modulus (modulus of elasticity, tangent modulus) (E) is defined as the ratio of stress to the corresponding strain below the elastic limit of test specimen; and it is calculated by dividing stress to strain. Unit of modulus of elasticity is in GPa for rocks, and MPa for plastic materials. Modulus of elasticity is calculated as follows:

$$E_t = \frac{\sigma_t}{\varepsilon} \qquad [3.8]$$

Where;

σ_t : Stress in MPa

ε: Strain

Moreover, elastic modulus is calculated on the linear portion of the slope of a stress-strain curve constituted using continuous data flow. A typical sample stress-strain curve for a brittle TSL and the linear elastic portion is given in Figure 3.36.

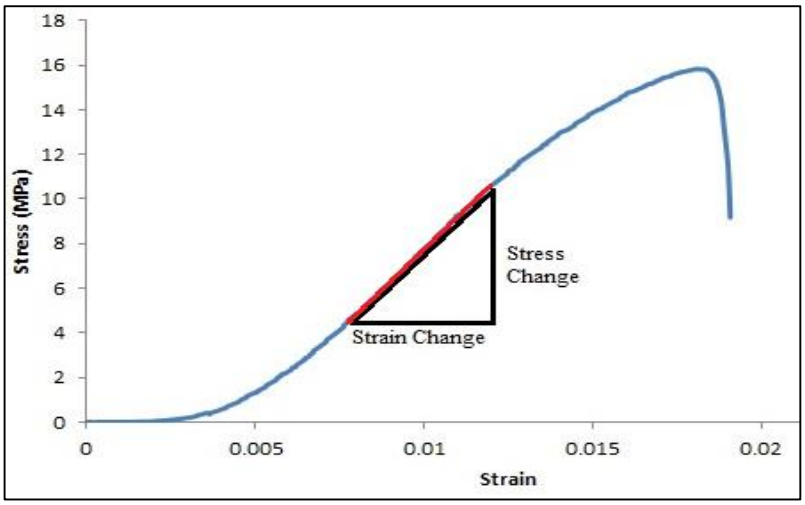

Figure 3.36. Sample Stress- Strain Curve of a TSL (Liner 2)

Poisson's ratio is defined as the negative ratio of lateral to axial strain of a specimen which can be calculated using the following formula;

$$\nu = \frac{-\Delta\varepsilon_y}{\Delta\varepsilon_x} \qquad [3.9]$$

Where;

ε_y : Ratio of length change of lateral direction to initial lateral length.

ε_x: Ratio of length change of axial direction to initial axial length.

In addition, hundreds of data readings are recorded continuously during the tests. Sample stress-strain curve for a brittle TSL and the linear elastic portion is given in Figure 3.37

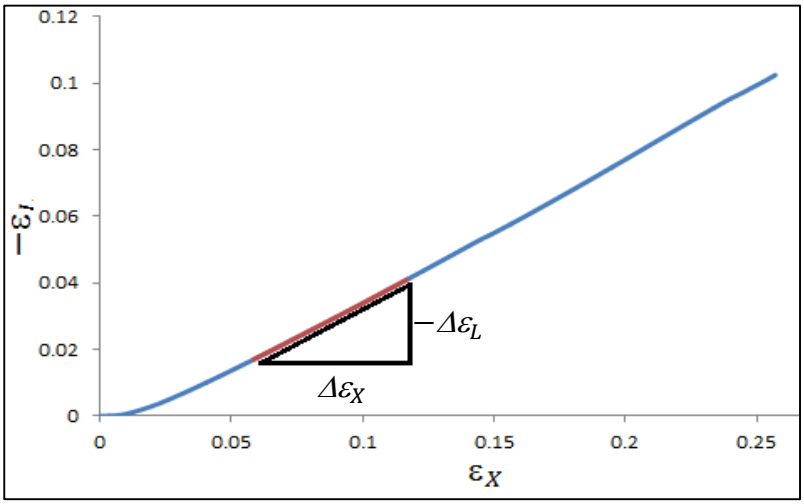

Figure 3.37 Sample –Lateral versus Axial Strain Curve (Liner 1)

After the initial trials, Liner 2 is observed to be more rigid than Liner 1. It means that the test time and the elongation capability of Liner 2 is shorter than Liner 1. Moreover, Liner 1 did not fail during the tests. Figure 3.38 shows two different specimens at the end of the compression test.

Figure 3.38 Representative Specimen Shapes after Test (Liner 1, Liner 2)

As in tensile tests part, the test results are presented for both products in the coming sections. First of all, summary graphs and tables for Liner 1 compression test are given.

Compression Test Results of Liner 1

45 compression test samples are prepared for Liner 1 for calibration and measurement purposes. At the end of the experiments, 25 valid tests are performed to plot stress strain and lateral-axial strain curves for all specified curing time. Since failure state was not observed during the tests, testing time is decided by considering required time in order to see linear elastic path in stress-strain curve. Therefore, the tests are ended at 10 mm length deformation (limiting displacement for LVDT) (about 7 minutes) and 1.50 mm/min. load rate is applied during the test.

Since the test specimens did not fail during the tests, the UCS values could not be found. On the other hand, elastic loading region is identified very accurately. This region enables to find elastic modulus and Poisson's ratio parameters. Figure 3.39and Figure 3.40 shows raw load-displacement and lateral-axial displacement curves for each curing time.

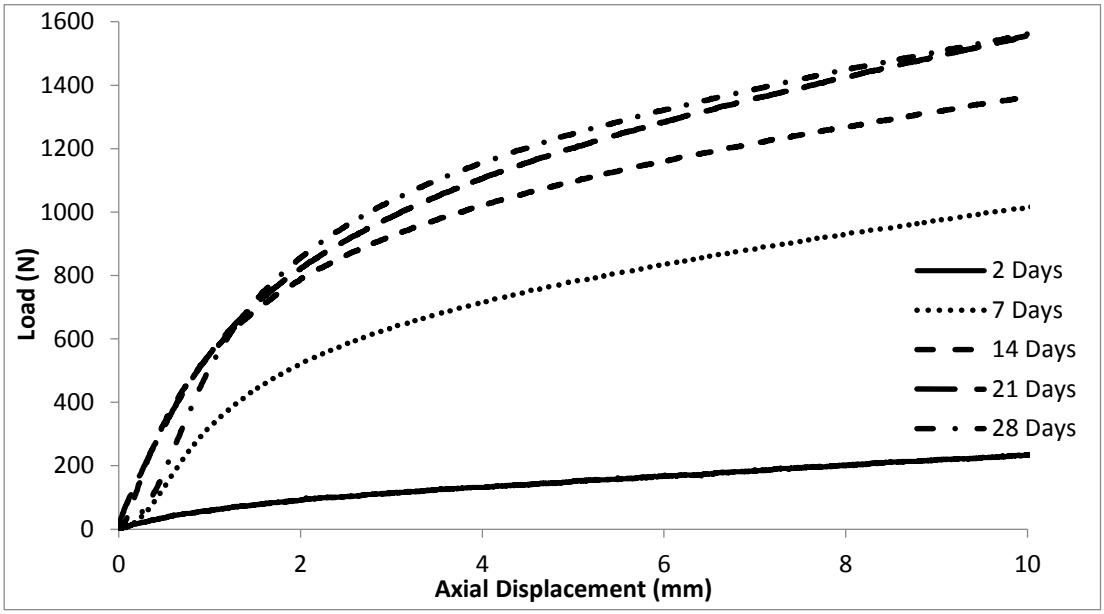

Figure 3.39 Representative Load-Displacement Curves for 5 Different Curing Time (Liner 1)

As seen in Figure 3.39, load carrying capacity is directly proportional to curing time. This curve helps to obtain elastic modulus of the test specimens. We can say that elastic modulus growth depends on curing time. Moreover, as in Figure 3.39, material has a bilinear load-displacement and stress-strain curves. Elastic modulus parameter of the liner is assessed using the initial linear portion of stress-strain curve. After a while, characteristics of the curves change and the slopes of lines decreases monotonically. However, test standards suggest considering initial linear portion for calculating elastic modulus parameter.

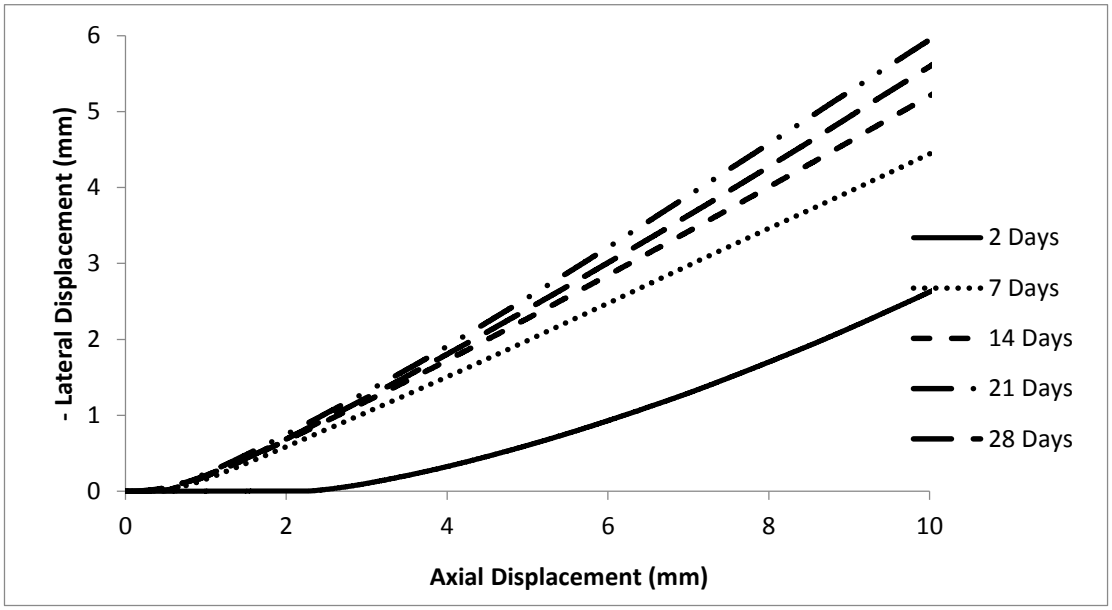

Figure 3.40 Representative –Lateral versus Axial Displacement Curves for 5 Different Curing Time (Liner 1)

Poisson's ratio parameter can be calculated with a help of axial and lateral displacement recording; Poisson's ratio also slightly depends on curing time.

In elastic modulus and Poisson's ratio calculations, there is no outlier detection according to Q test. All valid test results, stress strain curves and sample figures (before and after test) are presented in Appendix.2.Under this title; only some important summary graphs are given. As it can be seen from Figure 3.41 that elastic modulus strongly depends on curing time. The relationship can be expressed by a logarithmic trend line having a correlation coefficient of 0.84.

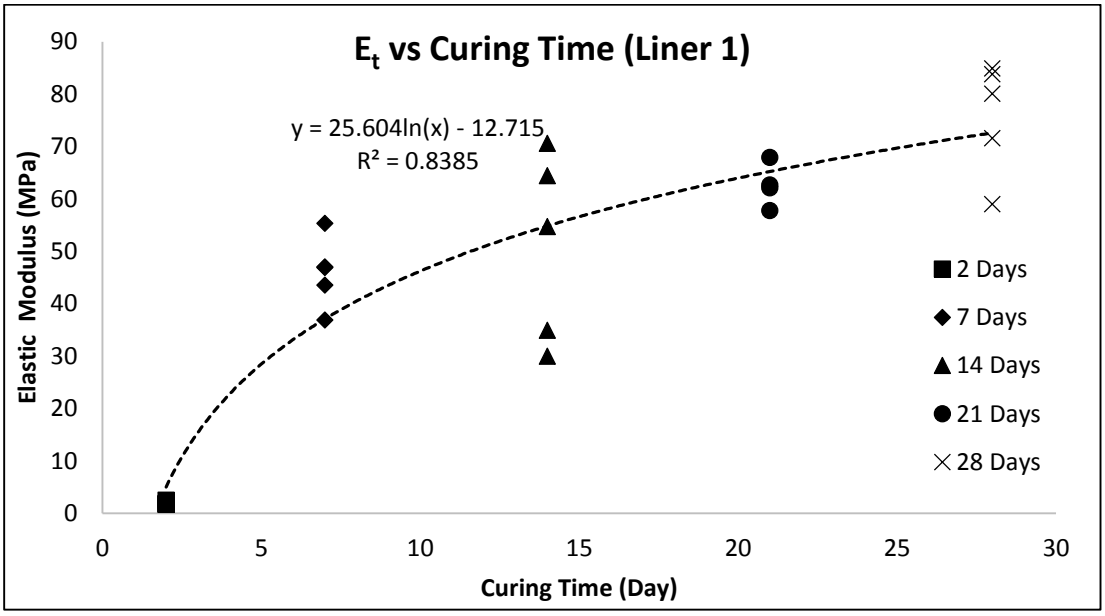

Figure 3.41 Elastic Modulus Change versus Curing Period

Average elastic moduli results are presented in Table 3.13.

Table 3.13 Average Elastic Modulus in Specified Curing Time

Curing Time	Avg. E (MPa)
2 Day	1.98 ± 0.33
7 Days	45.94 ± 6.67
14 Days	50.96 ± 17.88
21 Days	60.08 ± 6.74
28 Days	75.87 ± 10.77

Second summary graph is on Poisson's ratio versus curing time relationship. As a result of the compression tests, very similar Poisson's ratio values are obtained. Resultant Poisson's ratios are in the range of 0.31 to 0.44. Moreover, it is observed that Poisson's ratio also depends on curing time. Increasing curing time raises the value of Poisson's ratio parameter. The relationships can be expressed by a logarithmic trend line with a 0.78 correlation coefficient. Figure 3.42 shows this relationship. The average Poisson's ratio values are presented in Table 3.14.

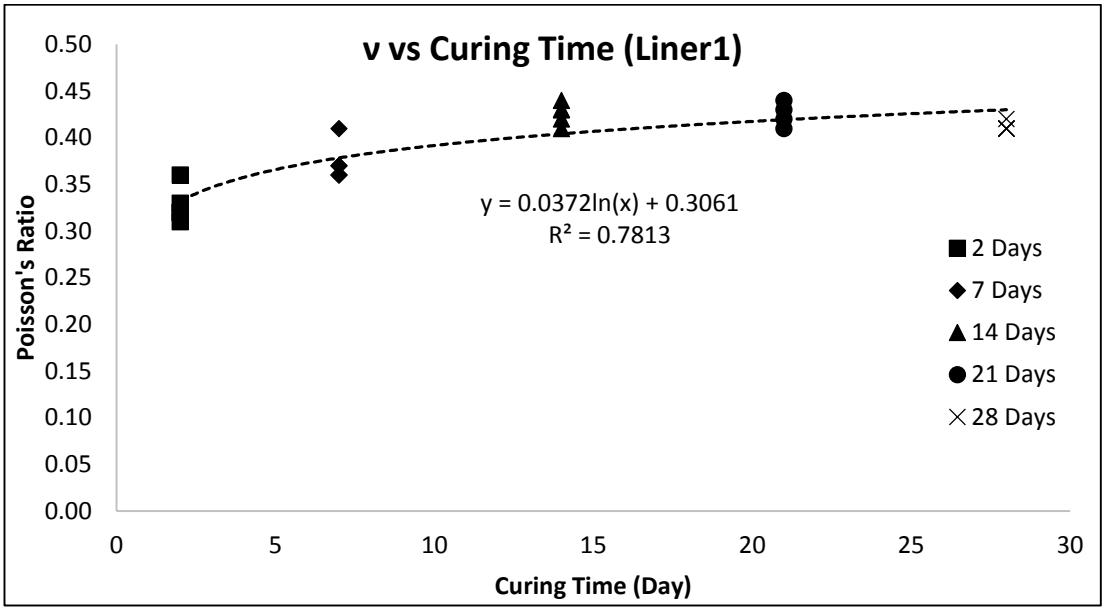

Figure 3.42 Poisson's Ratio Change versus Curing Time

Table 3.14 Average Poisson's Ratio Values in Specified Curing Times

Curing Time	Avg. ν
2 Day	0.33 ± 0.02
7 Days	0.37 ± 0.02
14 Days	0.43 ± 0.01
21 Days	0.42 ± 0.01
28 Days	0.41 ± 0.01

To sum up, compression strength value of Liner 1 could not be determined due to chemical composition of material which makes the material behave in a rubber like way. On the other hand, elastic modulus and Poisson's ratio parameters of Liner 1 are evaluated from the experiments. Moreover, their curing time change is investigated. As expected, both parameters depend on curing time. Poisson's ratio and elastic modulus proportionally improves with curing time. These relationships can be expressed by a logarithmic trend line equation. Table 3.15 presents related equations and correlation coefficients of the given graphs. .

Table 3.15 . Equations and Correlation Coefficients of Given Curves

Equation Name (y)	Equation	R^2
Elastic modulus	y = 25.604ln(x) - 12.715	0.83
Poisson's ratio	y = 0.0372ln(x) + 0.3061	0.78

Compression Test Results of Liner 2

In order to determine the compression properties of the brittle TSL material, 40 test specimens are prepared for testing purpose. 32 tests are conducted in order to get a 25 valid test results. During the laboratory tests, specimens fail in about 60 seconds with 1.45 mm/min constant load rate. 3 different result graphs are presented under this title.

The compressibility of Liner 2 is lower than Liner 1. During laboratory tests, recorded average compressibility ratio is found between 0.7 and 2.0 % of specimen length. As in Liner 1 calculation, stress-strain and lateral-axial strain graphs are plotted initially. Figure 3.43 and **Error! Reference source not found.** show the raw load displacement and lateral- axial displacement curves for each specified curing time.

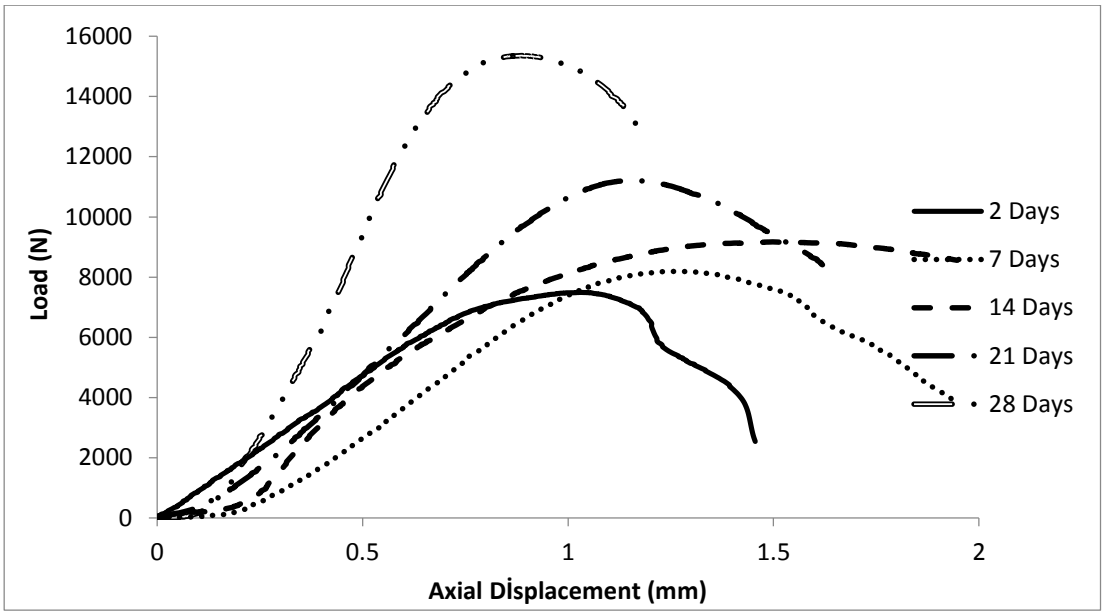

Figure 3.43 Representative Load versus Displacement Curves for 5 Curing Time (Liner 2)

As seen from Figure 3.43 failure load is directly proportional with curing time. Also, it can be concluded that the material behaves stiffer with increasing curing time. Compressive strength and elastic modulus parameters will be investigated using these data.

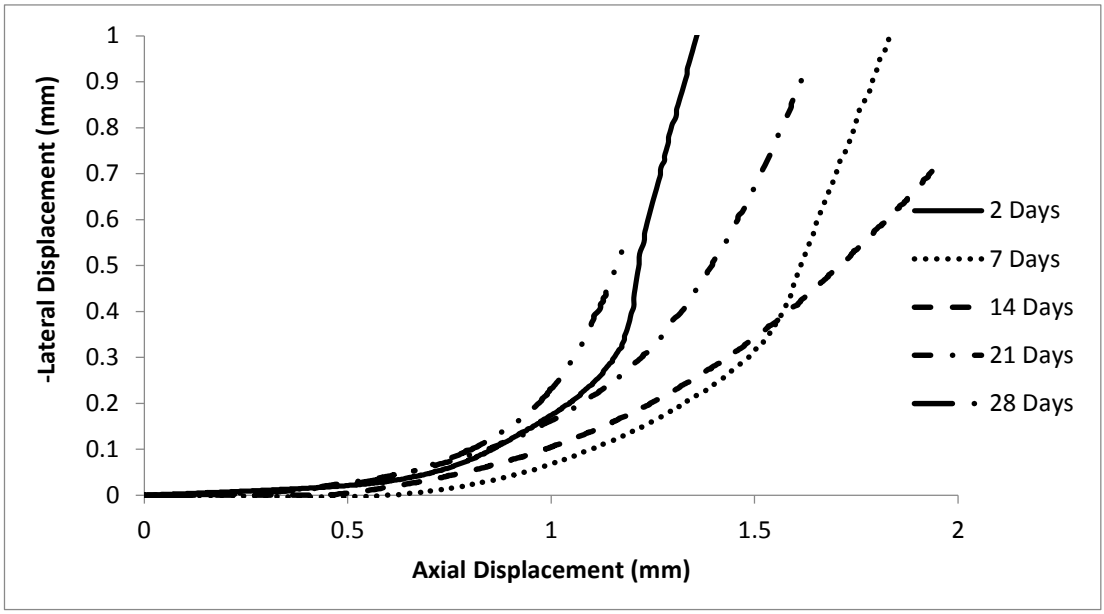

Figure 3.44 Representative –Lateral-Axial Displacement Curves for 5 Different Curing Time (Liner 2)

Axial and lateral displacement recordings are utilized for the calculation of Poisson's ratio. It can be estimated that Poisson's ratio depends on curing time. Moreover, outlier test (Q test) is conducted for the suspicious experiment results. The test computation proves that there is no over- or under-estimated value in the compressive test results for Liner 2. Figure 3.45 shows the relationship between UCS and curing time. The UCS strongly depends on the curing time; the relationship can be expressed using a logarithmic trend line with 0.58 correlation coefficients.

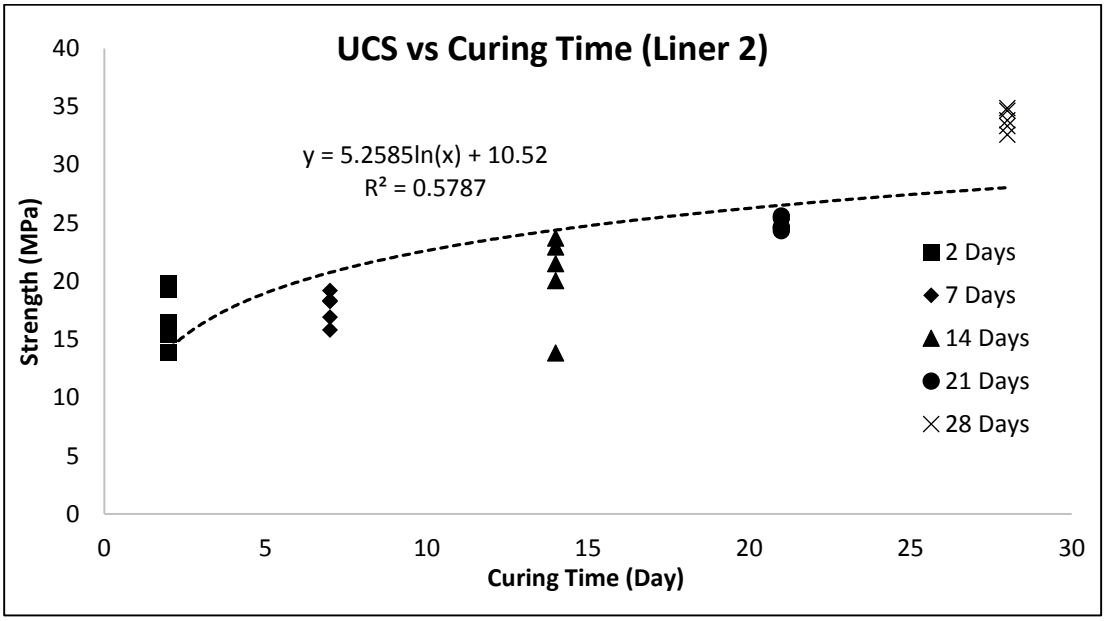

Figure 3.45 UCS versus Curing Time Relationship

Average UCS values with specified curing time are presented in Table 3.16. As can be seen from Table 3.16, increase in curing time causes 1 to 2 times increase of Liner 2's compressive strength.

Table 3.16 Average UCS Values versus Curing Time

Curing Time	Avg. UCS (MPa)
2 Day	16.98 ± 2.54
7 Days	17.71 ± 1.33
14 Days	20.41 ± 3.93
21 Days	24.92 ± 0.55
28 Days	33.85 ± 0.95

Elastic modulus variation can also be explained by curing time. Figure 3.46 shows that elastic modulus increases with curing time, as expected. Although linear trend line is the most representative trend line for this data, linear increasing is not suitable way to express UCS growth. Analyses show that there is no any outlier possibility in the data.

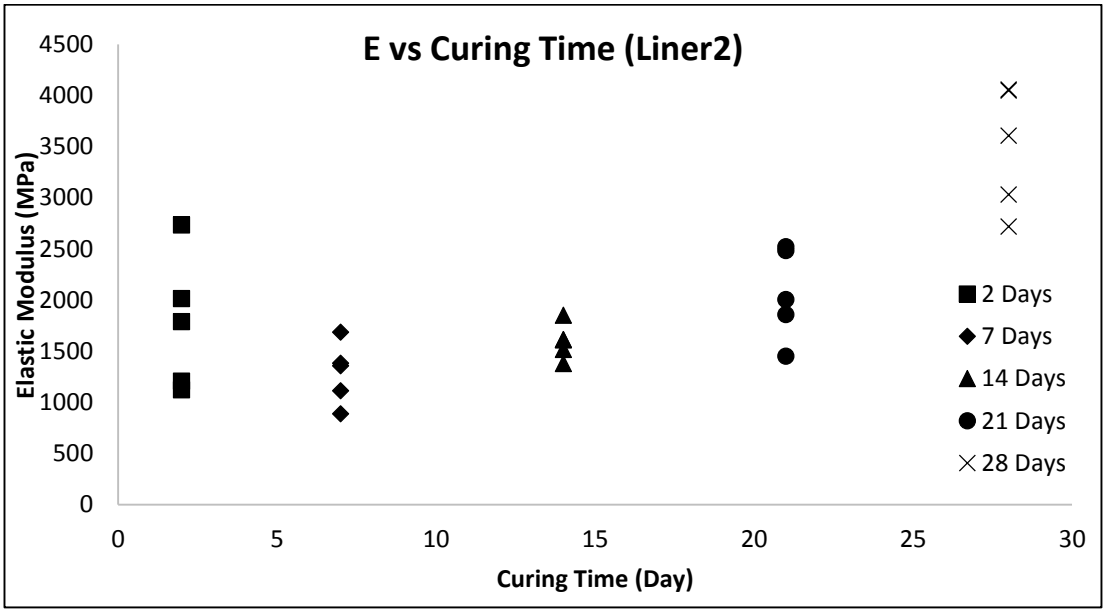

Figure 3.46 Elastic Modulus versus Curing Time Relationships (Liner 2)

According to Figure 3.46, 2nd day test results are relatively higher than expected values. 2nd day test results cause the decrease of correlation coefficient. Average elastic modulus test results are given in Table 3.17.

Table 3.17 Average Elastic Modulus versus Curing Period

Curing Time	Avg. E (MPa)
2 Day	1774 ± 657
7 Days	1286 ± 301
14 Days	1595± 173
21 Days	2065 ± 449
28 Days	3493 ± 603

Third result graph is on Poisson's ratio versus curing time dependency. As a result of the compression tests, unusual Poisson's ratios are obtained. In the literature, Poisson's ratio of TSL material is generally assumed to be between 0.3 and 0.4. Calculated Poisson's ratios are extremely small values compared to the literature. Moreover, it is observed that there is no correlation between Poisson's ratio and curing time (Figure 3.47). This can be due to the polypropylene fiber content of the material since it

restricts the lateral deformation. Average Poisson's ratio values are presented in Table 3.18.

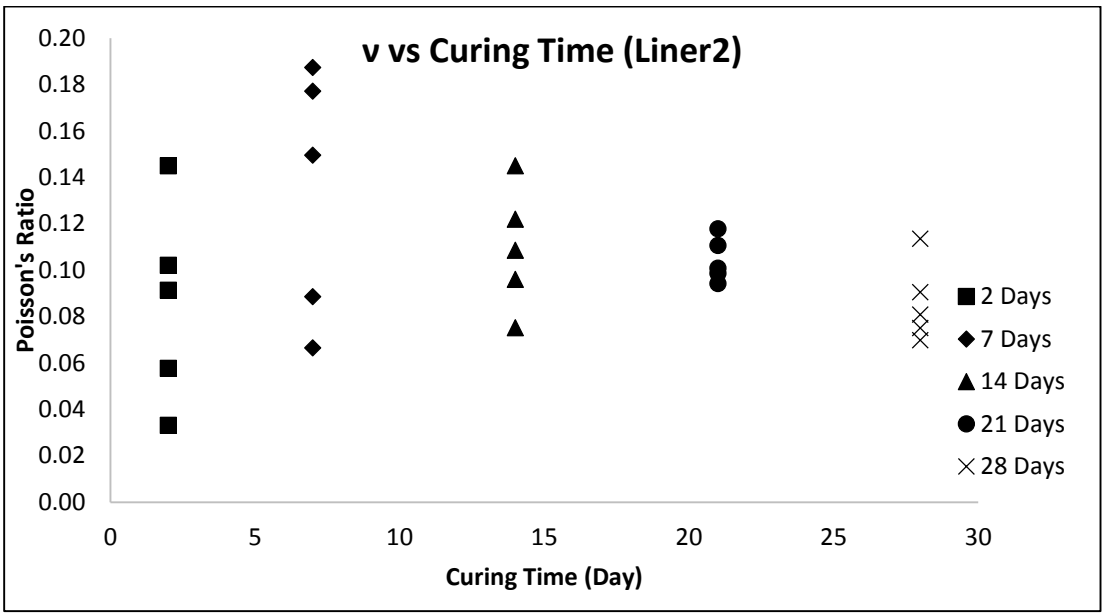

Figure 3.47 Poisson's Ratio Change versus Curing Time

As a result of the Poisson's ratio investigation; an average Poisson's ratio is found as 0.10 for brittle TSL. Poisson's ratio values are given in Table 3.18.

Table 3.18 Average Poisson's Ratio Values for a Specified Curing Time

Curing Time	**Avg. ν**
2 Day	0.09 ± 0.04
7 Days	0.13 ± 0.05
14 Days	0.11 ± 0.03
21 Days	0.10 ± 0.01
28 Days	0.09 ± 0.02

To sum up, UCS, elastic modulus and Poisson's ratios are calculated; and their relationships with curing time are investigated. As expected, UCS parameter strongly depends on curing time. As curing time increases, UCS and elastic modulus also grow. These relationships can also be defined with logarithmic equations. Table 3.19 presents the related equation and the correlation coefficient of the related graph. On

the other hand, Poisson's ratio change could not be expressed by curing time change. Note that, all the test results and the sample figures are presented in Appendix B.

Table 3.19 Equations and Correlation Coefficients of Given Curves

Equation Name (y)	Equation(x: curing time)	R^2
UCS	y = 5.2585ln(x) + 10.52	0.58

Finally, elastic modulus versus compressive strength correlation equation is also plotted for Liner 2 to be used in the future studies. This equation enables a practical elastic modulus estimation for brittle type TSLs. Equation of the curve is as follows:

$$Elastic\ Modulus\ (MPa)\ =\ 2338.9\ ln\ (UCS\ (MPa))\ -\ 5176 \qquad [3.10]$$

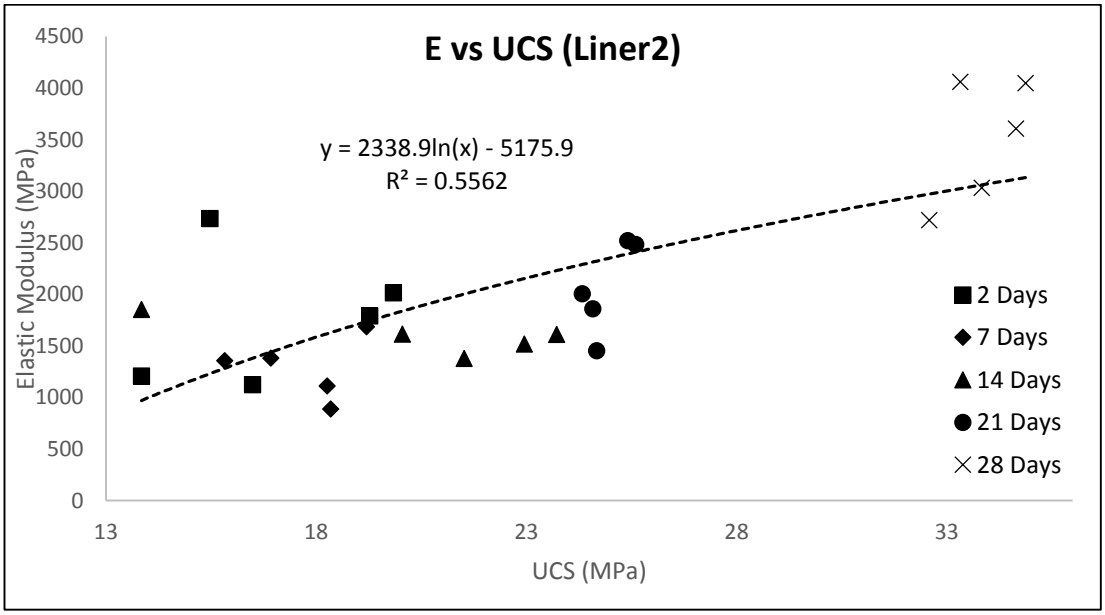

Figure 3.48 Elastic Modulus versus Compressive Strength Relationships

Comparison of Compression Test Properties of Two Products

Since UCS values of Liner 1 could not be found, there is no possibility of comparing the UCS values.

As Liner 2 is a stronger and a stiffer material, elastic modulus of Liner 2 is also higher than Liner 1. Figure 3.49 shows elastic modulus growth versus curing time of two

products. For better comparison purposes, logarithmic plot is used in this graph since elastic modulus values of the tested products are significantly different. At the end of 28 days curing period, Liner 1 (ductile) has less than 100 MPa elastic module value. On the other hand, Liner 2 reaches about 3.5 GPa elastic modulus for the same curing time.

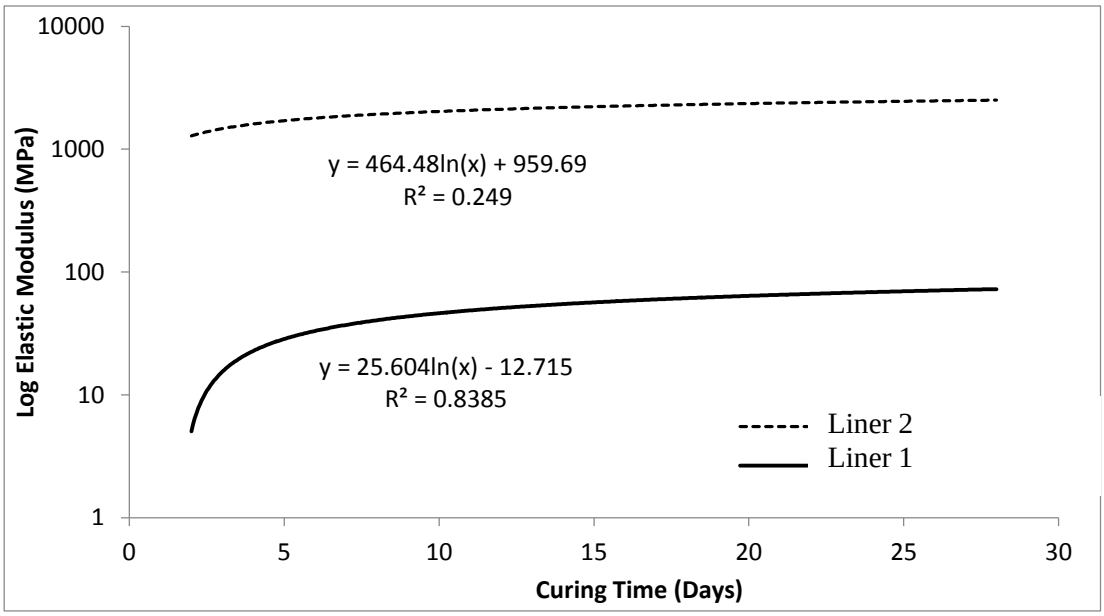

Figure 3.49. Elastic Modulus Growths with Curing Time

When Poisson's ratios are compared, Liner 1 and Liner 2 has an average Poisson's ratio of 0.39 and 0.10, respectively. Variations in Poisson's ratios of Liner 1 depend on the curing time. Conversely, calculated Poisson's ratios for Liner 2 have extremely small values which give an average value of 0.10. There is no dependency between the Poisson's ratios of Liner 2 and the curing time.

Degree of Brittleness of Liners

In order to be able to compare the brittleness of both liners, the degree of brittleness which is the ratio of uniaxial compressive strength and tensile strength is found. As can be seen from Table 3.20, Liner 2 is more brittle compared to Liner 1.

Table 3.20 Ratios of UCS and Tensile Strength for Both Liners

	Liner 1					**Liner 2**				
Curing Day	**1&2**	**7**	**14**	**21**	**28**	**1&2**	**7**	**14**	**21**	**28**
Uniaxial Compressive Strength (MPa)	0.78	2.55	3.65	3.46	3.71	16.98	17.71	20.42	24.92	33.85
Tensile Strength (MPa)	0.58	2.93	4.21	4.26	5.08	2.15	3.93	4.97	5.05	5.27
Ratio	1.34	0.87	0.87	0.81	0.73	7.90	4.51	4.11	4.93	6.42
Average	**0.90**					**5.60**				

CHAPTER 4

NUMERICAL MODELLING

This part presents the numerical modelling of the laboratory tests. Distinct element method (DEM) is relatively new technique in modelling of underground openings. One challenging issue for this chapter is the determination of TSL input parameters to be used in the future studies. Chapter 4.1 to 4.5 describe overview of DEM, test geometry and input parameters and model results.

4.1 Overview of DEM

DEM, i.e. Discrete Element Method, was firstly proposed by Cundall and Strack (1979); and it is utilized to model movement and interaction of circular assembles in analysis of rock and soil mechanics problems. In addition to circular particles, discrete element model also includes walls as a boundary. Walls allow one to apply velocity boundary conditions to assemblies of balls for purposes of compaction and confinement. The balls and walls interact with one another via the forces that arise at contacts.

This method is originally used as a tool to perform research into the behaviour of granular material; representative elements containing hundreds of particles are tested numerically. The particle model is used to comprehend element behaviour (with uniform conditions) while continuum method is used to solve real problems that involve complicated deformation patterns (with the element behaviour derived from the particle-model tests).

A physical problem on the movement and interaction of circular or spherical particles with a finite mass can be modelled directly by PFC2D- PFC3D software. PFC software

has a wide range of application in various disciplines. These applications exploit the ability of the program to model the interaction of many discrete objects, the large-strain capability or the ability to treat the process of fracturing as the progressive breaking of discrete bonds. Main utilization areas of PFC2D are noted below. With the development of liner characterization, new implementation areas can be added to this list in the future.

• Bulk handling process; mixing and conveying,
• Bulk flow of material in bins, chutes, silos and pipes,
• Mine caving process; fracture, collapse, fragmentation and flow of rock blocks,
• Seismic response and collapse of structures composed of beams represented by arrays of bonded particles,
• Impact of objects composed of bonded particles: dynamic breakage,
• Compaction of powder in molds,
• Fundamental studies of granular materials: yield, flow, volume changes and so on,
• Fundamental studies of solids, represented by bonded assemblies of particles: damage accumulation, fracture and acoustic emission,
• Slurry flow and fluidized beds, in which particles are transported by, and interact with, a moving fluid,

PFC basically enables finite displacements and rotations of discrete bodies, including complete detachment, and recognizes new contacts. Newton's 2nd law of motion is solved via explicit finite-difference procedure for each time step interval. The full equation of motion is solved at each step and time step adjusts automatically according to local conditions. Note that, only two force components and one moment component exist in a PFC2D model.

The calculations performed in the DEM allow a transition zone between the rule of Newton's second law to the particles and a force-displacement law at the contacts. Newton's second law is used to determine the motion of each particle arising from the contact and body forces acting upon it, while the force-displacement law is used to update the contact forces arising from the relative motion at each contact. The presence

of walls in PFC2D requires only that the force-displacement law account for ball-wall contacts. Newton's second law is not applied to walls, since the wall motion is the boundary of analysis specified by the user (Itasca, 2008)

In the DEM, the interaction of the particles is treated as a dynamic process until the internal forces ensure the equilibrium of particles. The contact forces and displacements of a stressed particle assembly are found by tracing the movements of the individual particles. Movements result from the propagation through the particle system of disturbances caused by specified wall and particle motion and/or body forces. This is a dynamic process in which the speed of propagation depends on the physical properties of the discrete system. Figure 4.1 Show the general notation using in theory of DEM.

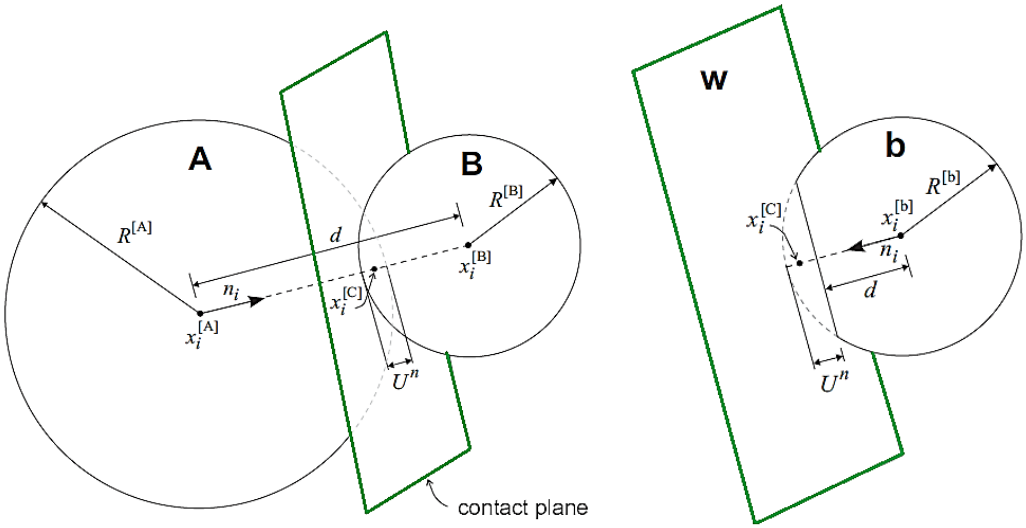

Figure 4.1 General Notation Used to Describe Ball- Ball (left) and Ball- Wall (Right) Contacts

As stated in PFC2D Manual (Itasca, 2008), the dynamic behaviour is represented numerically by a timestepping algorithm in which it is assumed that the velocities and accelerations are constant within each timestep. The start of each timestep, the set of contacts is updated from the known particle and wall positions. The force-displacement law is then applied to each contact to update the contact forces based on the relative motion between the two entities at the contact and the contact constitutive model, then, the law of motion is applied to each particle to update its velocity and

position based on the resultant force and moment arising from the contact forces and any body forces acting on the particle. Also, the wall positions are updated based on the specified wall velocities. (Figure 4.2)

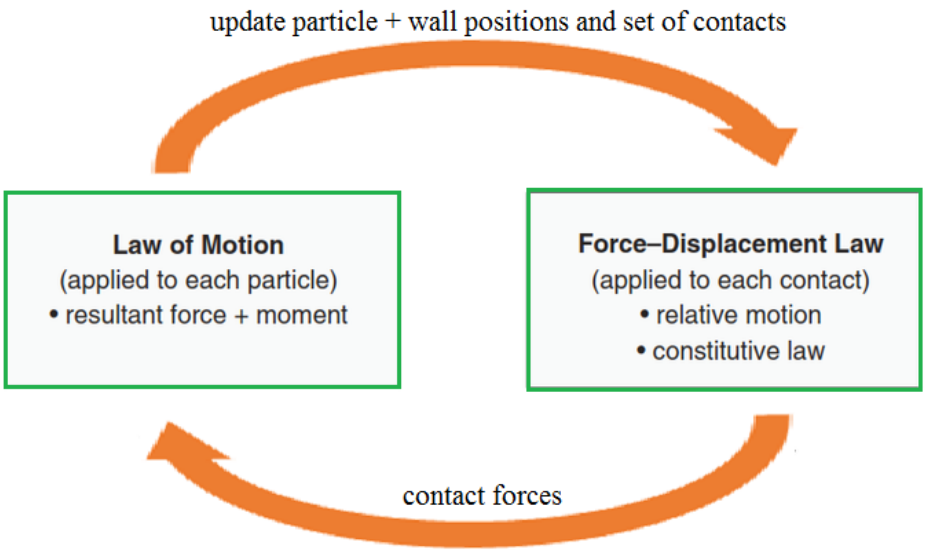

Figure 4.2. Calculation Cycle in PFC2D (Itasca, 2008)

A study done by Potyondy and Cundall in 2004, shows that it is possible to model the mechanical behavior of rock by using a method that assumes that rock has both grains and cement, which are deformable and breakable. The bonded-particle model (BPM), due to its ability to provide a platform for this conceptual method, is able to simulate the mechanical behavior of rock.

BPM gives opportunity to model contacts and bonds with microproperties, regarding the second law of Newton. By this way, macroproperties can be obtained with using bond failures, sliding movements and contact specifications which raised from the specified microproperties. Therefore, it can be assumed as a direct model technique instead of theoretical analysis which causes limitations on the model.

Following this substantial work, various test modelling studies were conducted based on bonded particle model. In these studies, rock, soil, and asphalt samples were used to obtain DEM input parameters. In addition, some researchers performed underground opening modelling by using previously acquired parameters. Since TSLs

are defined as heterogeneous material composed of cemented grains, BPM model is appropriate for TSL modelling. However, there is still lack of study about TSLs test calibration to be used in the modelling stage. Researchers generally assume those input parameters as a constant value without calibration. Curing time dependency is also neglected in the recent studies. In this basis, this thesis study reveals the importance of curing time for following mentioned input parameters; and it also examines the numerical modelling of experimental results.

The PFC software has an embedded code language, FISH. This language makes possible to define new user defined functions and features. For instance, new defined variables may be plotted or printed, special particle generators may be implemented, servo-control may be applied to a numerical test, unusual distributions of properties may be specified, and parameter studies may be automated. Moreover, Potyondy and Cundall's studies code is also available in fishtank functions in the software. This function supports BPM by means of material-genesis procedure and measurement of properties. This function contains 5 different laboratory test simulations, Brazilian test, direct tensile test, uniaxial and biaxial compression test, and fracture toughness test for simple and complex particle configuration. In this thesis study, Fishtank have been used to generate sample and to perform the modelling of uniaxial compression test and direct tensile test with some modification.

4.2 Specimen Geometry

In modelling, one representative test model is used for each of liner type, test type, and curing time. A total of 18 test models are carried out. For these runs, model geometries are held exactly same dimensions with the experiments.

Due to the inability of software to create complex shapes, only the narrower section of test specimens were modelled as shown in Figure 4.3. Yellow balls represent the gauge length and the remaining of the specimen and the length of this section is determined from measured initial distance between the grips of the loading machine during the

laboratory tests. Blue balls represent the residue part of the specimen inside clamps. Opposite velocities are applied to these strongly bonded blue balls.

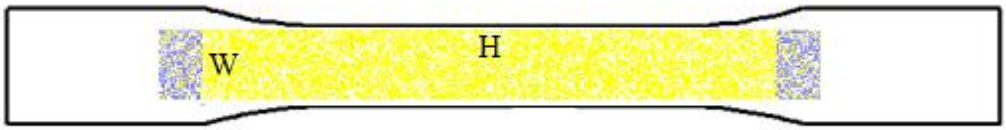

Figure 4.3 Tensile Test Geometry for Numerical Models.

For compression test geometries, 2D rectangular models (height (H)/width (W) > 2) are generated. Since laboratory test specimens have similar but different dimensions, all of the width and length measures are taken into consideration for each curing time in this step. Then, the average of the dimensions was taken as a representable value. Sample compression test geometry and platens are shown in Figure 4.4. During modelling, platen is moves toward each other with a constant velocity.

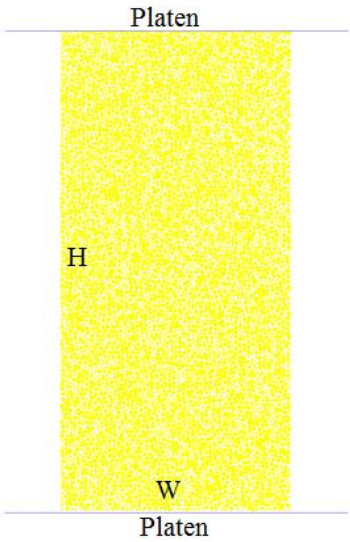

Figure 4.4 Compression Test Geometry

While the creation of geometry is relatively simple, decision making of constant input parameters is comparatively more time consuming and difficult part in the modelling stage. Each input parameter is described one by one in the following section.

4.3 Input Parameters

Input parameters must be selected carefully; and they should be representative for the TSL products since the numerical model results are highly sensitive to each parameter. Main input parameters of PFC2D is number of particles (ball radius), density of the particles, loading rate and friction coefficient.

4.3.1. Number of Particles or Ball Radius

The first parameter is the particle size. Particle size directly effects the computation time of a model. The optimum ball radius is selected regarding the most appropriate dimension which is large enough for fully representing the tested material behavior and also small enough to optimize the computation time.

Literature review and preliminary studies indicate that increasing ball radius slightly changes the strength and Young's modulus of the model (Cai, 2013). This thesis reveals that ball radius also effects the failure location of the specimen not significantly. In this sense, 6 different tensile models were generated to observe the importance of ball radius while other parameters were kept constant. As a result, minimum ball radius was determined to be between 0.11 mm and 1.00 mm. Figure 4.4 shows the sensitivity of ball radius versus strength and Young's modulus parameters. As illustrated in Figure 4.5, there is no apparent effect of ball radius change on strength and Young's modulus.

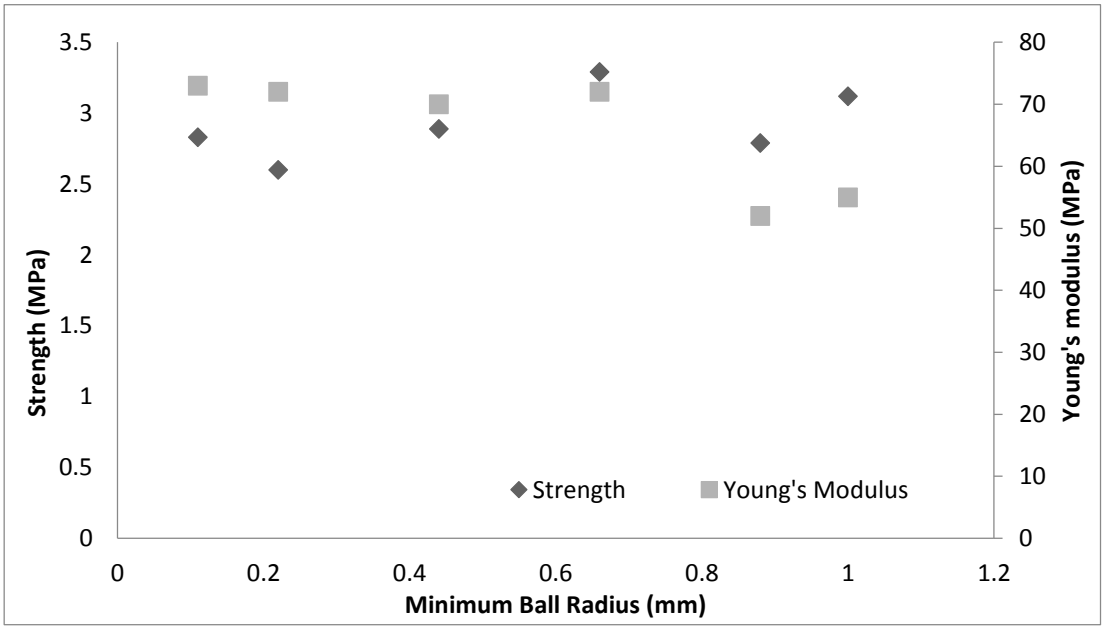

Figure 4.5 Effect of Ball Radius on Elastic Properties

According to the Cai (2013), the optimum number of particle should be about 6000 for granular asphalt sample models. In this basis, ball radius in PFC2D model satisfied the selection of about 6000 particles in the borders of predetermined sample dimensions. Therefore, overall ball radius is selected as 0.25 mm. In experiment phase, the grain size of powder components of TSLs are predicted as 0.2 mm radius at least. Therefore, ball radius in the computational model is taken as 0.2 in minimum at the modelling stage. Since the TSL powder component consists of various chemical components more than one, the radius of particles is then selected with a range between 0.2 to 0.3 mm with Gaussian Distribution Function, i.e. normal distribution. Figure 4.6 shows the relationship between ball radius variations and failure locations for the models having balls 0.11×10^{-3} m to 1.00×10^{-3} m radius. But ball radius change does not affect the failure load and axial displacement, as can be seen from the stress- strain curves in Figure 4.5.

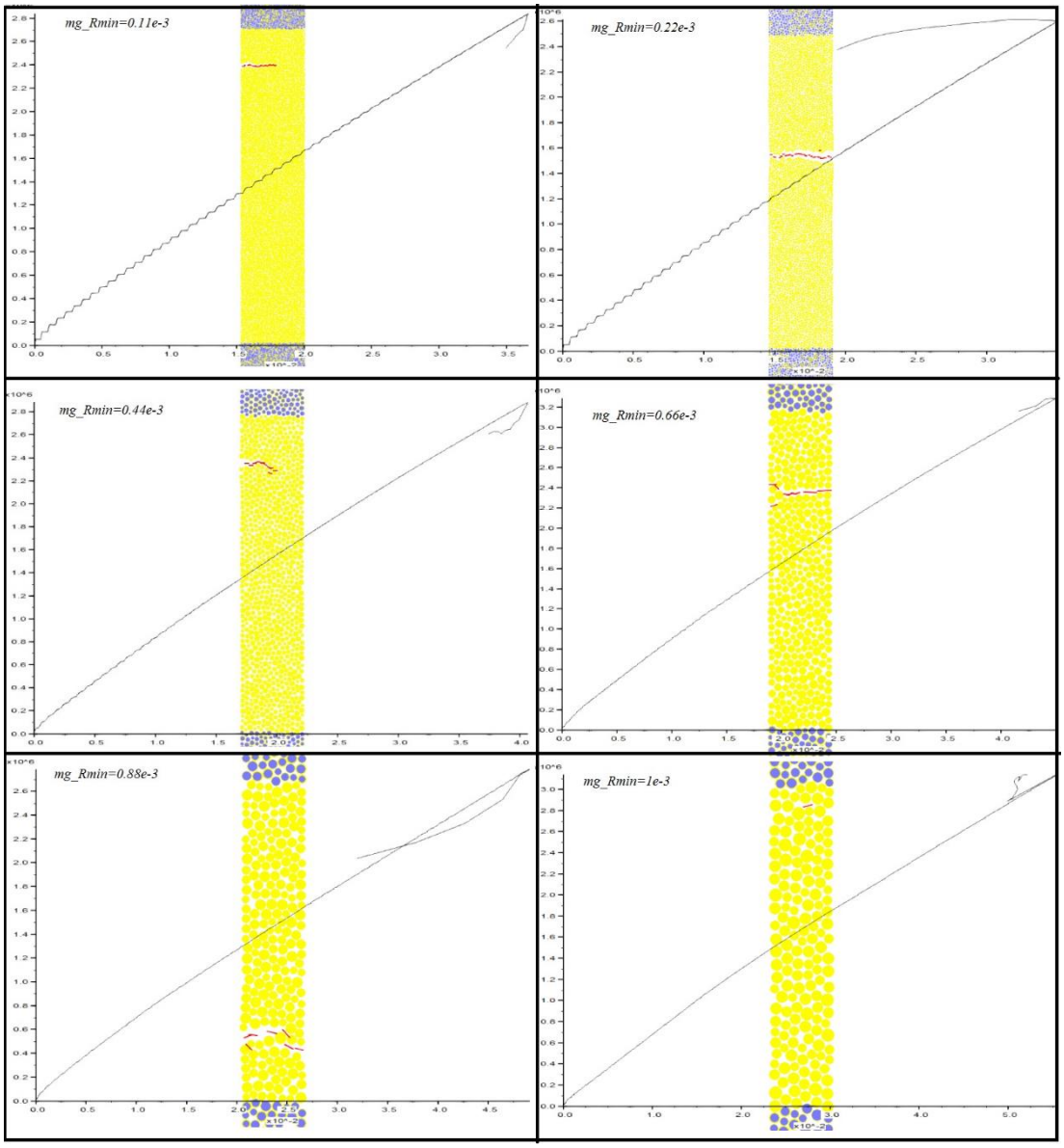

Figure 4.6 Stress-strain curves and failure locations of generated tensile test model

4.3.2. Density of the Particles

It is required to assign particle densities to the model in order to compute the accelerations of particles, considering the second law of Newton. The densities of the mixture are acquired from the catalogue data sheets obtained from the manufacturers. The densities are re-measured in the laboratory, and the values are detected nearly to be same as the catalogues. The density of the Liner 1 (ductile TSL) was about 690 kg/m^3 and the density of the second Liner (brittle TSL) was about 2010 kg/m^3.

4.3.3. Loading Rate

Loading rate is one of the most important parameter in the laboratory studies. A study conducted by Kias (2013) about the investigation of the effect of the load rate on BPM model, the uniaxial compressive strength test was conducted with different specified loading rates. As a result of this study, seen in Figure 4.7, there is no noticeable effect of loading rate on the elastic region of the stress-strain curve.

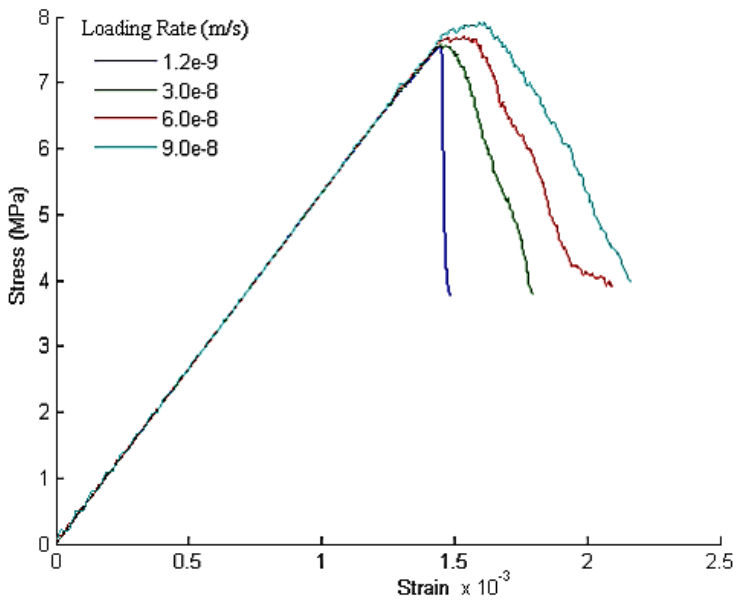

Figure 4.7 . Effect of Loading Rate on Unconfined Compression Stress-Strain Curves (Kias C. 2013)

Under the scope of the thesis, a similar study is also conducted for direct tensile test. The effect of loading rate is defined by platen strain rate (PSR) command in PFC2D software. In order to verify above mentioned results, 6 different model runs are performed. The runs states that exaggerated loading rate causes higher tensile strength and tensile modulus values (PSR> 5). Considering the processing time of the computer, platen strain rate is selected as 1 in all numeric models. Figure 4.8 shows the stress-strain behavior for different loading rates. According to the figure, load rate has not any significance effect on failure load in case of PSR value less than 5.

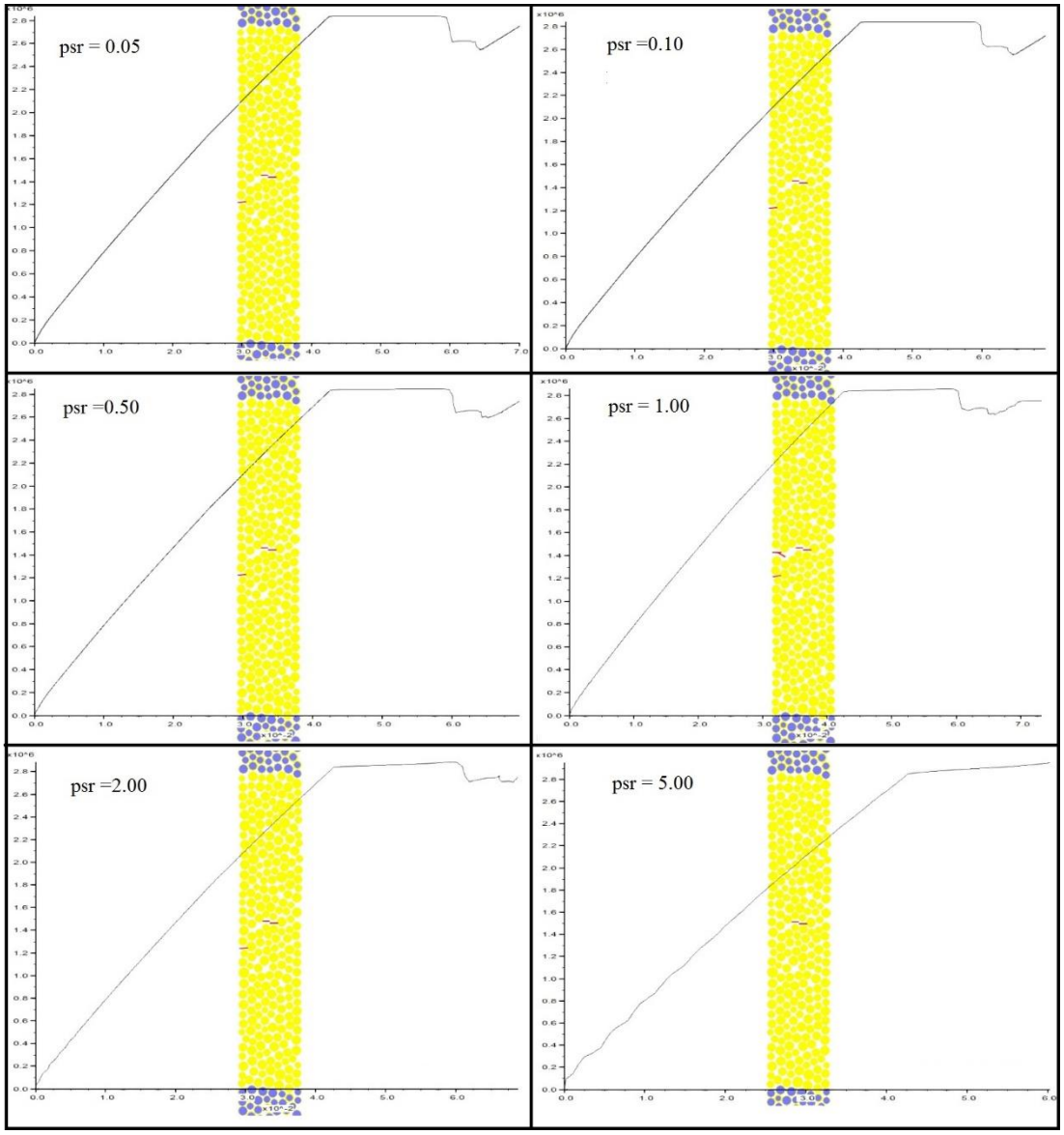

Figure 4.8 . Effect of Loading Rate on Stress-Strain Curves

4.3.4. Friction Coefficient

Friction coefficient (μ), is a dimensionless scalar value, describes the ratio of the force of friction between two bodies. The coefficient of friction varies depending on the material characterization. In rock mechanic studies, coefficient of friction is defined as the ratio of the shear over normal stress (τ/σ_n) acting between the surfaces during sliding. In this study, in order to determine optimum friction coefficient parameter for 2 products, Mohr Coulomb Envelopes are plotted. As a result, coefficient of friction is

found 0.20 and 0.75 for 2 products, respectively. Figure 4.9 shows the plotting of Mohr Envelope for Liner 2.

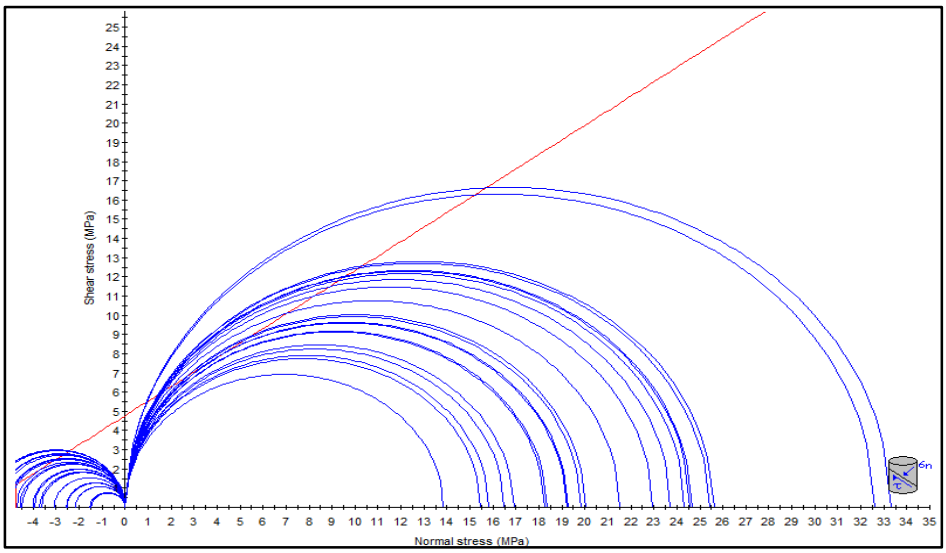

Figure 4.9 Mohr-Coulomb Envelope of Liner 2

In numerical studies, previously described 4 parameters are kept constant. Other micro and macro properties of ball and bond are taken as variable parameters for each model. Micro properties listed below are utilized to reach the macro properties (strength, modulus of elasticity):

1. Elastic modulus of the ball (taken from the result of laboratory test),
2. Elastic modulus of the parallel bond (trial and error iteration until observing the actual elastic modulus obtained from the laboratory test),
3. Overall normal strength of the parallel bond (trial and error iteration until observing the actual failure stress value from the laboratory test) and standard deviation of the value $(\bar{\sigma_c}, \bar{\lambda})$,
4. Overall shear strength of the parallel bond is taken as the same as normal strength of parallel bond and standard deviation of the value too$(\bar{\tau_c}, \bar{\lambda})$.

During the numerical models, the major aim is to obtain the same macro properties (strength, modulus of elasticity) of the products for each curing time. For this purpose, parallel bonds, Young's modulus, normal and shear strength parameters are

investigated by trial and error iterations. An average of 6 iterations is performed for each curing duration to reach the actual macro properties.

4.4 Tensile Test Model Results

In tensile test modelling, 4 models for Liner 1 and 5 model for Liner 2 is conducted. For specimen generation part, overall specimen dimensions for each curing time are taken into consideration. As mentioned before, since program is not enable to generate complex shapes, only the narrow part of the specimen is generated with overall 5500 balls having 0.25± 0.05 mm radius. In order to obtain failure in the middle part of the specimen, top and bottom parts are strengthened. Moreover, a constant velocity of 0.07 m/s in opposite direction is applied to these strengthened balls.

Modelling of Liner 1 is comparatively more time consuming since it owns a ductile material characteristic. Especially the 1 day cured sample model of Liner 1 is not enabled due to extreme strain capability for corresponding small stress amount. Correlation between stress-strain curves of experimental and computational outputs is significant to validate the model results. Figure 4.10 shows a model consisting of 5600 balls for a tensile test with different stages of extension. Broken bonds are represented in red color.

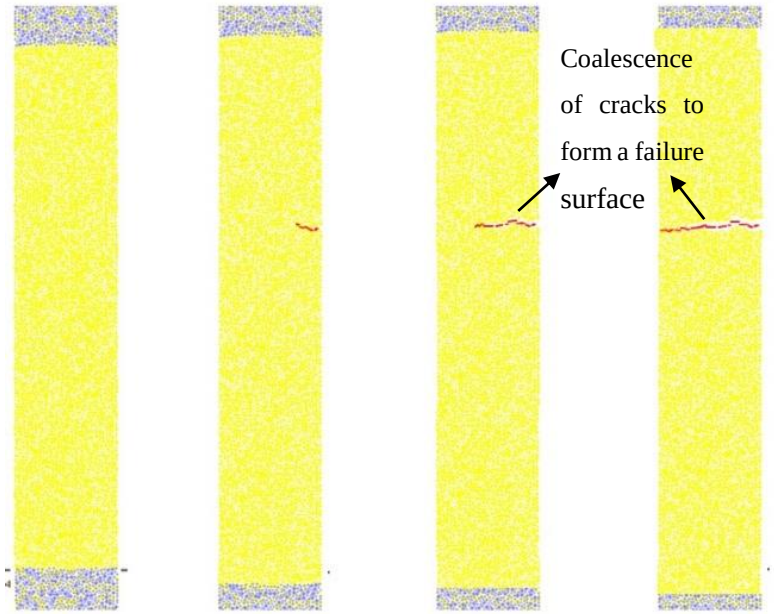

Figure 4.10 Tensile Model in the Different Stages of Pull-out Modelling Process.

Resultant micro properties and input parameters for Liner 1 are presented in Table 4.1. Representable stress- strain curve obtained in 14 days cured samples for both products are presented in Figure 4.10 and 4.11 respectively. Moreover, rest of the stress-strain curves can be seen in Appendix C. Input parameters and test results for the products are tabulated Table 4.1 to Table 4.4 respectively.

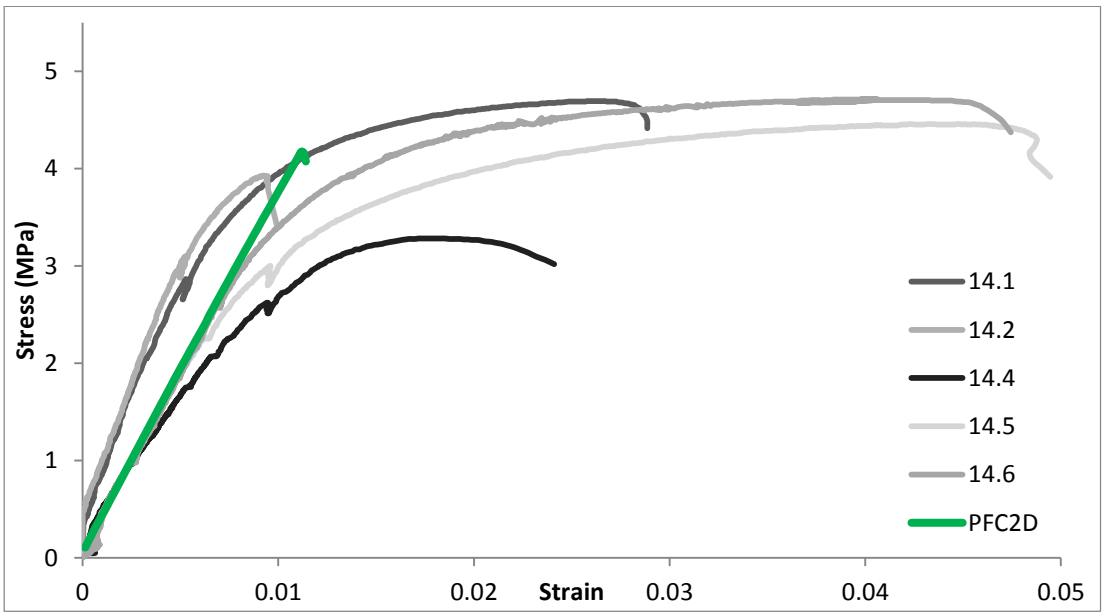

Figure 4.11 Tensile Stress-Strain Curve of 14 Day Cured Liner 1 Sample & PFC Model

As seen in Figure 4.11, elastic part of the stress strain curve can be modelled properly with PFC. Since there is a variation in experimental curves performed at the same date, there is no any expectation to obtain exactly the same linear elastic behavior for both experimental and computational results. A representative PFC model in Figure 4.10 is shown for 14 day curing of Liner 1. After the linear elastic region it is not possible to model the strain softening (ductile) region of the tests by bonded particle model, due to its limitations.

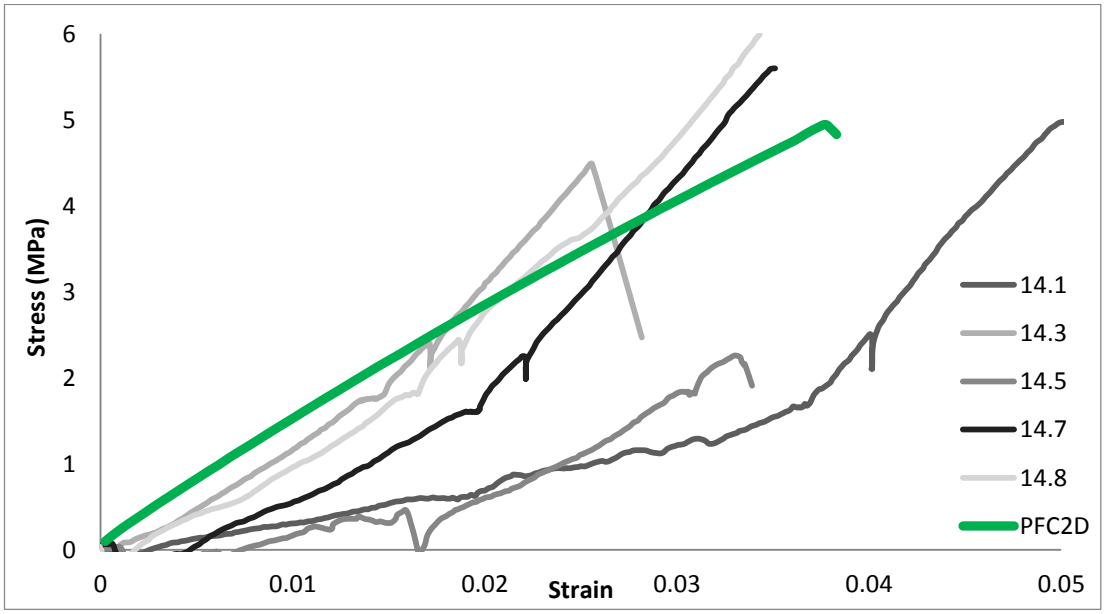

Figure 4.12 Tensile Stress-Strain Curve for 14 Day Cured Liner 2 Sample & PFC Model

Table 4.1. Constant PFC Input Parameters of Liner 1

Min. Particle radius (mm)	0.2
Max. Particle radius (mm)	0.3
Model thickness (mm)	4
Friction coefficient	0.2
Particle density (kg/m^3)	690
Applied initial stress (MPa)	0.1
Parallel Bond normal/shear strength ratio	1
Length of Strengthened part (mm)	10

Table 4.2 Variable PFC Input Parameters and results of Liner 1

Curing Days		7	14	21	28
Sample Dimensions	**Width (mm)**	11.70	11.69	10.95	10.89
	Length (mm)	79.05	82.15	85.90	82.60
Lab. Test Results	**Target UCS (MPa)**	2.93 ± 0.10	4.21 ± 0.61	4.26 ± 0.52	5.08 ± 0.79
	Target E (MPa)	286.91 ± 47.98	394.27 ± 96.27	833.77 ± 207.32	758.2 ± 367.91
Model values	**Obtained UCS (MPa)**	2.95	4.23	4.26	5.07
	Obtained E (MPa)	275.5	375.6	825.7	768.3
	Parallel bond E (MPa)	36.20	48.25	104.36	90.1
	Parallel bond strength (MPa)	1.81±0.01	2.47 ± 0.4	3.05 ± 0.4	3.07 ± 0.5
	Obtained - P. bond strength ratio	1.63	1.71	1.40	1.65
	Obtained - P. bond E ratio	7.61	7.78	7.91	8.52

Table 4.3 Constant PFC Input Parameters of Liner 2

Min. Particle radius (mm)	0.2
Max. Particle radius (mm)	0.3
Model thickness (mm)	4
Friction coefficient	0.75
Particle density (kg/m^3)	2010
Applied initial stress (MPa)	0.1
Parallel Bond normal/shear strength ratio	1
Length of Strengthened part (mm)	10

Table 4.4 Variable Input Parameters and PFC results of Liner 2

Curing Days		1	7	14	21	28
Sample Dimensions	**Width (mm)**	13.66	13.60	13.55	13.41	13.43
	Length (mm)	62.23	67.72	73.90	70.21	67.77
Lab. Test Results	**Target UCS (MPa)**	2.15 ± 0.68	3.93 ± 1.02	4.97 ± 0.67	5.05 ± 0.98	5.27 ± 0.45
	Target E (MPa)	58.82 ± 15.91	118.78 ±44.18	125.04 ± 11.96	131.75 ± 17.88	138.61 ± 19.29
Model values	**Obtained UCS (MPa)**	2.16	3.93	4.97	5.04	5.31
	Obtained E (MPa)	60.10	119.60	126.10	130.60	139.28
	Parallel bond E (MPa)	10.17	20.36	21.01	21.16	23.34
	Parallel bond strength (MPa)	1.19 ± 0.40	2.09 ± 0.50	2.73 ± 0.40	2.81 ± 0.50	2.98 ± 0.35
	Obtained - P. bond strength ratio	1.81	1.88	1.82	1.80	1.77
	Obtained - P. bond E ratio	5.78	5.83	5.95	6.22	5.93

Elastic modulus and bond strength parameters of parallel bond results as stated in Table 4.2 and 4.4 can be regarded as academically valuable since there is no any available study in the relevant literature. The researchers can utilize these study findings in their future researches as Liner 2 for brittle liner modelling and Liner 1 for ductile liner modelling for any support behaviour of TSLs in PFC: such as TSL lined tunnels or roadways etc. In addition, characteristic variations of the products depending on the curing times can also be utilized in the future studies.

It should also be noted that for both products in Table 4.2 and Table 4.4, UCS and modulus values of the tests and models matches very well. Moreover, the ratios between laboratory test modulus and model parallel bond modulus ratio changes between 5.78 to 8.52. In the same way the ratio between the laboratory test UCS and model parallel bond strength changes between 1.40 to 1.88. Therefore one can take these ratios and directly calculate the PFC modelling input values for parallel bond strength and parallel bond modulus without going through labor some modelling simulations.

The growth in strength values of parallel bond for two products depending on the curing time can be investigated in Figure 4.13. Elastic modulus changes depending on the curing time is presented in Figure 4.14.

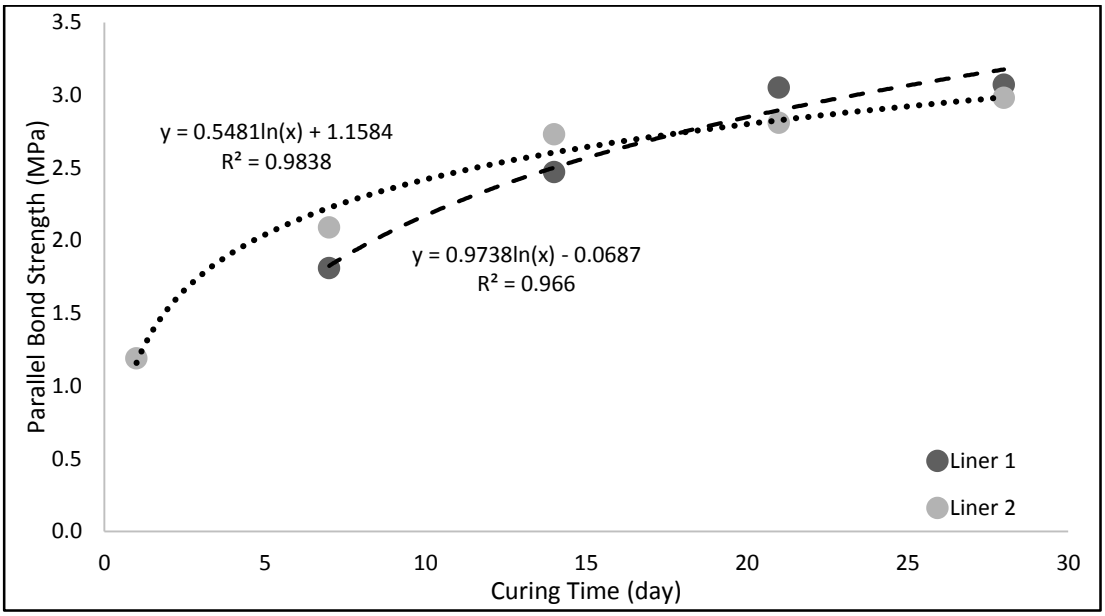

Figure 4.13 Parallel Bond Strength versus Curing Time (Tensile Tests)

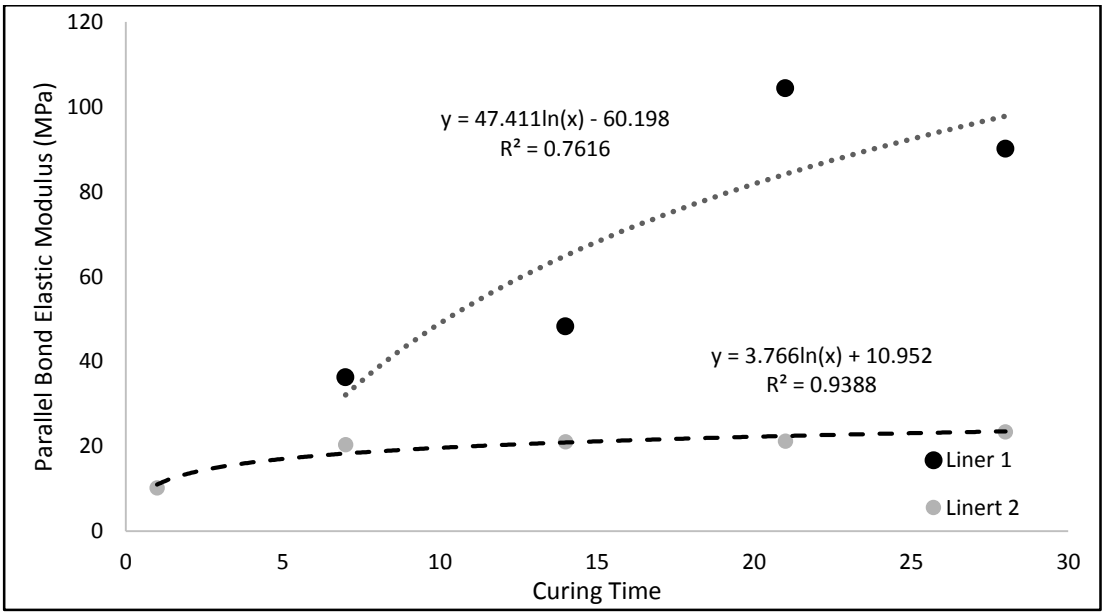

Figure 4.14 Parallel Bond Elastic Modulus versus Curing Time (Tensile Tests)

Regression equations in Table 4.5 give time dependent values of bond strength and elastic modulus if the time value (x) is specified as an input in the equations.

Table 4.5 Equations and Correlation Coefficients of Given Curves (Tensile Tests)

	Equation Name (y)	**Equation**	**R^2**
Liner 1	P. bond strength	y = 0.9738ln(x) - 0.069	0.97
	P. bond Elastic modulus	y = 47.411ln(x) - 60.198	0.76
Liner 2	P. bond strength	y = 0.5481ln(x) + 1.158	0.98
	P. bond Elastic modulus	y = 3.766ln(x) + 10.952	0.94

x: Curing time in days

As a result of tensile test modelling, it is observed that the theoretical elastic region can be simulated by simple linear model method. For ductile type materials, BPM technique is not suitable. Other model tools such as simple ductile or simple viscoelastic model can show more realistic result for the elastoplastic region of the stress strain curve. For brittle materials, simple linear model simulation is enough to give acceptable results.

Note that similar bond properties are also found in the coming compression test modelling part.

4.5 Compression Test Model Results

Compression test modelling is extensively observed in rock and soil mechanics studies as a test simulation tool. However, there is not any compression test modelling about TSLs in the literature. In the thesis, 4 simulations for Liner 1 and 5 simulations for Liner 2 are conducted. The specimen dimensions utilized in the models according to the curing day are presented in Table 4.7 and 4.9. A total of 5500 balls were generated with 0.25± 0.05 mm radius in PFC. Rigid walls were constituted at the top and bottom of the specimen and constant small velocity (0.055 m/s) is applied to these platens in order to compress the specimen.

Similar to tensile test modelling part, 2 days cured Liner 1 specimen couldn't be simulated due to small loading capacity. A small value of load with 0.1 MPa was applied to the model for the seating of the particles and also in order to prevent the rotation of the specimen. However, rotation of 2 days cured Liner 1 couldn't be prevented due to low load carrying capacity of the product. Figure 4.15 shows general views of modelled specimen in the different stages of PFC compression test modelling. Failed bonds can also be investigated from the red zones in the Figure 4.14.

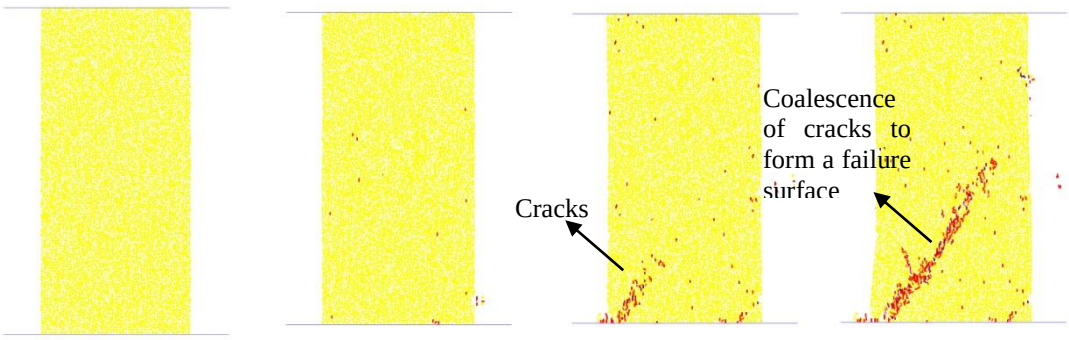

Figure 4.15 PFC Compression Model in the Different Stages of Simulation Process.

As a result of modelling process, similar stress-strain curves are obtained. Sample stress- strain curve and expected failure location of 14 days cured samples for both 2 products can be viewed in Figure 4.16 and Figure 4.17, respectively. Other curves and specimen appearances can be seen in Appendix C.

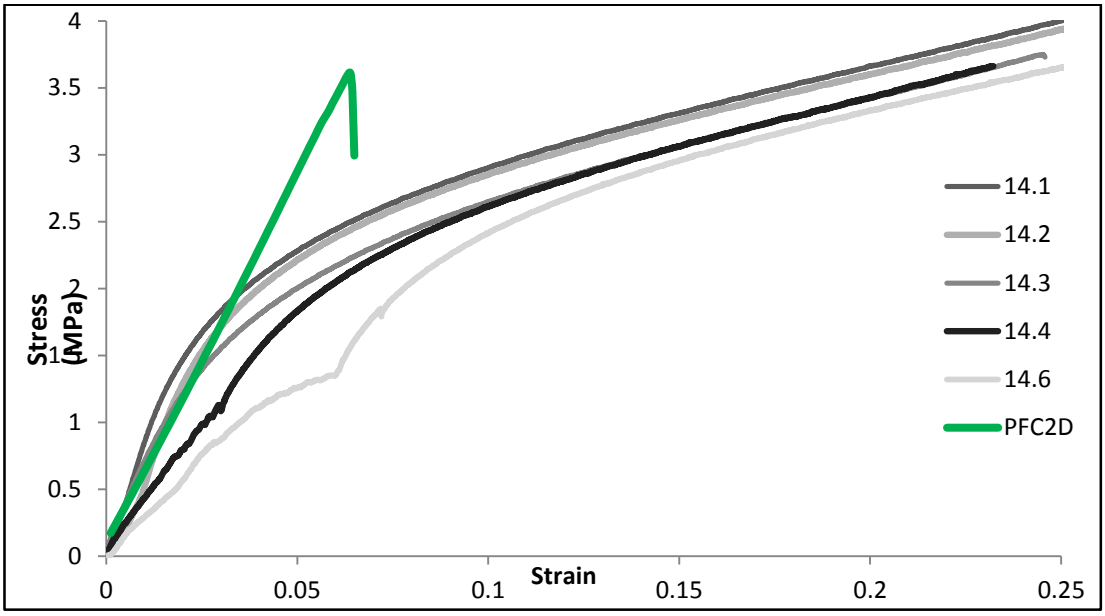

Figure 4.16 Stress-Strain Curve for 14 Day Cured Liner 1 Sample & PFC Model

According to the stress strain curve, elastic part of the run seems to be highly matching with to the laboratory results. On the other hand, no comparative results could be obtained in the elastoplastic region because it requires extra coding in PFC. Since the modelling is performed with representative laboratory sample results of the associated curing day, curves with exactly same behavior cannot be expected. PFC model in Figure 4.16 does not match either of them but it rather matches their slope.

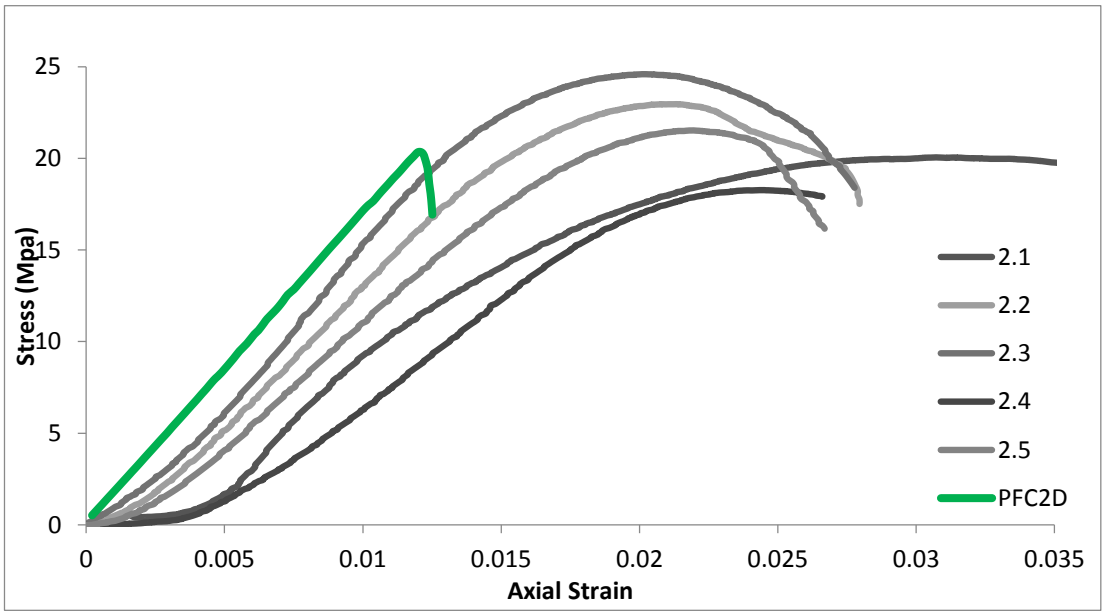

Figure 4.17 PFC Model of Stress-Strain Curve for 14 Day Cured Liner 2 Sample

Although Liner 2 is a relatively brittle material, the laboratory tests show that it is not really a brittle material, it shows some ductile post peak behaviour which might be attributed its fiber content.

Program input parameters and results are presented for Liner 1 and Liner 2 in Table 4.6 to 4.9. Table 4.6 and 4.8 give constant input parameters. On the other hand, Table 4.7 and 4.9 present the variable inputs and results of the compression test modelling part. It should be mentioned that for both products in Table 4.8 and Table 4.9 UCS and elastic modulus values of runs and laboratory test results match quite well.

It should also be noted that for both products in Table 4.7 and Table 4.9 , UCS and modulus values of the tests and models matches very well. Moreover, the ratios between laboratory test modulus and model parallel bond modulus ratio changes between 1.45 to 1.72. In the same way the ratio between the laboratory test UCS and model parallel bond strength changes between 1.35 to 1.71. Therefore one can take these ratios and directly calculate the PFC modelling input values for parallel bond strength and parallel bond modulus without going through labor some modelling simulations.

Table 4.6 Constant PFC Input Parameters of Liner 1

Min. Particle radius (mm)	0.2
Max. Particle radius (mm)	0.3
Friction coefficient	0.2
Particle density (kg/m^3)	690
Applied initial stress (MPa)	0.1
Parallel Bond normal/shear strength ratio	1

Table 4.7 PFC Compression Test Variable Input Parameters and Results of Liner 1

Curing Days		7	14	21	28
Sample Dimensions	**Width (mm)**	23.19	23.96	23.61	24.05
	Height (mm)	51.33	50.45	51.32	50.55
Lab. Test Results	**Target UCS (greater than) (MPa)**	2.55 ± 0.21	3.65 ± 0.24	3.46 ± 0.08	3.71 ± 0.12
	Target E (MPa)	45.94 ± 6.67	50.96 ± 17.88	60.08 ± 6.74	75.87 ± 10.77
Calibrated values	**Obtained UCS (MPa)**	2.54	3.62	3.46	3.73
	Obtained E (MPa)	42.64	50.34	60.61	78.75
	Parallel bond E (MPa)	26.91	31.67	41.98	56.26
	Parallel bond strength (MPa)	1.59	2.23	2.34	2.24
	Obtained - P. bond strength ratio	1.60	1.62	1.48	1.66
	Obtained - P. bond E ratio	1.71	1.61	1.43	1.35

Table 4.8 PFC Compression Test Constant Input Parameters of Liner 2

Min. Particle radius (mm)	0.2
Max. Particle radius (mm)	0.3
Friction coefficient	0.75
Particle density (kg/m^3)	2010
Applied initial stress (MPa)	0.1
Parallel Bond normal/shear strength ratio	1

Table 4.9. PFC Compression Test Variable Input Parameters and Results of Liner 2

Curing Days		**2**	**7**	**14**	**21**	**28**
Sample Dimensions	**Width (mm)**	23.98	23.89	23.91	24.01	24.04
	Height (mm)	53.25	51.05	49.70	51.41	48.48
Lab. Test Results	**Target UCS (MPa)**	16.98 ± 2.54	17.71 ± 1.33	20.42 ± 3.93	24.92 ± 0.55	33.85 ± 0.95
	Target E (MPa)	1774.20 ± 656.97	1285.5 ± 301.11	1594.5 ± 172.80	2064.6 ± 448.91	3493.5 ± 602.82
Calibrated values	**Obtained UCS (MPa)**	17	17.72	20.35	24.31	33.66
	Obtained E (MPa)	1770	1285	1574	2062	3504
	Parallel bond E (MPa)	1177.7	838	1007	1341	2404
	Parallel bond strength (MPa)	10.32	10.29	12.33	17.14	22.19
	Obtained - P. bond strength ratio	1.65	1.72	1.66	1.45	1.53
	Obtained - P. bond E ratio	1.51	1.53	1.58	1.54	1.46

In the laboratory compression tests of Liner 1, no failure is obtained in the sample. Specimens reached to the maximum stress value taken as target UCS in numerical studies.

In addition, variation of bond strength and bond elastic modulus with increasing curing time is also investigated in compression modelling part. In contrast to the tensile modelling part, output difference between two products is remarkably high in compression modelling. Figure 4.18 and 4.19 show the change of bond strength and bond elastic modulus with curing time for two products. Since the values are highly different in y axes, curves are plotted in logarithmic scale.

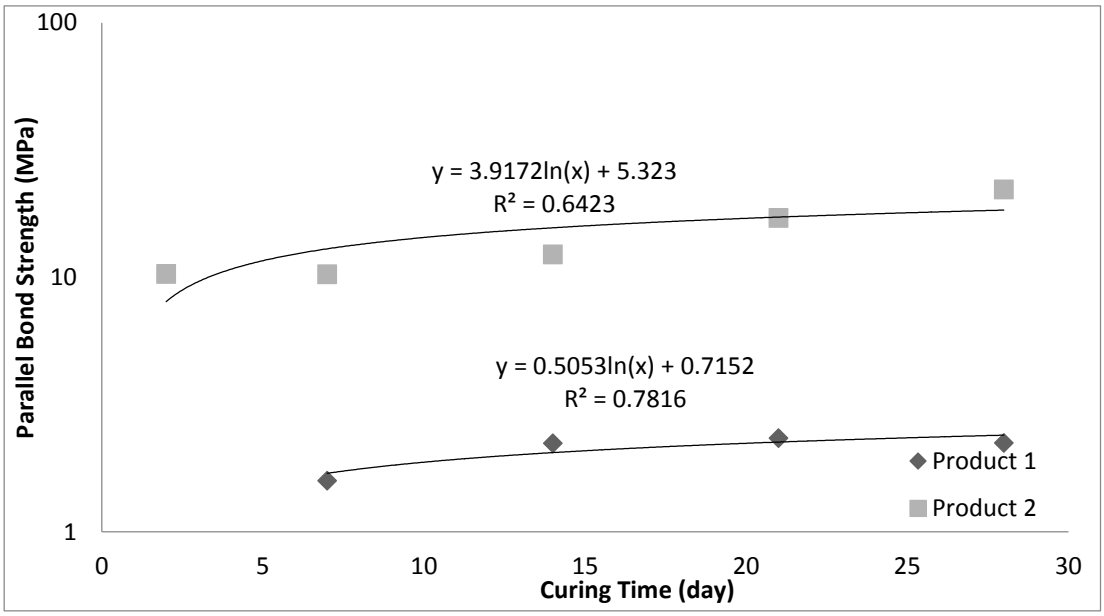

Figure 4.18 Parallel Bond Strength versus Curing Time (Compression Tests)

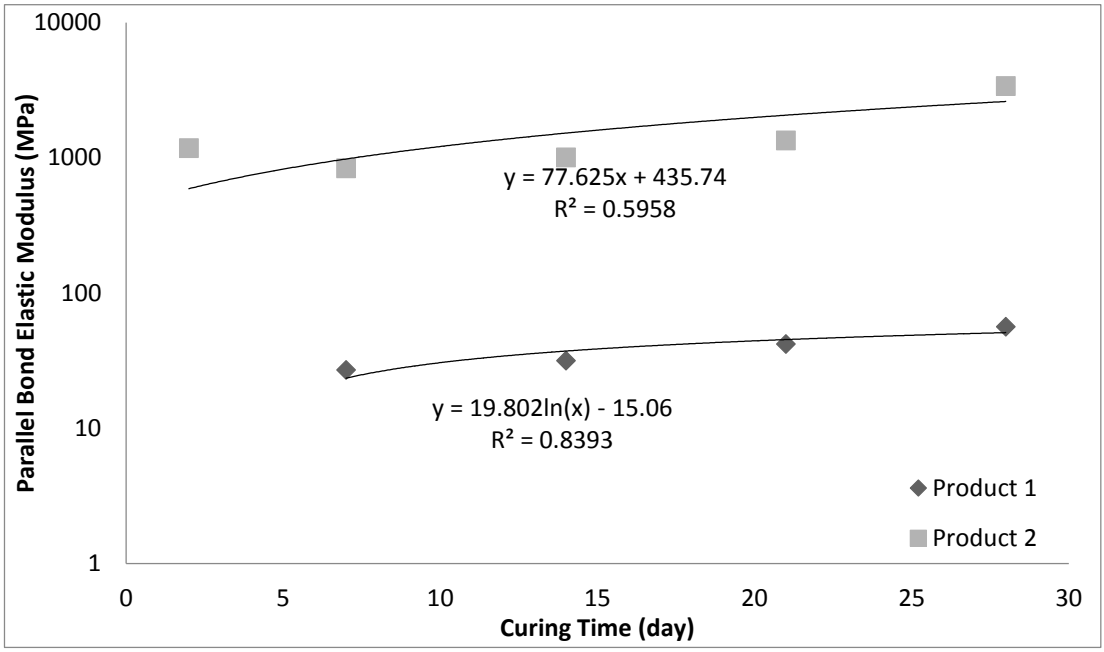

Figure 4.19 Parallel Bond Elastic Modulus versus Curing Time (Compression Tests)

Regression equations as given in Table 4.10 can be utilized to find out time dependent bond strength and elastic modulus with giving the time value (x) to the equations as an input.

Table 4.10 Equations and Correlation Coefficients of Given Curves (Compression)

	Equation Name (y)	**Equation**	**R^2**
Liner 1	P. bond strength	y = 0.5053ln(x) + 0.715	0.78
	P. bond Elastic modulus	y = 19.802ln(x) - 15.060	0.84
Liner 2	P. bond strength	y = 3.9172ln(x) + 5.323	0.64
	P. bond Elastic modulus	y = 77.625x + 435.740	0.60

x: Curing time in days

Compression test model results show that the theoretical elastic region can be modelled by a linear PFC model, as in tensile test modelling. Other model tools; such as, ductile or viscoelastic model can present more realistic result for computing and interpreting the elastoplastic region in the stress strain curve. For brittle materials, simple linear PFC model runs give more appropriate results. Since the researchers in literature assume that TSL have a linear elastic behavior, this modelling technique can be convenient in the modelling of TSL with PFC.

4.6 Comparison of Tensile and Compression PFC Models

In this section, two different PFC models are compared. Modelled values of bond strength and bond elastic modulus can be utilized in future studies. At this point, it is required to remind that calibrated bond stress and bond elastic modulus parameters are very different for tensile and compression test models. A summary table for both tests and for both products are given in Table 4.11. In the modelling of the support behaviour of TSLs for underground openings, researchers should consider which failure type is potentially expected in the support mechanism of the TSL (either tensile or compressive) and then use the relevant inputs of TSL for PFC.

It can be said that this is one of the drawbacks of modelling with PFC that one obtains different material properties; such as, bond strength and bond elastic modulus based on the type of model (compression or tension) constructed.

Table 4.11 Summary Table of PFC Models

		Model Parallel Bond Strength (MPa)					Model Parallel Bond Modulus, E (MPa)				
Curing Day		1	7	14	21	28	1	7	14	21	28
Liner 1	Tensile Model	-	1.81	2.47	3.05	3.07	-	36.27	48.25	104.36	90.1
	Comp. Model	-	1.59	2.23	2.34	2.24	-	26.91	31.67	41.98	56.26
Liner 2	Tensile Model	1.19	2.09	2.73	2.81	2.98	10.17	20.36	21.01	21.16	23.34
	Comp. Model	10.32	10.29	12.33	147.14	22.19	1177	838	1007	1341	2404

CHAPTER 5

CONCLUSIONS AND RECOMMENDATIONS

This study presents the effects of curing time an elastic material properties of TSLs. For this purpose, tensile and compression tests are conducted. In these tests two different TSL products supplied by two different TSL manufacturers are tested comparatively. When selecting these products, it is aimed that they have different chemical compositions and behave differently under loading. During the laboratory studies, samples that are prepared in the laboratory conditions with different specified curing times (1, 7, 14, 21 and 28 days for tensile tests; 2, 7, 14, 21, 28 days for compression tests) are tested based on ASTM standards (D-638 and D-695-10). Sample preparation steps and significant factors are explained in detail. Tensile strength, tensile modulus, elongation at break, compressive strength, elastic modulus and Poisson's ratio parameters are calculated for each sample. After all the tests are conducted and related equations are found, numerical modelling is done. During numerical modelling it is aimed to simulate the laboratory test with the help of a widely used distinct element software PFC2D. Since the constitutive behaviour of TSLs are yet to be known. Test simulations are conducted for each curing time for both products, and 20 different simulations are carried out. As a result of numerical studies, 2 significant parameters which are bond strength and bond elastic modulus are found by an iterative, trial and error method. Moreover, the effect of curing time for these parameters are obtained. These parameters which are the key inputs, are useful for large scale simulations of TSLs in PFC2D and also help to better understand the support mechanism of TSLs.

Main conclusions of this study are as follows:

- In sample preparation part due to different chemical compositions of TSLs, mixing and curing times are variable and shrinkage of samples may happen for the water based TSLs. At the end of 28 days curing time, the specimen dimensions significantly changes. In field application, this problem may cause a decrease in the thickness of the liner.

- As expected, the tensile strength and tensile modulus for both liners are directly related with curing time. As curing time increases tensile strength increases. The related logarithmic relationships and correlation coefficients are given in Chapter 3.

- As curing time increases the elongation capability of the liner decreases which result in higher tensile modulus. For ductile type liners elongation capability is inversely proportional to tensile strength. Moreover, the elongation capability of Liner 1 is determined to be almost 10 times lower than the manufacturer's claim for 7, 14, 21 and 28 day cured samples.

- For the first time in TSL testing literature, axial tensile displacement is measured from the gauge length of the specimens. A common malpractice of measuring the sample axial displacement from the loading machine versus from the sample's gauge length in tensile testing is observed to be very significant. Obtained results are very different for Liner 1. LVDT measured elastic modulus underestimates the value by 4 to 10 times compared to axial extensometer. On the other hand, LVDT measurements overestimates elongation at break by 3 times.

- Polypropylene fibre additives increase tensile strength of the liner, while decreasing their elongation capacity.

- Chemical composition of liners directly affects the compression test results. Liner 1 (ductile liner) does not fail in compression tests even at 100% axial strain. Therefore a lower bond compressive strength value is found for Liner 1.

- As in tensile testing part, compressive strength and elastic modulus observed to be increasing with increasing curing time for both products. The relationships and coefficients are presented in Chapter 3.

- Curing time has very little effect on Poisson's ratio. For Liner 1, after 7 days of curing time, it can be said that Poison's ratio becomes constant and has a value of 0.42. On the other hand, for Liner 2 there is no apparent correlation between Poisson's ratio and curing time. Poisson's ratio of 0.1 is found for Liner 2. The possible reason for a smaller Poisson's ratio is that it may be because of the polypropylene fibre additives preventing the lateral deformation of the test sample and brittle nature of Liner 2.

- For both liners, PFC2D models are done for tensile and compression tests for each curing time. A total of 18 runs modelled. For both products PFC is able to model linear portion of tensile stress-strain curve of the tests. PFC models matches the laboratory measured test parameters (UCS, elastic modulus, tensile strength, strain) quite well. By the help of the models PFC parameters such as parallel bond strength and parallel bond modulus of TSLs which can be used by TSL modellers and lessens the rigorous simulation process that a PFC modellers has to go through, say for an excavation with TSL liner support. It should also be mentioned that the ratios between laboratory test modulus and model parallel bond modulus ratio changes between 1.25 to 1.75. In the same way the ratio between the laboratory test UCS and model parallel bond strength changes between 1.3 to 1.7. Therefore one can take these ratios and directly calculate the PFC modelling input values for parallel bond strength and parallel bond modulus without going through labor some modelling simulations.

- Two important PFC modelling input parameters; bond elastic modulus and bond strength equations are found as a function of curing time for both TSLs.

- It can be said that one of the drawbacks of modelling with PFC that one obtains different material properties; such as, bond strength and bond elastic modulus based on the type of model (compression or tension) constructed.

According to the given conclusions, suggested recommendations and future works are listed as follows:

- In laboratory specimen molding progress, releasing agent should be used, instead of rigid molds, flexible molds can be useful to prevent damaging of test specimen.

- In compression test specimen preparation progress, molding method is inefficient, coring technique is the best way to prepare suitable test specimen.

- During tensile tests, axial displacement should be measured from the gauge length of the specimen with the help of an axial extensometer,

- In order to investigate the long term performance of TSLs it may better to carry out longer curing time tests, like 3 months, 1 year.

- Although tensile and compressive strength tests are conducted in detail, in order to see the effect of curing time on other important design parameters such as adhesion strength, different tests should be conducted.

- Temperature and humidity are also significant parameters for liners, detailed tests considering these parameters may give important results.

- For TSL selection, gaining the target strength on time is important. Manufacturers should reduce the strength gaining time of products.

- Manufacturers should re-formulate to get higher early tensile strength.
- In field application of TSL, tough and more deformable liners are needed.

- Modelled values of bond strength and bond elastic modulus can be utilized in future studies. At this point, it is required to remind that calibrated bond stress and bond elastic modulus parameters are very different for tensile and compression test models. A summary table for both tests and for both products are given in Table 4.11. In the modelling of the support behaviour of TSLs for underground openings, researchers should consider which failure type is potentially expected in the support mechanism of the TSL (either tensile or compressive) and then use the relevant inputs of TSL for PFC.

- For future studies in order to obtain full stress strain curve of ductile liners, simple ductile and simple viscoelastic models should be investigated. This way, the support mechanism may be better understood.

- PFC modelling of ductile liners should be improved for ductile portion of their behaviour.

REFERENCES

Ahn T., (2011), *"Thermal and Mechanical Stuides of Thin Spray-on Liner (TSL) for Concrete Tunnel Linings."* Phd. Thesis of the University of Western Ontario.

Archibald J.F. Espley S.J. St. Lausch P. (1997). "*Field and Laboratory Response of Mineguard Spray-on Polyurethane Liners"*. Proc. Int. Symp. on Rock Support, Lillehammer, pp. 475-490.

Archibald, J.F., and Dirige, P.A. (2006). *"Thin, Spray-on Lining Applications for Rockburst, Blast and Fire Damage Mitigation*". Proceedings of the 41st U.S. Rock Mechanics Symposium.

Archibald, J.F., and Degagne, D.O. (2000). "*Recent Canadian Advances in the Application of Spray-on Polymeric Linings*", Mining Health and Safety Conference, Sudbury, Ontario.

Archibald J.F. &Lausch P. (1999). *"Thin Spray-on Linings for Rock Failure Stabitization".* Proc. 37th US Rock Mechanics Symp., Vail. Rock Mechanics for Industry, Balkema, Rotterdam, pp. 617-624.

ASTM Standard D-638-10, (2010), *"Standard Test Method for Tensile Properties of Plastics-1,"* ASTM International, West Conshohocken, PA, USA DOI: 10.1520/D0638-10

ASTM Standard D-695-10, (2010), *"Standard Test Method for Compressive Properties of Rigid Plastics,"* ASTM International, West Conshohocken, PA, USA

Cai W., (2013) "Discrete Element Modelling of Constant Strain Rate and Creep Tests on a Graded Asphalt Mixture" University of Nottingham, Doctor of Philosophy Thesis

Cundall, P.A. & Strack, O.D.L., (1979). *"Discrete Numerical Model for Granular Assemblies",* Geotechnique, 29, pp. 47-65.

Dirige A., Archibald J. (2009), "Numerical Modeling Simulations of Spray-on Liners Support Potential in Highly Stressed and Rockburst Prone Rock Conditions". Proceedings of the 3rd CANUS Rock Mechanics Symposium, Toronto,

EFNARC, 2008. "*Specification and Guidelines on Thin Spray-on Liners for Mining and Tunneling*". ENC 250TSL v7.2 25-07-08.

Espley, S., Tannant, D.D., Baiden, G., and Kaiser, P.K. (1999). *"Design Criteria for Thin Spray-on Membrane Support for Underground Hardrock Mining".* Canadian Ins. of Mining and Metallurgy Annual Meeting, Calgary

Esterhuizen A.P., Bosman J.D., (2009) *"Practical Experience with The use of Thin Sprayed Liners At two Rivers Platinum Mine",* 43rd U.S. Rock Mechanics Symposium and 4th U.S.-Canada Rock MechanicsSymposium, Asheville

Finn, D. (2001). "*Polymer Membrane Tests*". Surface Support Liners: Membranes, Shotcrete and Mesh, Australian Centre for Geomechanics, Australia. Sect.20.

Hannon A., (2009) "*Thın Sprayed Lıners (TSLs) and a Safe Workıng Place".* The Southern African Institute of Mining and Metallurgy Hard Rock Safe Safety Conference,Sun City. pp. 99-114

Harding W. (2008). *"Numerıcal Modellıng of Thin Spray-on Liners Using FLAC".*Research Project, University of New South Wales, Australia

Itasca, *(2008) Online Manual of Particle Flow Code in 2 Dimensions,* Users guide

Hadjigeorgiou J, ed., (2003) *"Proceedings of the Third International Seminar on Surface Support Liners: Thin Spray-On Liners, Shotcrete, and Mesh",* Quebec City, Canada,

Jensen P., (2013). *"Managing the Engineering, Health & Safety Aspects of Thin Spray-On Liner Application"* Msc. Thesis, Luleå University of Technology.Department of Civil, Environmental and Natural Resources Engineering.

Kias C. M. (2013) *"Investigation of Unstable Failure in Underground Coal Mining Using the Discrete Element Method",* Colorado School of Mines Doctor of Philosophy Thesis (Mining and Earth Systems Engineering).

Kuijpers, J. (2001). "*Evaluation of Membrane Support Behaviour*". Surface Support Liners: Membranes, shotcrete and Mesh. Australian Centre for Geomechanics, Perth. Sect.21.

Kuijpers, J.S., Sellers, E.J., Toper, A.Z., Rangasamy, T., Ward, T., Van Rensburg, A.J., Yilmaz, H., and Stacey, R., (2004). "*Required technical specifications and standard testing methodology for Thin Sprayed Linings*". SIMRAC Final Report. Research agency: CSIR Division of Mining Technology. Project No: SIM 020206.

Lacerda L.(2004), *"Shotcrete and Other Surface Support Liners", SME Annual Meeting, Denver, Colorado*

Lacerda, L., and Rispin, M., (2002). "*Current Ground Support Membrane Applications in North American Underground Mines*". 2nd Int. seminar on Surface Support Liners: Thin Sprayed Liners, Shotcrete, Mesh. Crowne Plaza Sandton, RSA.

Lau V., Saydam S., Cai Y., Mitra R., (2008) *"Laboratory Investigation of Support Mechanism for Thin Spray-on Liners".* The 12th International Conference of International Association for Computer Methods and Advances in Geomechanics (IACMAG) Goa, India, PP. 1381-1388.

Lukey, C. Spinks, Baafi, E. Porter, I Nemcik, J., (2008). "*Polymer-Based Alternative to Steel Mesh for Coal Mine Strata Reinforcement".* 13th Australian Tunnelling Conference Melbourne, PP. 327-330.

Mason, D.P., Stacey, T.R., (2008) *"Support to rock excavations provided by sprayed liners".* Int J. Rock Mech Min Sci; 45, pp.773–788

Mason, D.P., Abelman, H., (2009), *"Support provided to rock excavations by a system of two liners".* Int. J. Rock Mech Min Sci; 46, pp.1197- 1205.

Mirzamani B., Tavassoli M. and Oraee K. (2011). *"Designing Shotcrete as Primary Support in Tunnels"*. Proc. 30th International Conference on Ground Control in Mining, pp. 320-325.

Mpunzi M. (2011). *"The Properties and Performance of Selected Thin Spray on Liners for Rock Support*".Msc. Thesis, University of Witwatersrand, Johannesburg,

Ozturk H. (2005), *"Adhesion between Thin Spray-on Liners and Rock or Concrete"*, Phd. Thesis, the University of British Columbia.

Ozturk H. & Tannant D.D., (2007) *"Factors Affecting Adhesive Strength of Different Thin Spray-on Liners*". Canadian Mining and Metallurgical Bulletin, 100(1100):1-7.

Ozturk H., (2011), *"Püskürtülen İnce Kaplamalarin Elastik Malzeme Özellikleri"*. Madencilik, Vol.50, No.2, pp. 41-45.

Ozturk H. (2012a), *"Work of Adhesion of Thin Spray-On Liners"* Rock Mechanics and Rock Engineering, pp. 1095-1102.

Ozturk H. (2012b), *"Fracture Mechanics Interpretation of Thin Spray-on Liner Adhesion Tests"*. International Journal of Adhesion and Adhesives, Vol. 34, pp.17-23

Pappas, D.M., Barton, T.M., and Eric S.W., (2003). "*The Long-Term Performance of Surface Support Liners for Ground Control in a Underground Limestone Mine*". 3rd Int. Seminar on Surface Support Liners: Thin Spray-On Liners, Shotcrete and Mesh, Quebec City, Canada. Sect.22.

Potvin, Y., (2002). "*Towards a Common Understanding of TSL Applications in Mines*". 2nd Int. Seminar on Surface Support Liners: Thin Sprayed Liners, Shotcrete, Mesh. SAIMM, Sandton, RSA, Sect.A1, pp.1-9.

Potyondy, D.O. & Cundall, P.A., (2004). "*A Bonded-Particle Model for Rock",* Int.J.Rock Mech.Min.Sci., 41, 1329-1364.

Pritchard C., Swan G. Henderson A., (1998). *"Tekflex as a Sprayon Screen Replacement in an Underground Hard Rock Mine"* 18th Conference On Ground Control in Mining. pp 90-97

Richardson J., Saydam S., (2009). "*Investigation of Thin Spray-On Liners using Numerical Modeling".* ARMA, American Rock Mechanics Association

Rispin, M., and Garshol, K.F., (2003). ""*Reactive" vs. "Non-Reactive" TSL's: a Comparison Illustrated with Two Prototype Technologies*". 3rd Int. Seminar on Surface Support Liners: Thin Spray-On Liners, Shotcrete and Mesh, Quebec City, Canada. Sect.24

Saydam, S &Docrat, Y, (2007), *"Evaluating the Adhesion Strength of Different Selants on Kimberlite'*, 11th Congress of the International Society for Rock Mechanics, Lisbon,

Saydam, S., Yilmaz, H. and Stacey, TR., (2004) *"A New Testing Approach for Thin Spray-on Liners: Double-Sided Shear Strength (DSS) Test*". Surface Support in Mining, Eds. Y. Potvin, T.R. Stacey, J. Hadjigeorgiou, Australian Centre for Geomechanics. Pages: 151-156.

Smith N., (2012). *"The use and application of Thin Spray Liners (TSLs) in Mining".* Seventh International Symposium, Rockbolting and Rock Mechanics in Mining. Aachen, Germany, pp.197-204

Spearing, A.J.S., and Champa, J., (2000). "*The Design, Testing and Application of Ground Support Membranes for use in Underground Mines*" Proc. MASSMIN.

Stacey, T.R., (2001). "*Review of membrane support mechanisms, loading mechanisms, desired membrane performance, and appropriate test methods".* J S. Afr. Inst. Min. Metall., vol. 101 pp. 343–351.

Stacey, T.R. and YU, X., (2004). *"Investigations into mechanisms of rock support provided by sprayed liners".* Ground Support in Mining and Underground Construction, Proc. 5th Int. Symp. On Ground Support, Perth, Australia, pp. 209–15.

Stacey, T.R., and Kasangula, M., (2003). "*Results from Testing of TSL's Using a Simple, Low Cost Laboratory Test*". 3rd Int. Seminar on Surface Support Liners: Thin Spray-On Liners, Shotcrete and Mesh, Quebec City, Canada. Sect.17

Steyn J., Gerber R J., Harrison A T., Ferreira P H., (2008). "*Investıgatıon Of The Characteristics of Thin Sprayed Lıners and Their use as an Additional Support Medium in Block Cave Mining"* The Southern African Institute of Mining and Metallurgy, pp.1-19

Swan G. & Henderson A., (1999). "*Water-based Spray-on liner implementation at Falconbridge Limited. Proceedings*" CIM/AGM, Calgary

Swan, G., Spencer, E.J., Graham, C., Hastings, D., Rayner, T.J., Livingstone, D., McDonald, N.W. and Bond, B., (2012). *"Towards Proving the Feasibility of a New, Composite Polymer Liner."* Eurock, Stockholm.

Tannant D., (2001), *"Thin Spray-on Liners for Underground Rock Support".* 17th International Mining Congress and Exhibition of Turkey, pp. 57-68.

Tannant D. D. & Wang C. (2003), *"Thin Tunnel Liners Modelled With Particle Flow Code"*. Engineering Computations, Vol.21, pp. 318-341.

Tannant D.D. & Wang C., (2007). *"DEM Boundary Conditions for Modeling Uniaxial and Biaxial Tests".* Proc. 1st Canada-US Rock Mechanics Symposium, Vancouver, pp. 385-392.

Wojno L. &Kuijper J.S., (1997). *"Spray-on, user Friendly and Flexible Support for Mine Excavations."* Proc. Int. Symp. An Rock Support, Lillehammer, pp.671-683.

Xia M., Zhou K., Baoping Z., (2009). *"Experimental Study and PFC Modelling of Failure Process of Brittle Rock Under Uniaxial Compression".* ARMA, American Rock Mechanics Association

Yilmaz, H., (2007). "*Shear-Bond Strength Testing of Thin Spray-on Liners*". J. S. Afr. Inst. Min. Metall., vol. 107, no. 8. pp. 519-530.

Yilmaz H.(2010), *"Tensile Strength Testing of Thin Spray-on Liner Products (TSL's) and Shotcrete"*. The Journal of The Southern African Institute of Mining and Metallurgy, Volume 110, pp. 559-569.

Zhenjun S., Porter I., Nemcik J., Baafi E. (2014), *"Comparing the Reinforcement Capacity of Welded Steel Mesh and a Thin Spray-On Liner Using Large Scale Laboratory Tests"*. International Journal of Mining Science and Technology. Article in Press.

APPENDIX A

TENSILE TEST CURVES AND SPECIMEN PHOTOS

A.1. Results of Liner 1

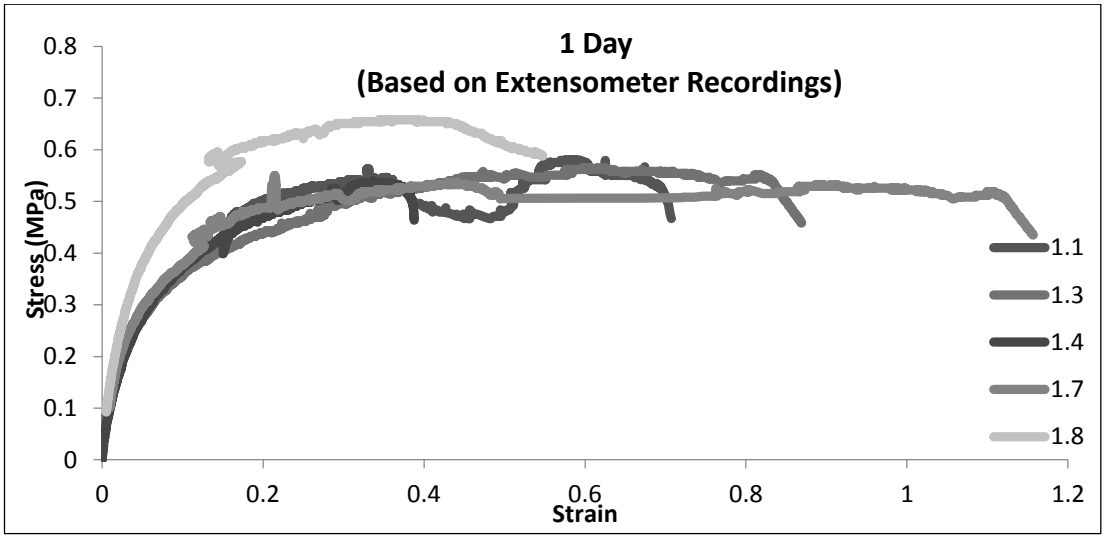

Figure A. 1 1 Day Cured Tensile Test Curves for Liner 1 (Based on Ext. Recordings)

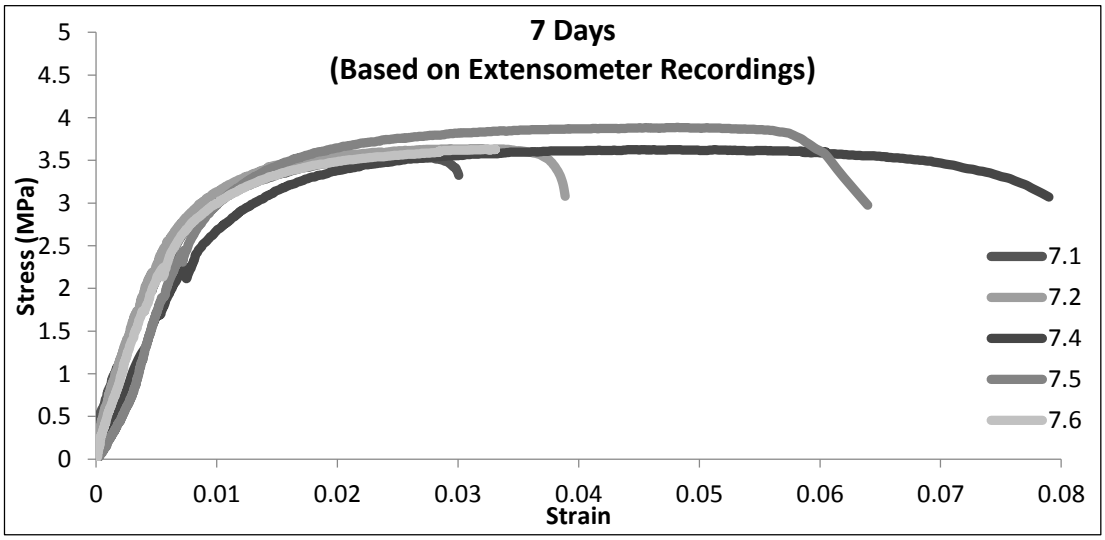

Figure A. 2 7 Days Cured Tensile Test Curves for Liner 1 (Based on Ext. Recordings)

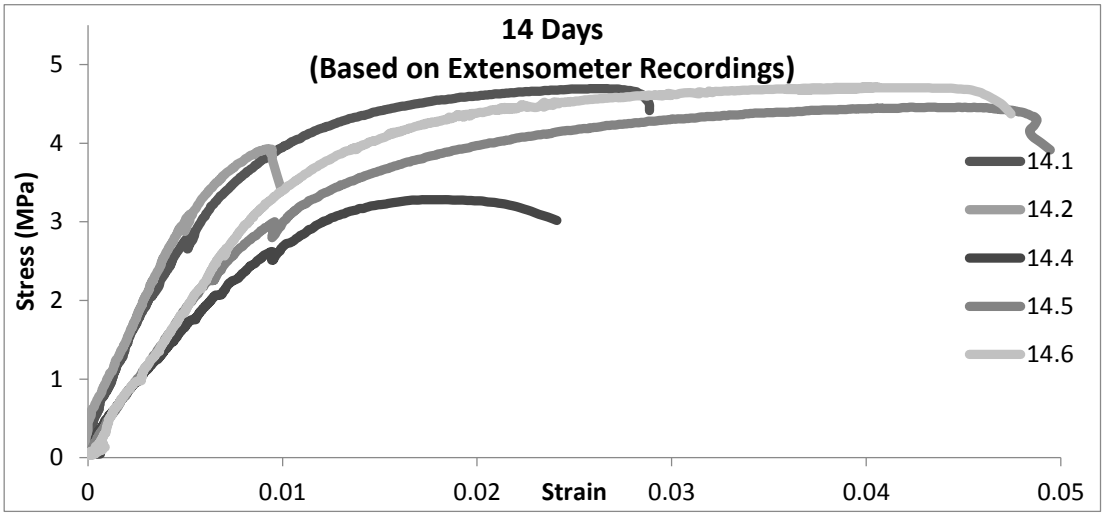

Figure A. 3 14 Days Cured Tensile Test Curves for Liner 1(Based on Ext. Recordings)

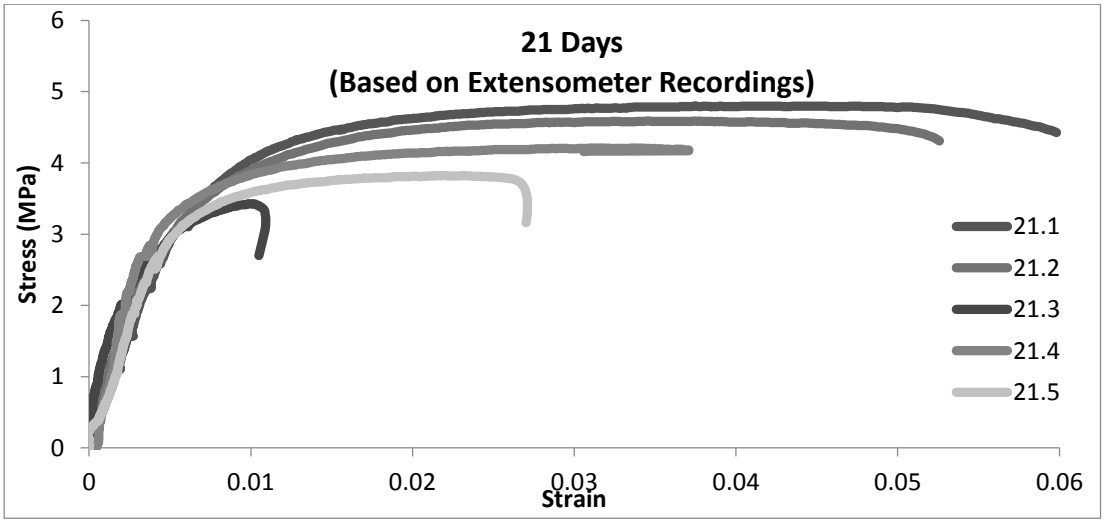

Figure A. 4 21 Days Cured Tensile Test Curves for Liner 1(Based on Ext. Recordings)

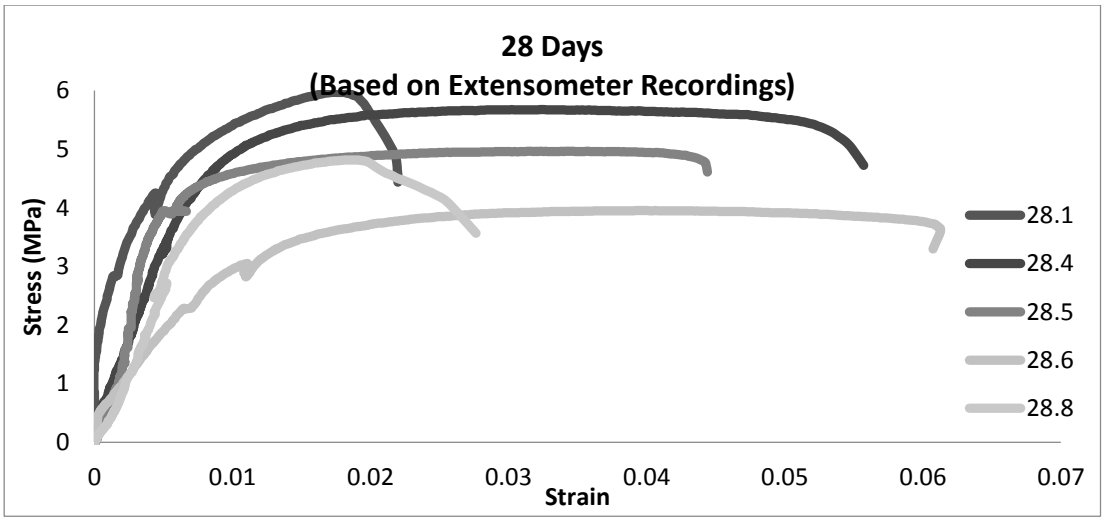

Figure A. 5 28 Days Cured Tensile Test Curves for Liner 1(Based on Ext. Recordings)

Figure A. 6 Tensile Test Specimen Photos of Liner 1(Before and After Test)

Figure A.6 Tensile Test Specimen Photos of Liner 1 (Before and After Test) (Continued)

Table A. 1 Tensile Test Result Table for Liner 1 (Based on Extensometer Recordings)

Curing Days	Specimen Number	σ_t (MPa)	E_t (MPa)	Avg. σt (MPa)	Avg. Et (MPa)	Elongation at Break (%)	Avg. Elongation at Break (%)
1	1.1	0.58	5.01	0.58 ± 0.05	4.51 ± 1.03	68	70.60 ± 27.36
	1.3	0.57	3.61			82	
	1.4	0.54	4.89			38	
	1.7	0.55	3.28			110	
	1.8	0.66	5.76			55	
7	7.1	2.83	281.05	2.93 ± 0.10	286.91 ± 47.98	3	4.73 ± 2.08
	7.2	2.91	341.7			3.75	
	7.4	2.9	231.23			8	
	7.5	3.11	251.26			5.6	
	7.6	2.9	329.34			3.3	
14	14.1	4.69	436.44	4.21 ± 0.61	394.27 ± 96.27	2.75	3.05 ± 1.57
	14.2	3.92	541.44			0.9	
	14.4	3.28	299.3			2.41	
	14.5	4.46	337.98			4.7	
	14.6	4.71	356.2			4.5	
21	21.1	4.8	629.76	4.26 ± 0.52	833.77 ± 207.32	6	3.80 ± 1.81
	21.2	4.26	598.27			3.25	
	21.3	4.59	906.8			5	
	21.4	3.43	982.6			1.25	
	21.5	4.21	1051.4			3.5	
28	28.1	5.97	1063.5	5.08 ± 0.79	758.2 ± 367.91	1.81	3.93 ± 1.71
	28.4	5.68	626.59			5	
	28.5	4.96	1206.4			4.25	
	28.6	3.95	311.87			6	
	28.8	4.82	582.66			2.61	

Table A. 2 Tensile Test Result Table for Liner 1 (Based on LVDT Recordings)

Curing Days	Specimen Number	E_t (MPa) LVDT	Avg. Et (MPa) LVDT	Elongation at Break LVDT(%)	Avg. Elongation at Break LVDT(%)
1	1.1	-	4.505 ± 0.51	67	71.60 ± 14.41
	1.3	4.1		74	
	1.4	4.57		53	
	1.7	4.15		93	
	1.8	5.2		71	
7	7.1	60.06	51.13 ± 6.41	9.6	11.99 ± 2.01
	7.2	46.15		12.8	
	7.4	50.23		12.7	
	7.5	44.4		14.53	
	7.6	54.82		10.3	
14	14.1	73.64	59.92 ± 17.96	8	9.71 ± 2.68
	14.2	60.22		7	
	14.4	34.85		9.54	
	14.5	79.81		10	
	14.6	51.09		14	
21	21.1	50.42	63.01 ± 12.85	14.1	11.62 ± 3.03
	21.2	65.39		10.9	
	21.3	80.203		13.55	
	21.4	68.94		6.66	
	21.5	50.11		12.9	
28	28.1	121.39	93.08 ± 45.50	6.14	10.23 ± 4.15
	28.4	75.13		11.1	
	28.5	38.66		16.6	
	28.6	82.42		10.42	
	28.8	107.79		6.92	

A.2. Results of Liner 2

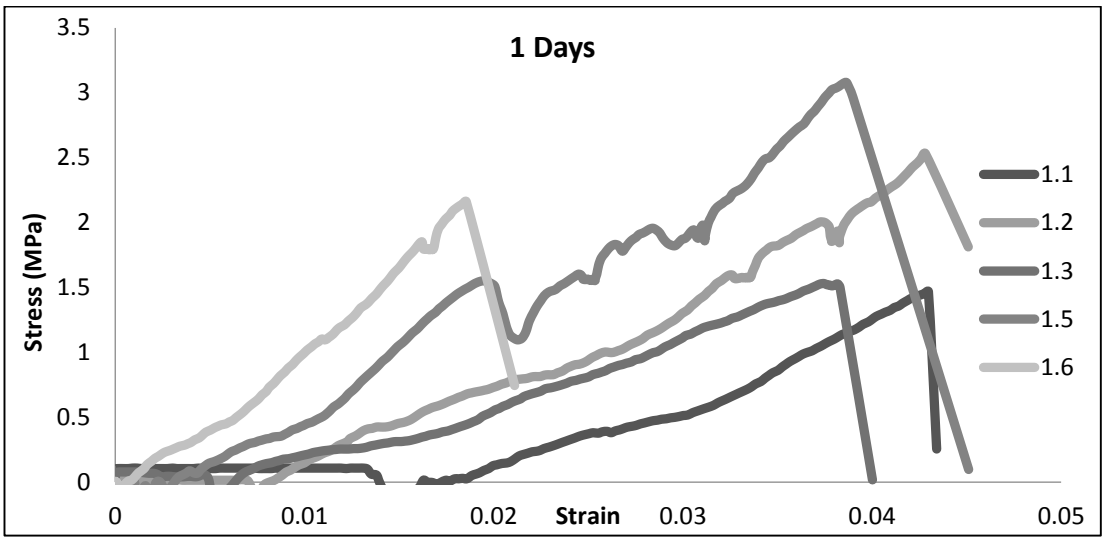

Figure A. 7 1 Day Cured Tensile Test Curves for Liner 2

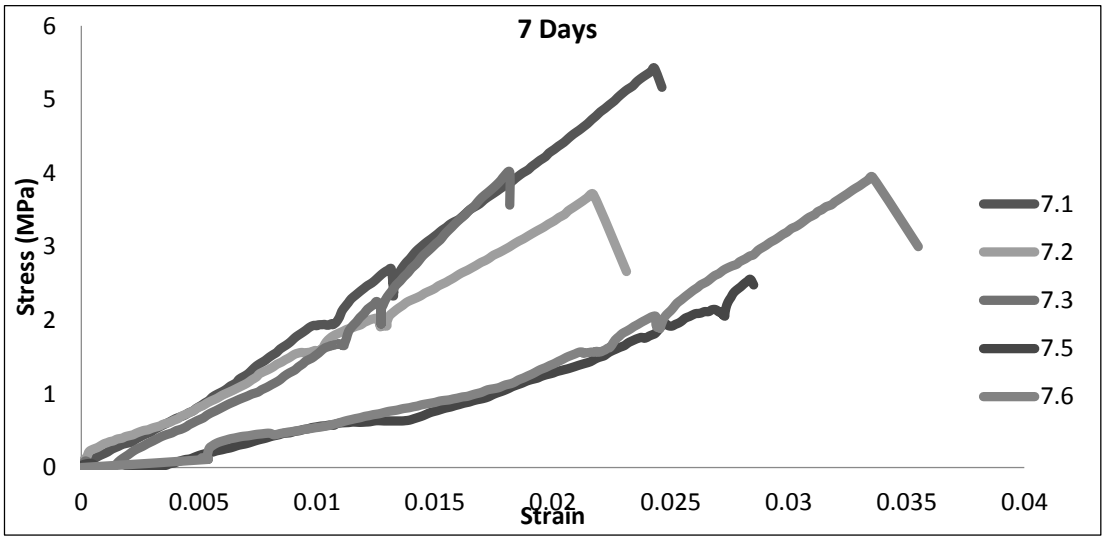

Figure A. 8 7 Days Cured Tensile Test Curves for Liner 2

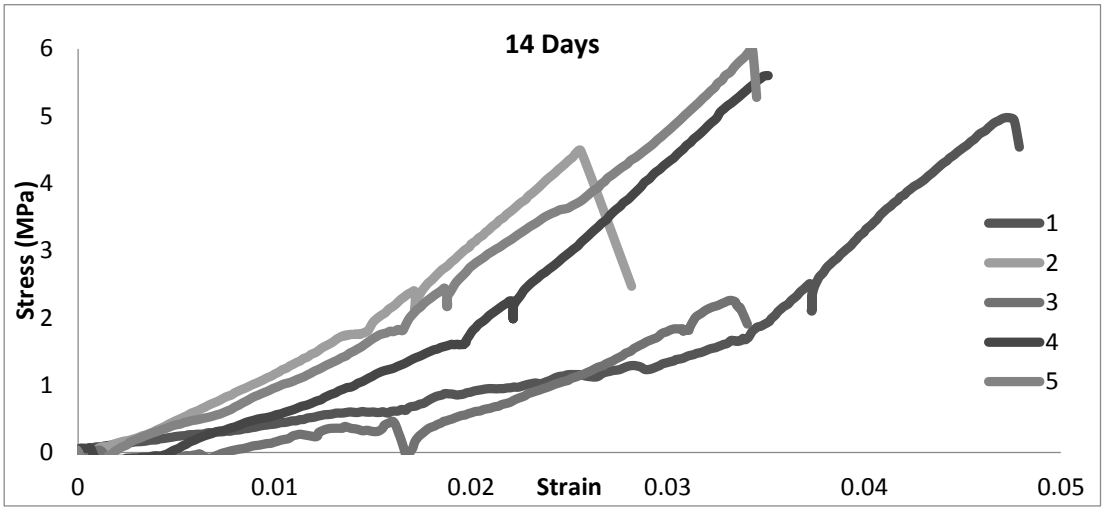

Figure A. 9 14 Days Cured Tensile Test Curves for Liner 2

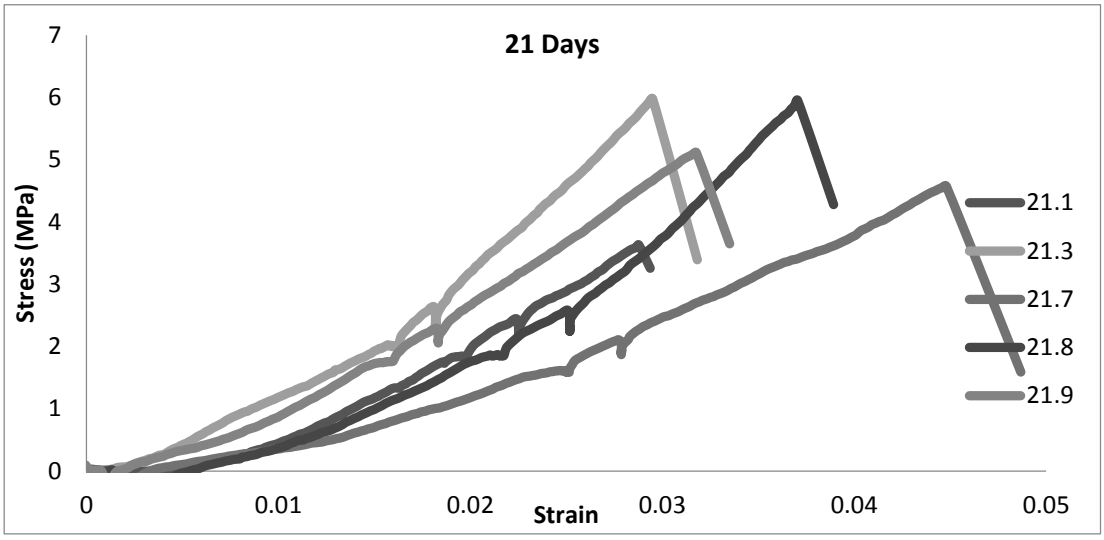

Figure A. 10 21 Days Cured Tensile Test Curves for Liner 2

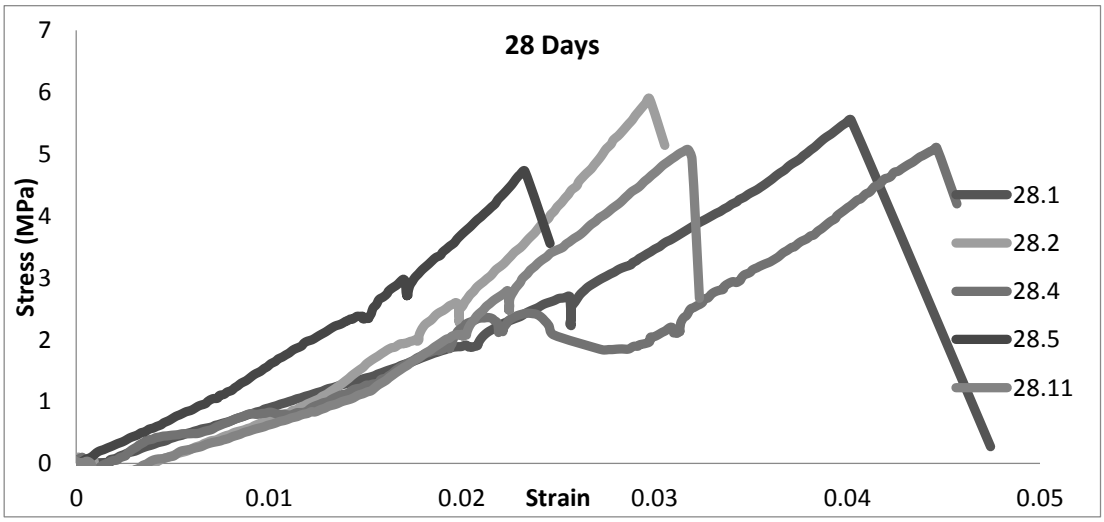

Figure A. 11 28 Days Cured Tensile Test Curves for Liner 2

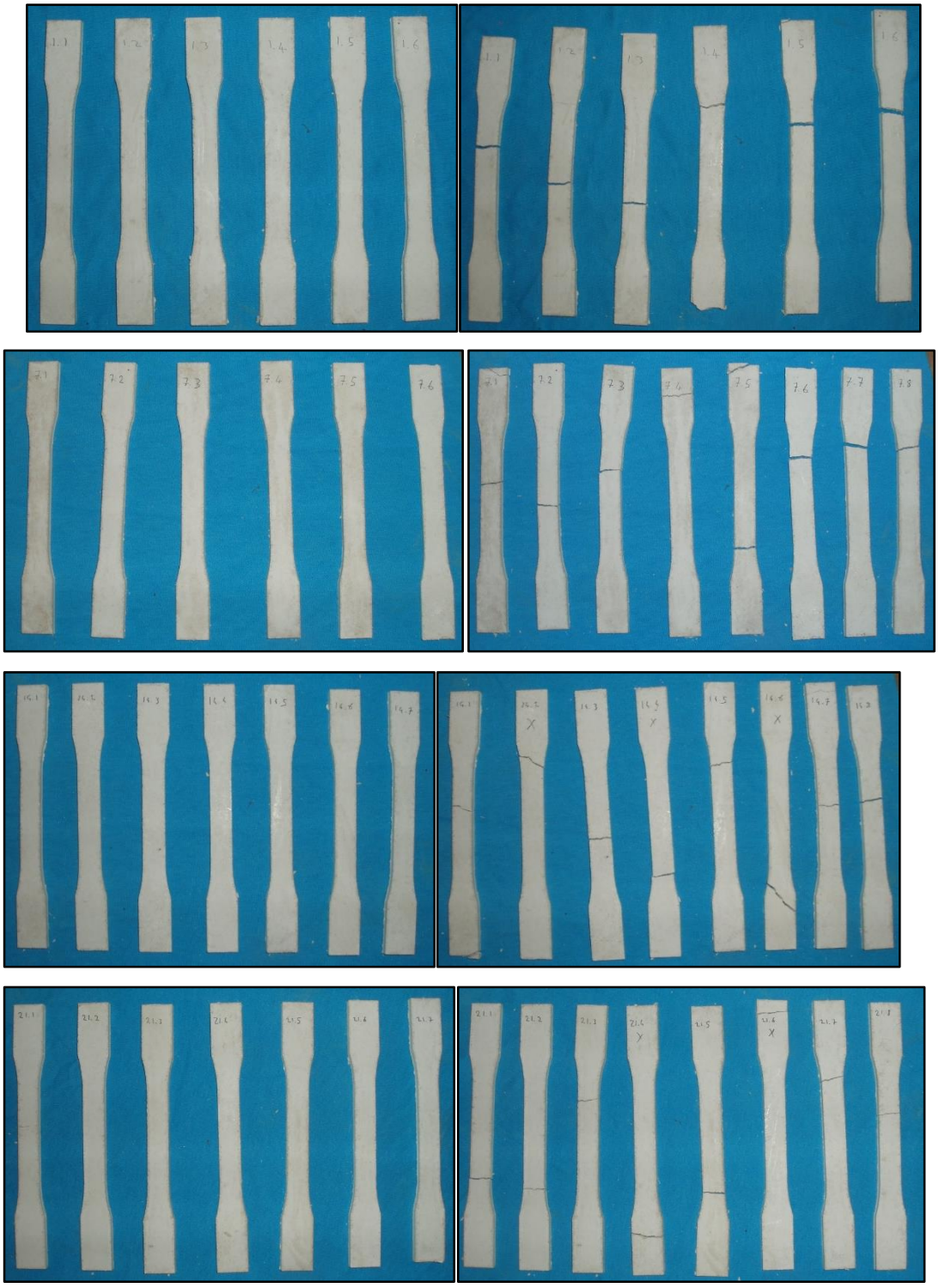

Figure A. 12 Tensile Test Specimen Photos of Liner 2(Before and After Test)

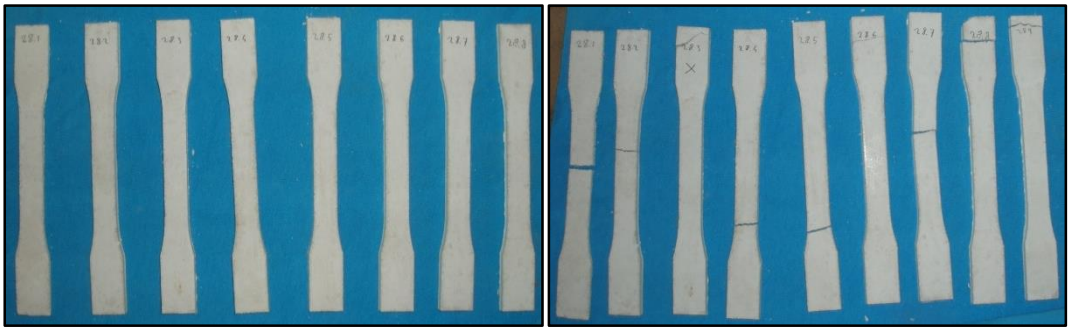

Figure A.12 Tensile Test Specimen Photos of Liner 2(Before and After Test)

(Continued)

Table A. 3 Tensile Test Result Table for Liner 2

Curing Duration	Specimen Number	σ_t (MPa)	E_t (MPa)	Avg. σt (MPa)	Avg. Et (MPa)	Elongation at Break (LVDT) (%)	Avg. Elongation at Break (%)
1	1.1	1.47	51.64	2.15 ± 0.68	58.82 ± 15.91	4.43	3.91 ± 1.03
	1.2	2.53	50.65			4.51	
	1.3	1.53	52.5			4	
	1.5	3.08	52.06			4.51	
	1.6	2.16	87.25			2.11	
7	7.1	5.43	156.38	3.93 ± 1.02	118.78 ± 44.18	4.04	3.19 ± 0.69
	7.2	3.71	135.78			3.5	
	7.3	4.01	158.85			2.22	
	7.5	2.56	74.61			2.85	
	7.6	3.95	68.27			3.35	
14	14.1	4.98	120.94	4.97 ± 0.67	125.04 ± 11.96	3.68	3.52 ± 0.11
	14.3	4.49	133.4			3.56	
	14.5	-	-			3.41	
	14.7	5.60	110			3.51	
	14.8	5.99	135.82			3.43	
21	21.1	3.63	139.27	5.05 ± 0.98	131.75 ± 17.88	2.93	3.64 ± 0.76
	21.3	5.97	134.74			3.18	
	21.7	4.57	100.59			4.86	
	21.8	5.95	145.91			3.89	
	21.9	5.11	138.23			3.35	
28	28.1	5.55	132.18	5.27 ± 0.45	138.61 ± 19.29	4.74	3.58 ± 0.99
	28.2	5.90	148.33			3	
	28.4	5.10	128.2			4.5	
	28.5	4.72	166.85			2.45	
	28.11	5.07	117.48			3.2	

APPENDIX B

COMPRESSION TEST CURVES AND SPECIMEN PHOTOS

B.1. Results of Liner 1

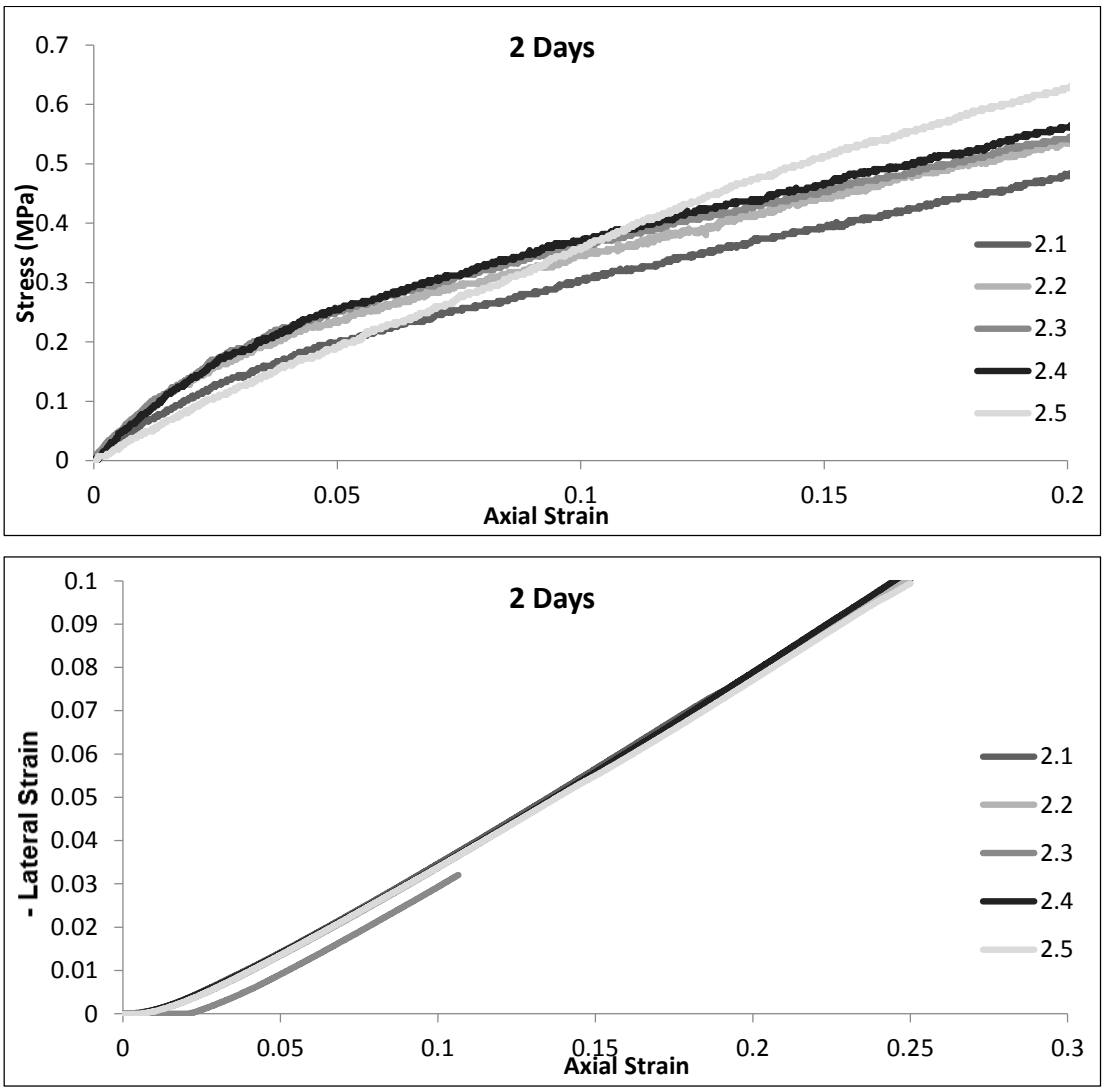

Figure B. 1 2 Days Cured Compression Test Curves for Liner 1

Figure B. 2 2 Days Cured Compression Test Specimen Photos of Liner 1

(Before and After Test)

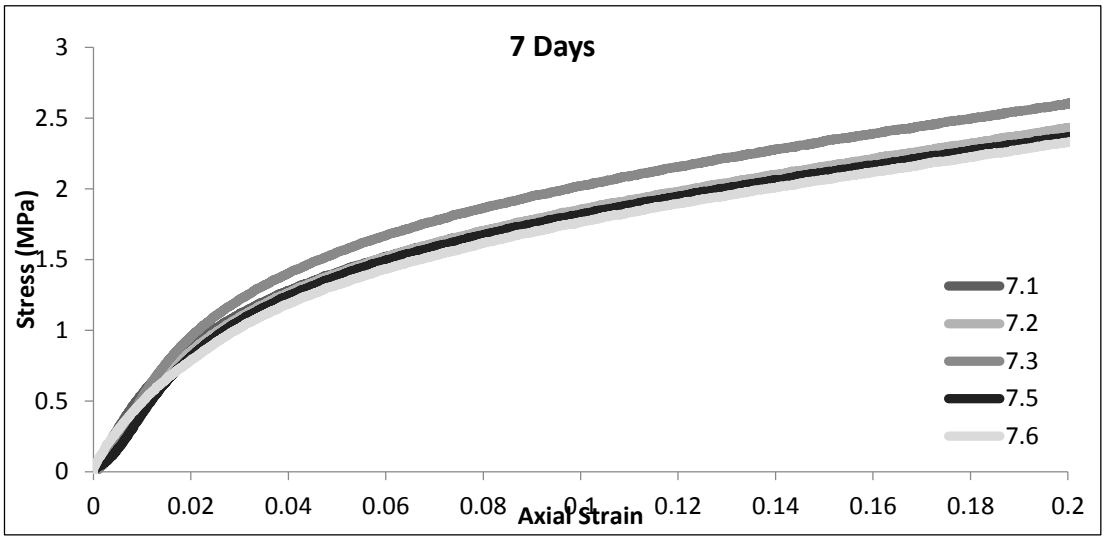

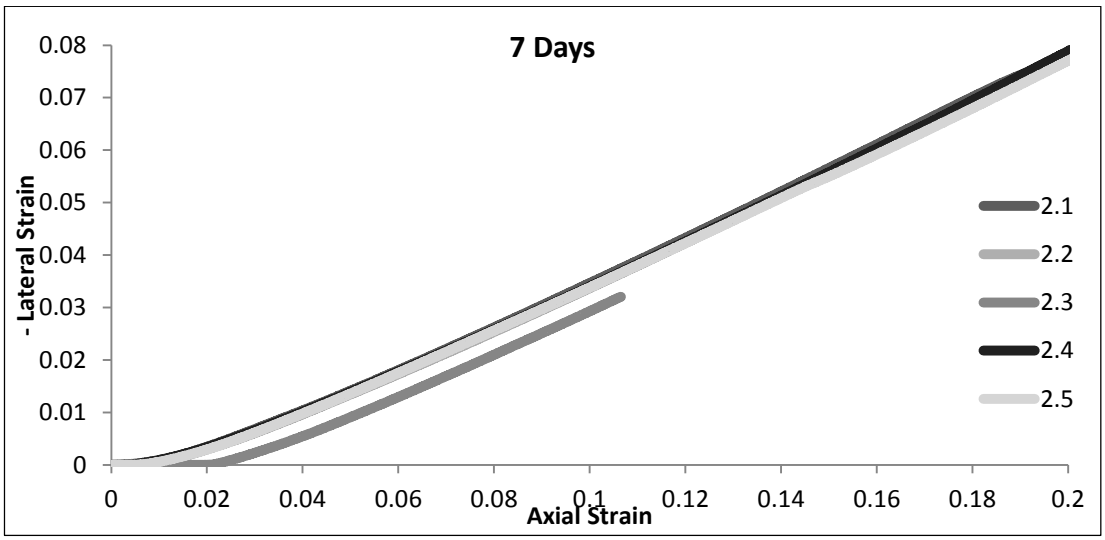

Figure B. 3 7 Days Cured Compression Test Curves for Liner 1

Figure B. 4 7 Days Cured Compression Test Specimen Photos of Liner 1

(Before and After Test)

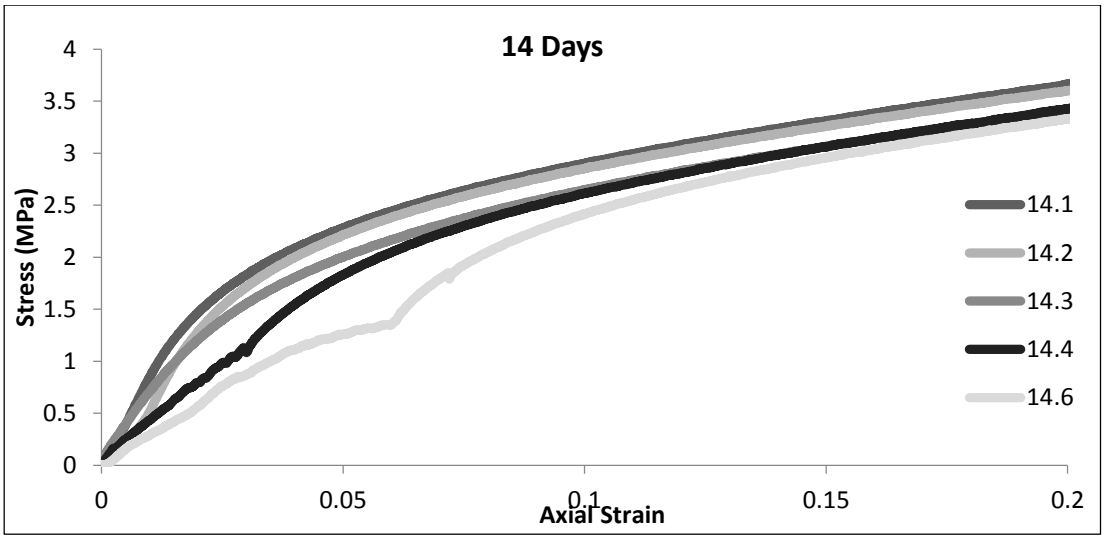

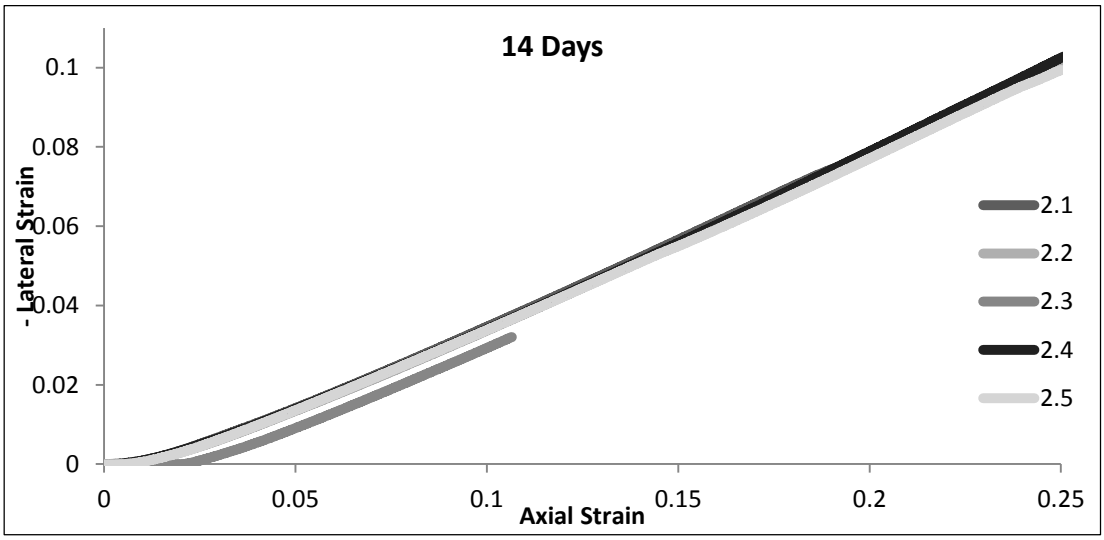

Figure B. 5 14 Days Cured Compression Test Curves for Liner 1

Figure B. 6 14 Days Cured Compression Test Specimen Photos of Liner 1

(Before and After Test)

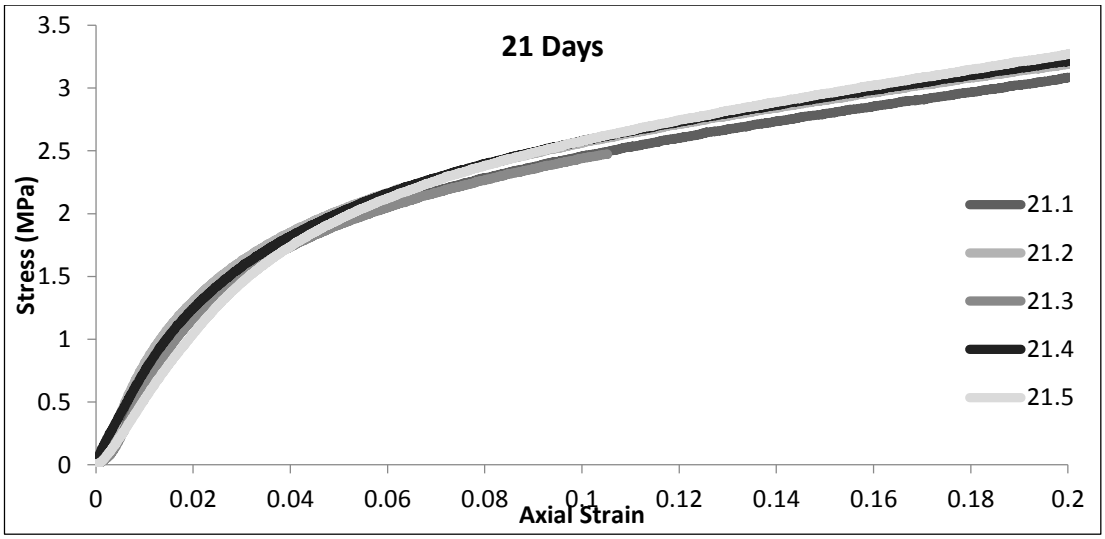

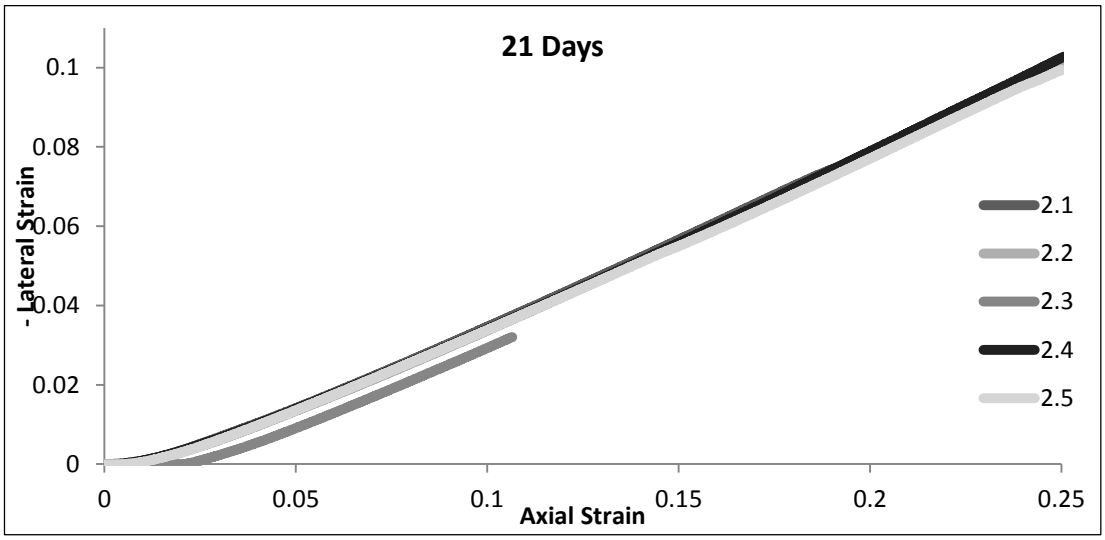

Figure B. 7 21 Days Cured Compression Test Curves for Liner 1

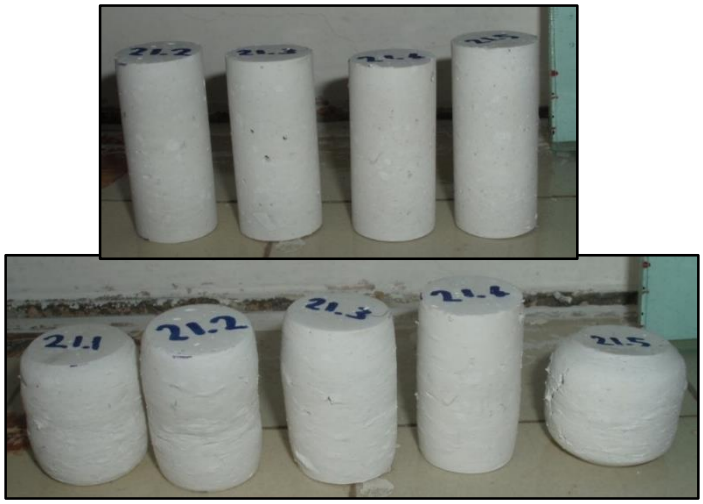

Figure B. 8 21 Days Cured Compression Test Specimen Photos of Liner 1

(Before and After Test)

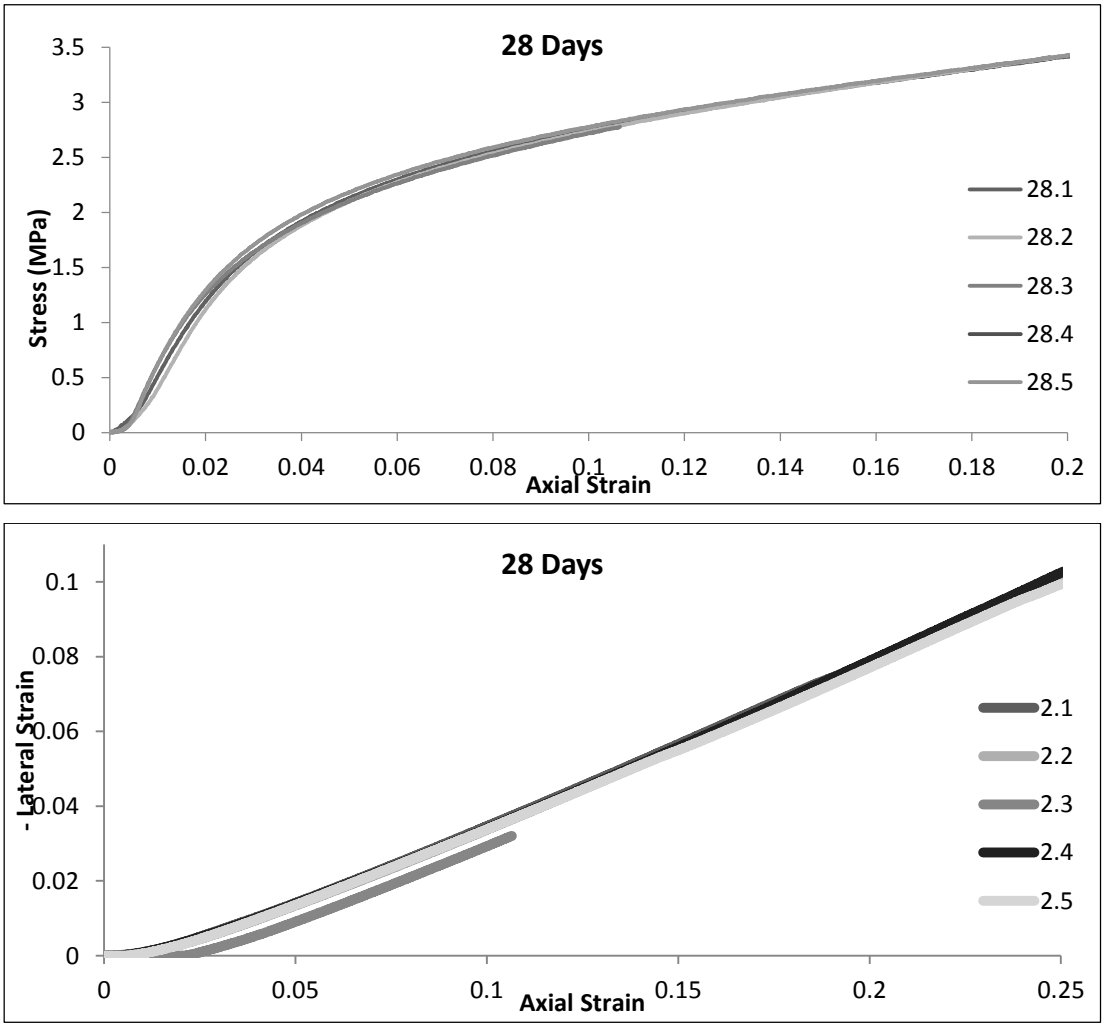

Figure B. 9 28 Days Cured Compression Test Curves for Liner 1

Figure B. 10 21 Days Cured Compression Test Specimen Photos of Liner 1

(Before and After Test)

Table B. 1 Compression Test Result Table for Liner 1

COMPRESSION TEST RESULT TABLE FOR LINER 1						
Curing Duration	**E (MPa)**	**Avg. E (MPa)**	**ν**	**Avg. ν**	**UCS (Greater Than)**	**Avg. UCS (Greater Than)**
2.1	1.76	1.98 ± 0.33	0.32	0.328±0.02	0.74	0.78 ±0.04
2.2	1.87		0.32		0.76	
2.3	1.81		0.33		0.74	
2.4	1.88		0.31		0.84	
2.5	2.56		0.36		0.80	
7.1	43.57	45.94 ± 6.67	0.41	0.37 ± 0.02	2.46	2.55 ± 0.21
7.2	46.91		0.36		2.62	
7.3	55.34		0.37		2.88	
7.5	47.02		0.36		2.42	
7.6	36.88		0.37		2.36	
14.1	70.60	50.96 ± 17.88	0.42	0.43 ± 0.01	3.74	3.65 ± 0.24
14.2	64.48		0.43		3.90	
14.3	54.77		0.44		3.51	
14.4	34.94		0.41		3.66	
14.6	30.02		0.43		3.45	
21.1	62.68	60.08 ± 6.74	0.42	0.42 ± 0.01	3.47	3.46 ± 0.08
21.2	62.15		0.41		3.52	
21.3	67.91		0.43		3.33	
21.4	57.79		0.44		3.51	
21.5	49.87		0.42		3.48	
28.1	59.01	75.87 ± 10.77	0.41	0.41 ± 0.00	3.76	3.71 ± 0.12
28.2	71.61		0.42		3.72	
28.3	83.78		0.41		3.51	
28.4	80.07		0.41		3.74	
28.5	84.90		0.41		3.81	

B.2. Results of Liner 2

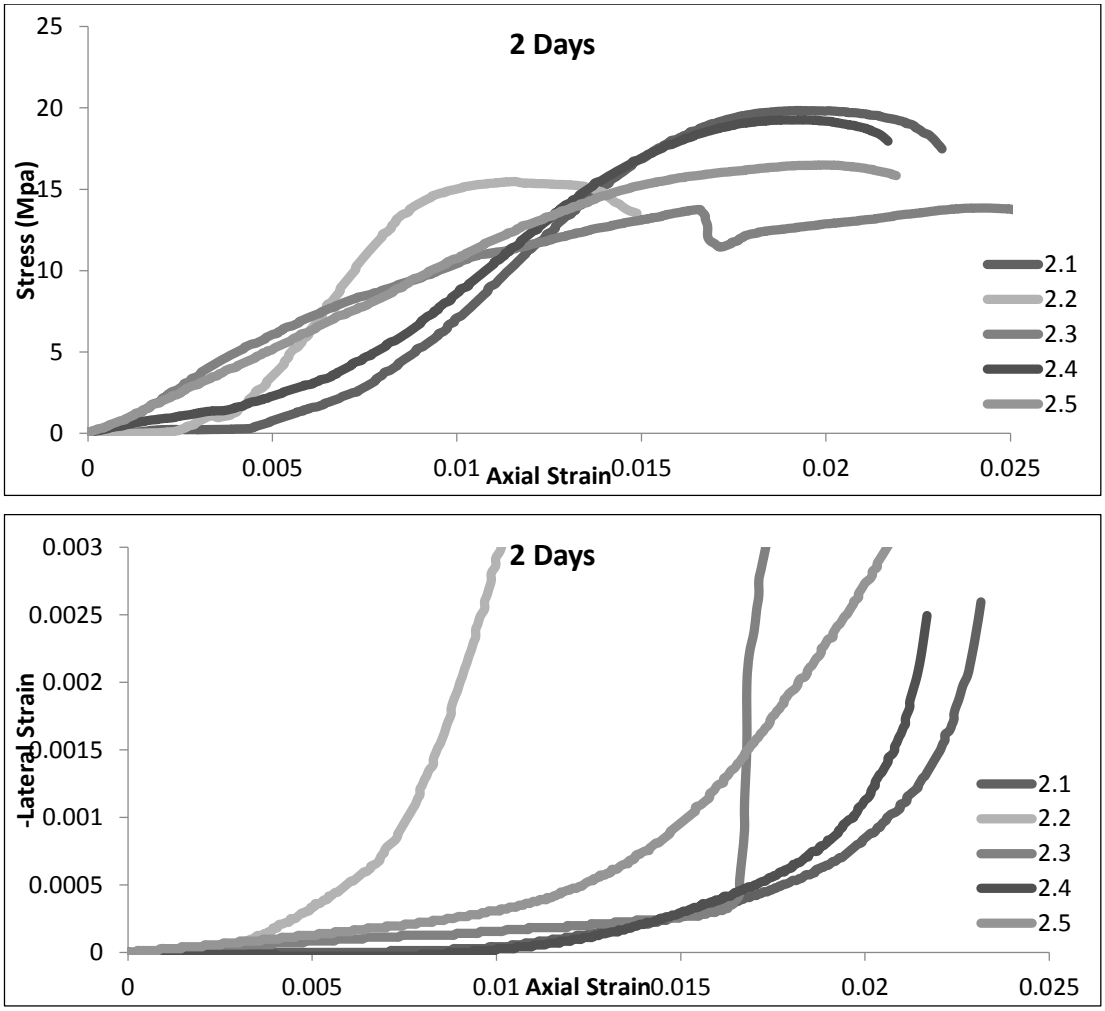

Figure B. 11 2 Days Cured Compression Test Curves for Liner 2

Figure B. 12 2 Days Cured Compression Test Specimen Photos of Liner 2

(Before and After Test)

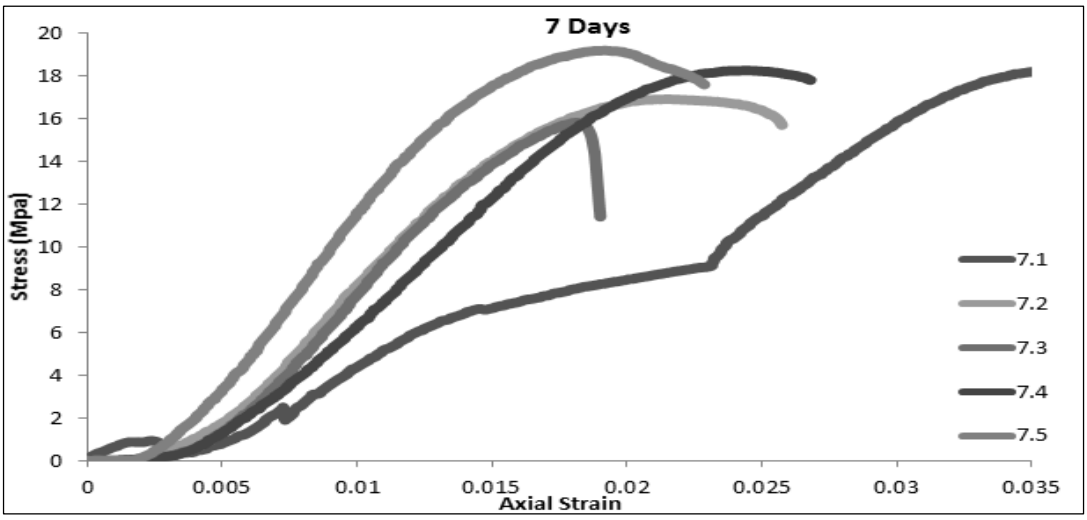

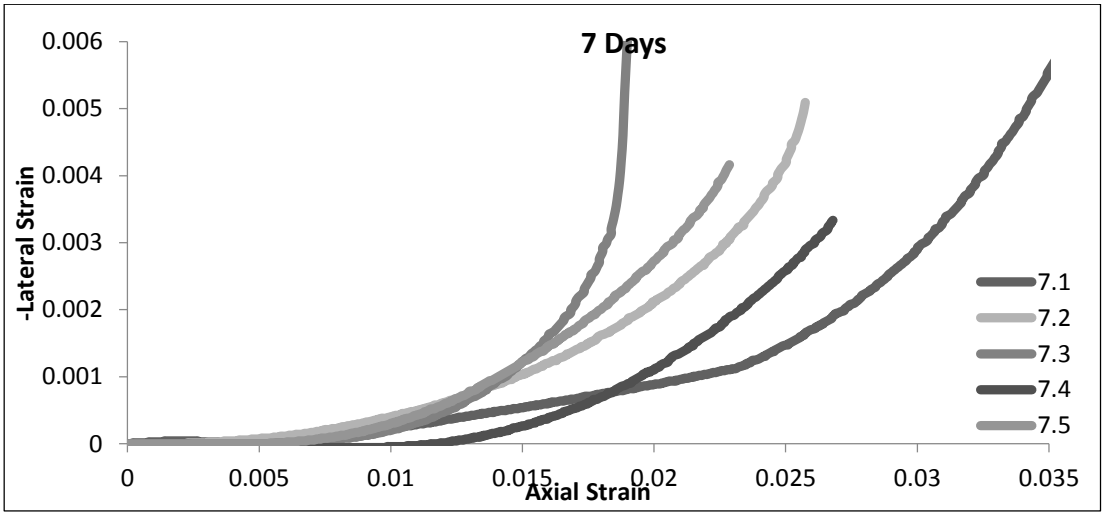

Figure B. 13 7 Days Cured Compression Test Curves for Liner 2

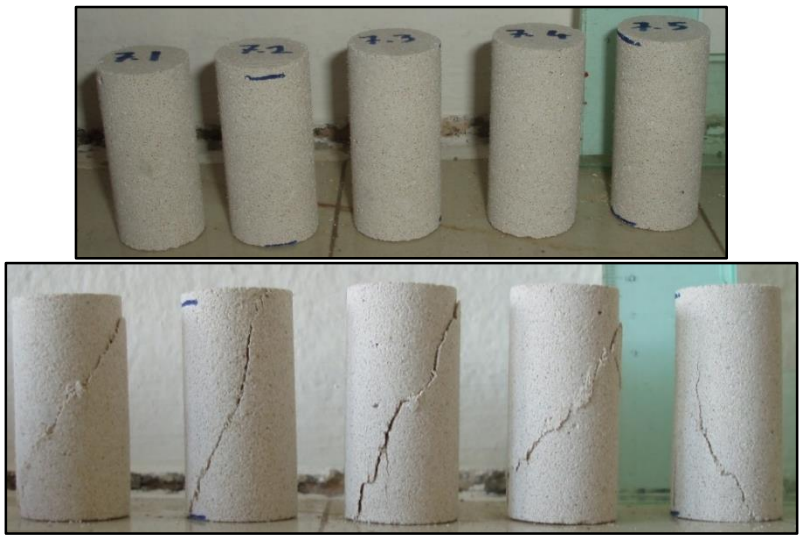

Figure B. 14 7 Days Cured Compression Test Specimen Photos of Liner 2

(Before and After Test)

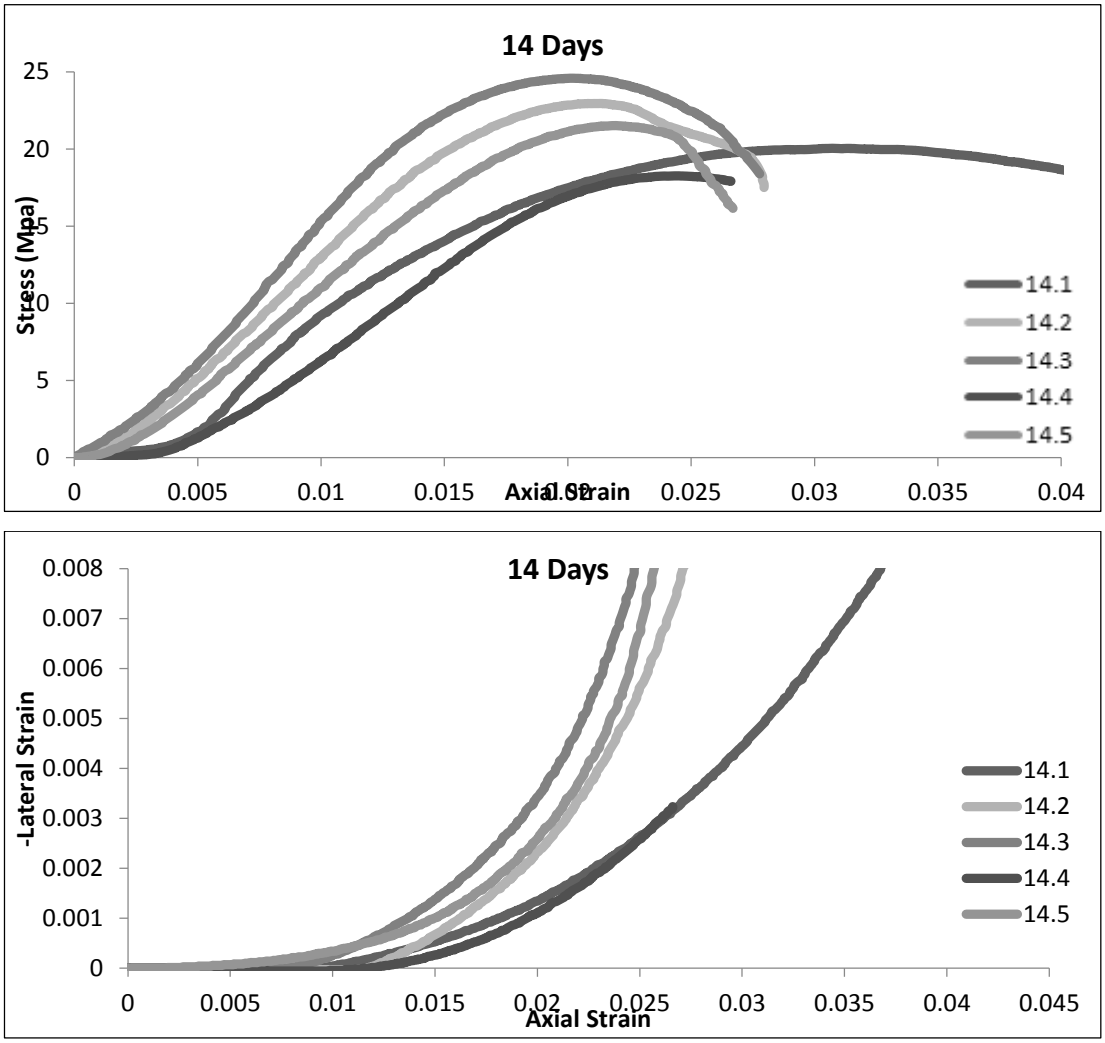

Figure B. 15 14 Days Cured Compression Test Curves for Liner 2

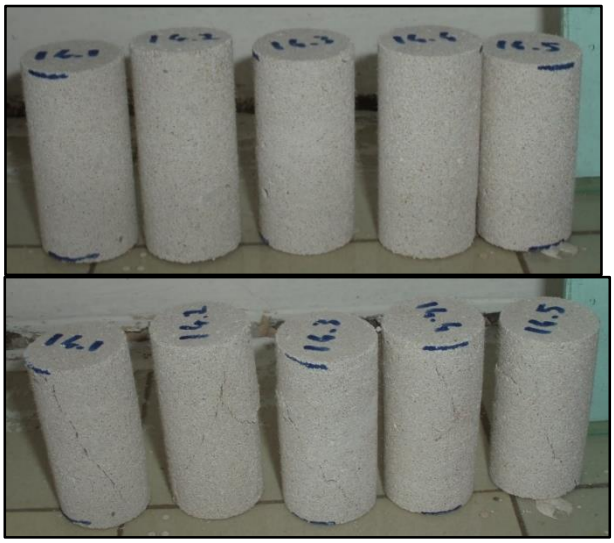

Figure B. 16 14 Days Cured Compression Test Specimen Photos of Liner 2

(Before and After Test)

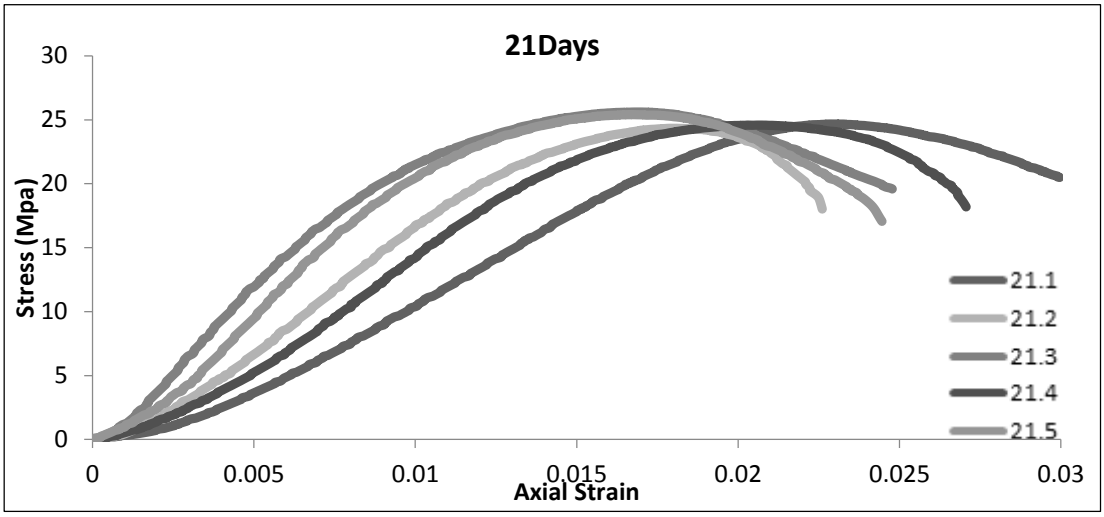

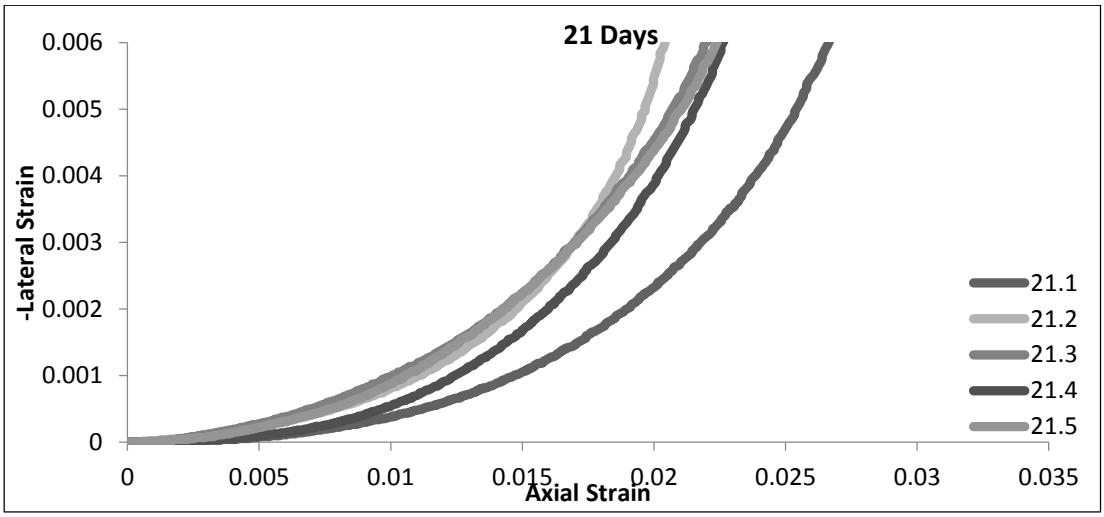

Figure B. 17 21 Days Cured Compression Test Curves for Liner 2

Figure B. 18 21 Days Cured Compression Test Specimen Photos of Liner 2

(Before and After Test)

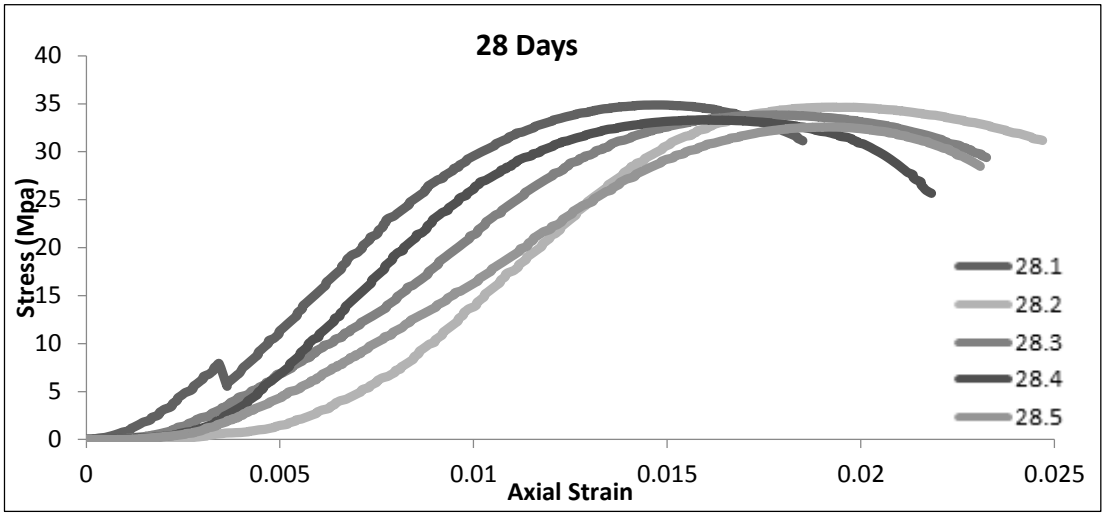

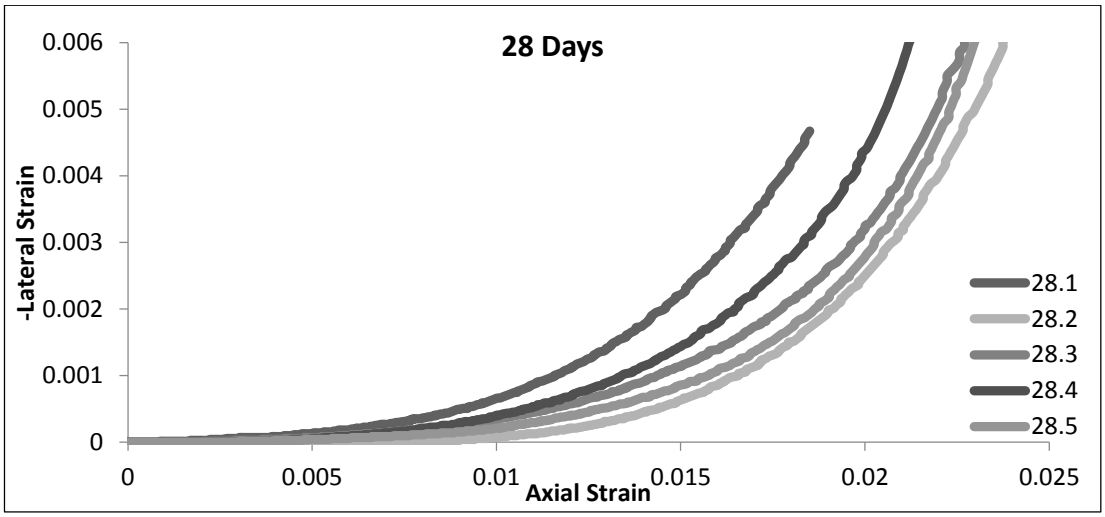

Figure B. 19 28 Days Cured Compression Test Curves for Liner 2

Figure B. 20 28 Days Cured Compression Test Specimen Photos of Liner 2

(Before and After Test)

Table B. 2 Compression Test Result Table for Liner 2

Curing Duration	E (MPa)	Avg. E (MPa)	ν	Avg. ν	UCS (MPa)	Avg. UCS (MPa)
2.1	2014.30	1774.20 ± 656.97	0.06	0.09±0.04	19.84	16.98 ± 2.54
2.2	2735.20		0.14		15.47	
2.3	1206.30		0.10		13.84	
2.4	1791.00		0.03		19.27	
2.5	1124.20		0.09		16.49	
7.1	888.39	1285.54 ± 301.12	0.07	0.13 ± 0.05	18.35	17.71 ± 1.33
7.2	1382.90		0.15		16.92	
7.3	1358.00		0.19		15.82	
7.5	1112.50		0.09		18.26	
7.6	1685.90		0.18		19.20	
14.1	1613.50	1594.52 ± 172.81	0.11	0.11 ± 0.03	20.05	20.42 ± 3.93
14.2	1516.50		0.14		22.95	
14.3	1852.50		0.10		13.84	
14.4	1610.50		0.12		23.72	
14.6	1379.60		0.08		21.52	
21.1	1451.70	2064.56 ± 448.91	0.10	0.10 ± 0.01	24.67	24.92 ± 0.55
21.2	2005.80		0.11		24.33	
21.3	2484.40		0.10		25.61	
21.4	1859.50		0.12		24.58	
21.5	2521.40		0.09		25.41	
28.1	4048.60	3493.12 ± 602.82	0.08	0.09 ± 0.01	34.88	33.85 ± 0.95
28.2	3607.30		0.11		34.65	
28.3	3033.20		0.07		33.84	
28.4	4058.50		0.09		33.32	
28.5	2718.00		0.08		3.81	

APPENDIX C

TEST SIMULATION CURVES AND FAILURE LOCATIONS

C.1. Tensile Test Simulation Results

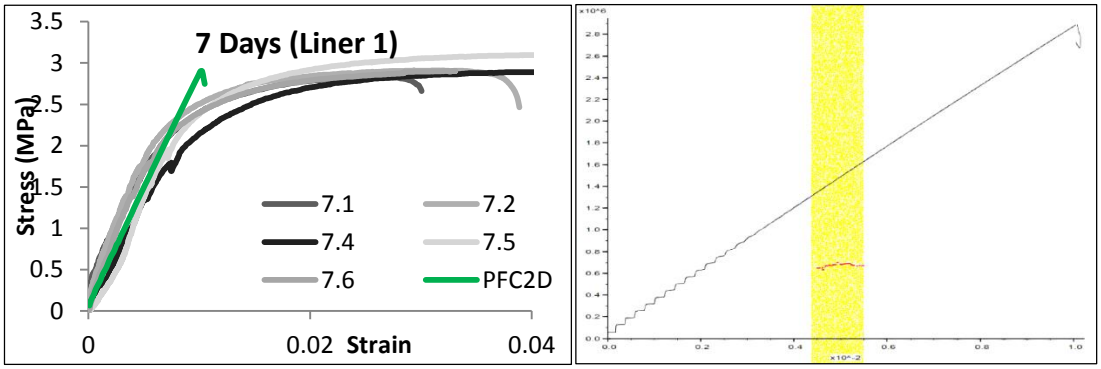

Figure C. 1 Obtained Tensile Test Curve & Failure Location for Liner 1 (7 Days)

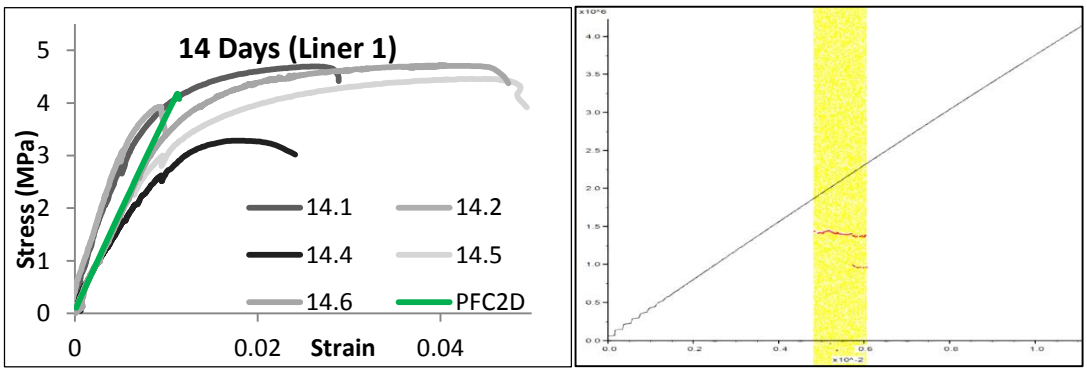

Figure C. 2 Obtained Tensile Test Curve & Failure Location for Liner 1 (14 Days)

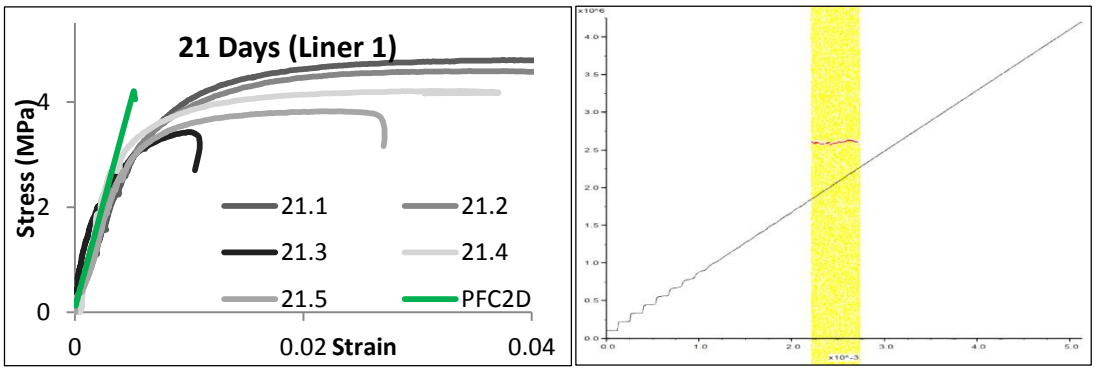

Figure C. 3 Obtained Tensile Test Curve & Failure Location for Liner 1 (21 Days)

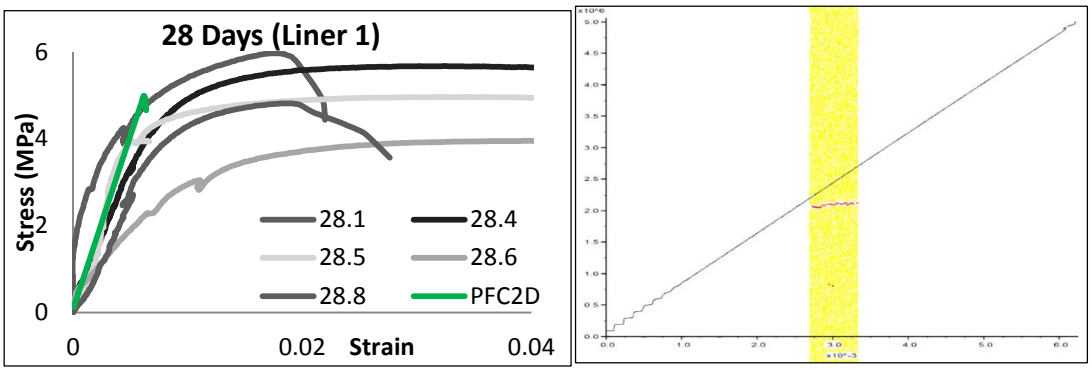

Figure C. 4 Obtained Tensile Test Curve & Failure Location for Liner 1 (28 Days)

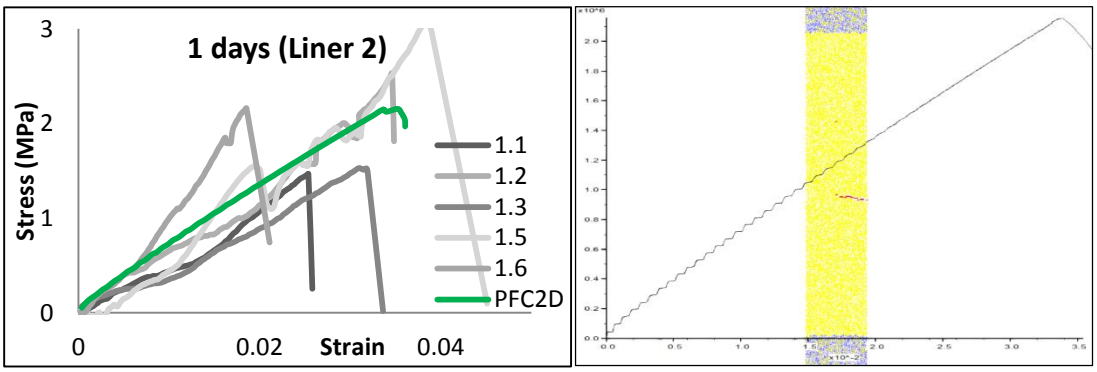

Figure C. 5 Obtained Tensile Test Curve & Failure Location for Liner 2 (1 Days)

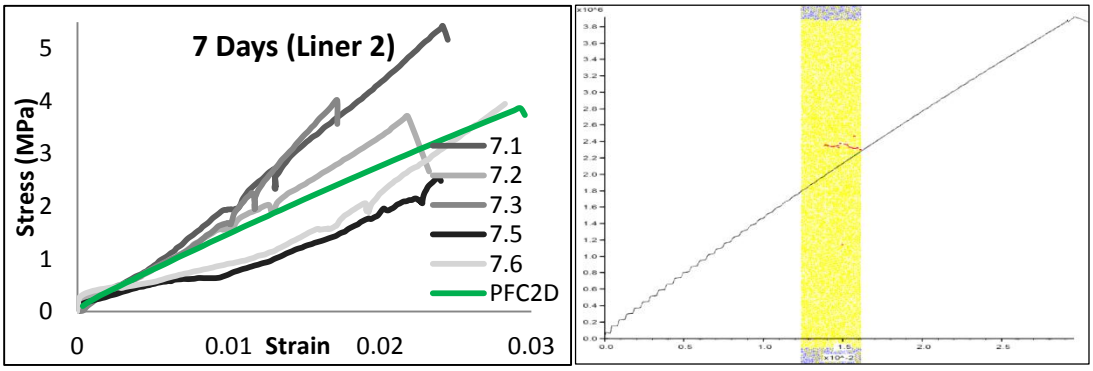

Figure C. 6 Obtained Tensile Test Curve & Failure Location for Liner 2 (7 Days)

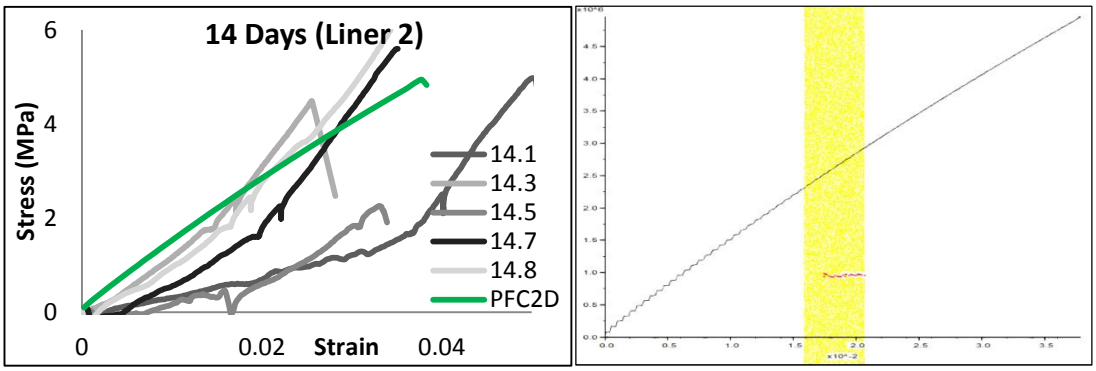

Figure C. 7 Obtained Tensile Test Curve & Failure Location for Liner 2 (14 Days)

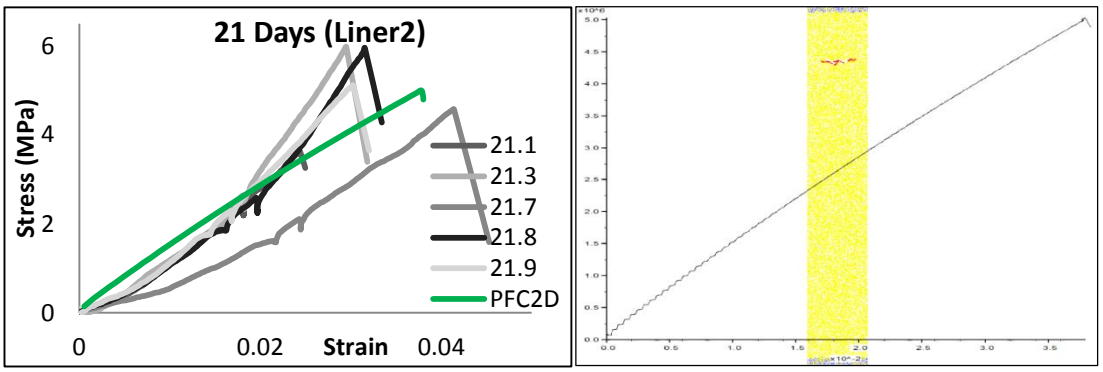

Figure C. 8 Obtained Tensile Test Curve & Failure Location for Liner 2 (21 Days)

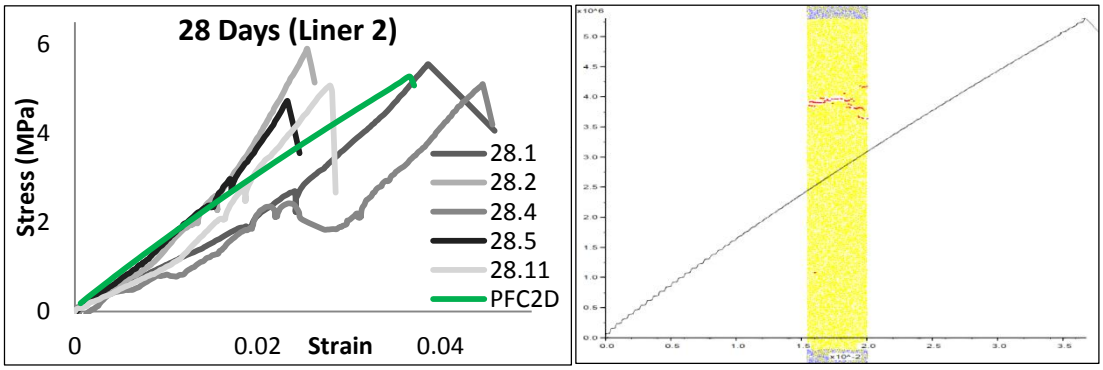

Figure C. 9 Obtained Tensile Test Curve & Failure Location for Liner 2 (28 Days)

C.2. Compression Test Simulation Results

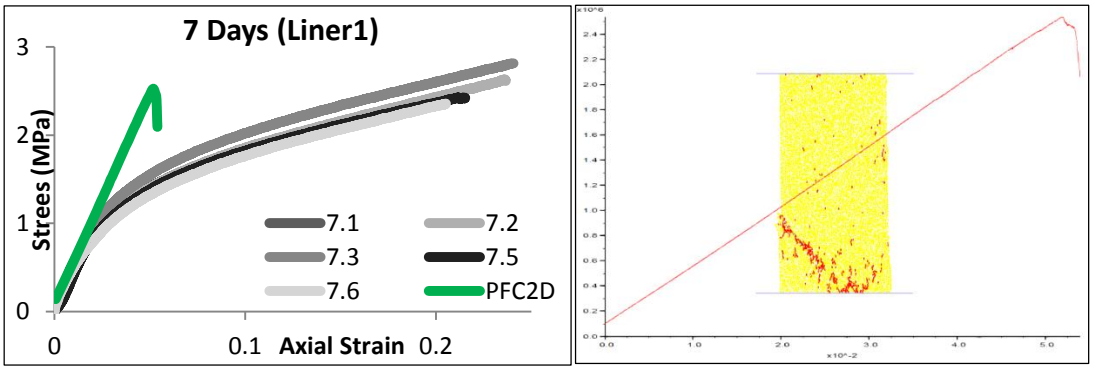

Figure C. 10 Obtained Compression Test Curve & Failure Location for Liner 1 (7 Days)

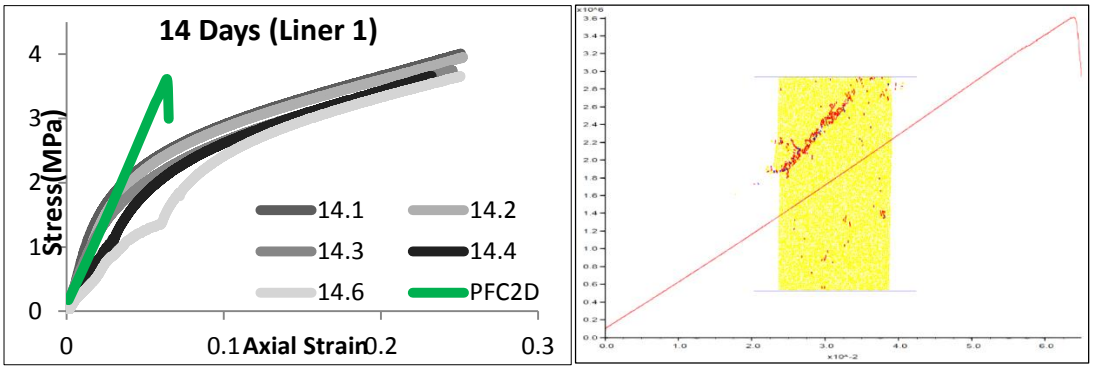

Figure C. 11 Obtained Compression Test Curve & Failure Location for Liner 1 (14 Days)

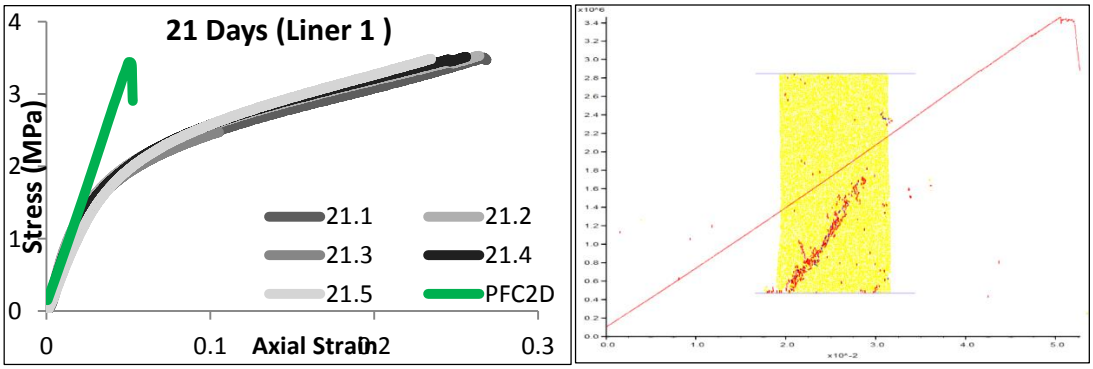

Figure C. 12 Obtained Compression Test Curve & Failure Location for Liner 1 (21 Days)

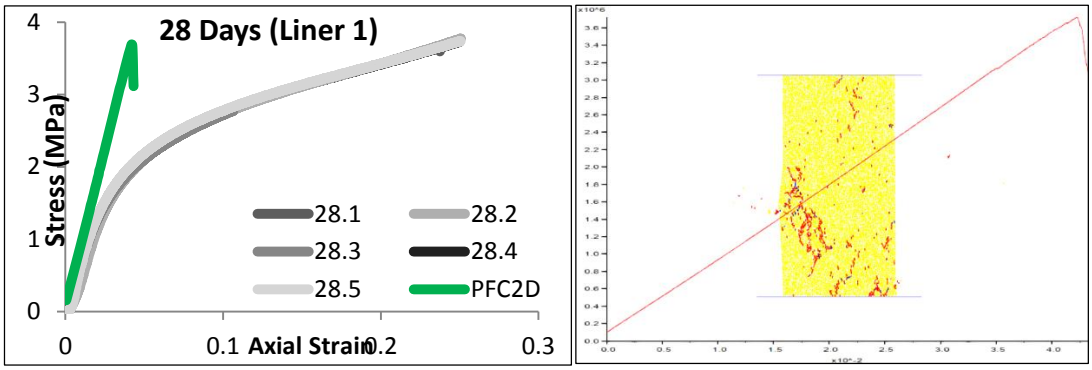

Figure C. 13 Obtained Compression Test Curve & Failure Location for Liner 1 (28 Days)

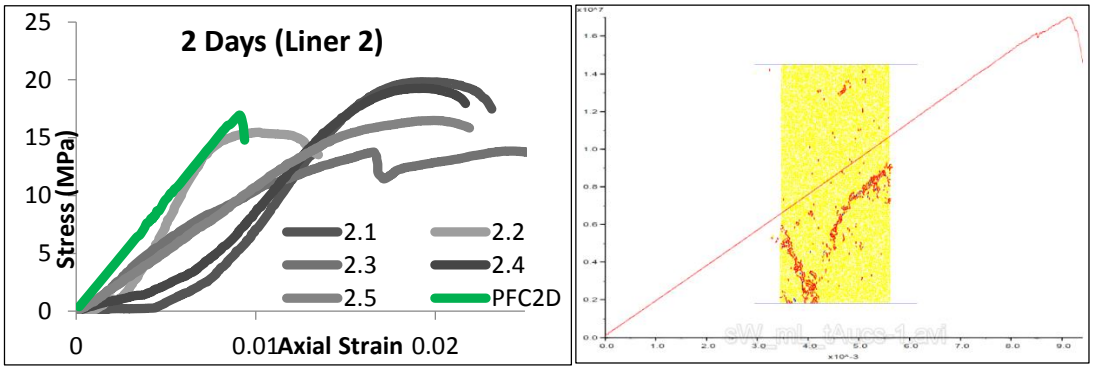

Figure C. 14 Obtained Compression Test Curve & Failure Location for Liner 2 (2 Days)

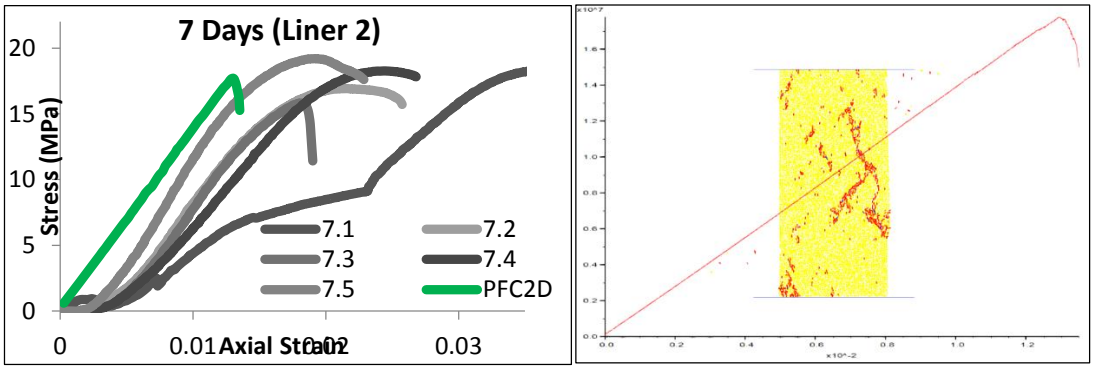

Figure C. 15 Obtained Compression Test Curve & Failure Location for Liner 2 (7 Days)

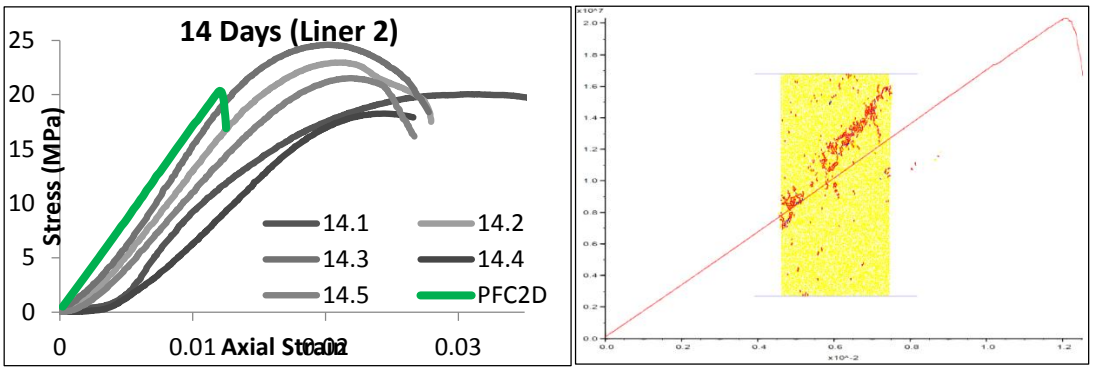

Figure C. 16 Obtained Compression Test Curve & Failure Location for Liner 2 (14 Days)

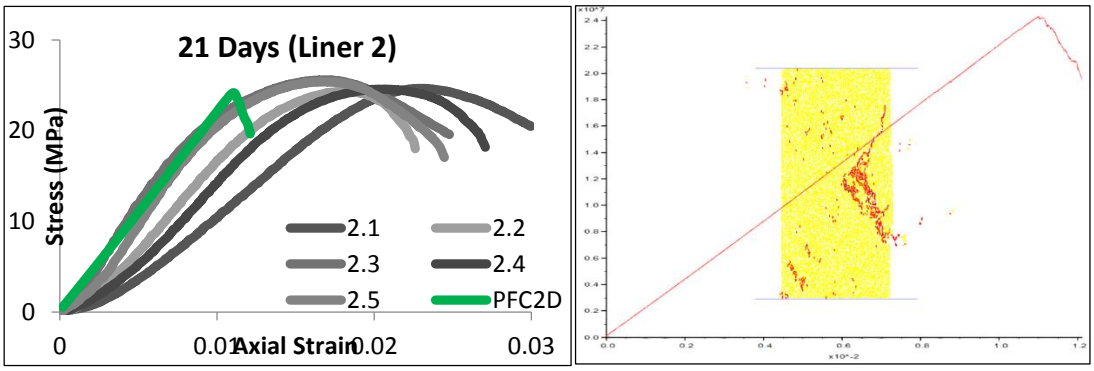

Figure C. 17 Obtained Compression Test Curve & Failure Location for Liner 2 (21 Days)

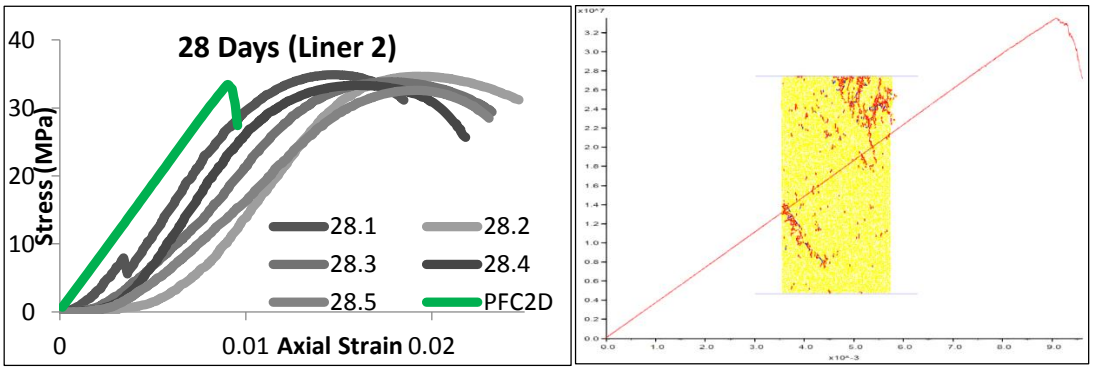

Figure C. 18 Obtained Compression Test Curve & Failure Location for Liner 2 (28 Days)